IMMOBILIZATION OF OLIVE LEAF EXTRACT ON CHITOSAN NANOPARTICLES AND INVESTIGATION OF THEIR EFFECTS ON CANCER CELL LINES

A Thesis Submitted to
the Graduate School of Engineering and Sciences of
İzmir Institute of Technology
in Partial Fulfillment of the Requirements for the Degree of

MASTER OF SCIENCE

in Chemistry

by
Burcu ÖZDAMAR

July 2014
İZMİR

We approve the thesis of **Burcu ÖZDAMAR**

Examining Committee Members:

Assoc. Prof. Dr. Gülşah ŞANLI

Department of Chemistry /İzmir Institute of Technology

Prof. Dr. Oğuz BAYRAKTAR

Department of Chemical Engineering /Ege University

Prof. Dr. Serdar ÖZÇELİK

Department of Chemistry /İzmir Institute of Technology

7 July 2014

Assoc. Prof. Dr. Gülşah ŞANLI

Supervisor, Department of Chemistry
İzmir Institute of Technology

Prof. Dr. Ahmet E. EROĞLU

Head of the Department of Chemistry

Prof. Dr. R. Tuğrul SENGER

Dean of the Graduate School of
Engineering and Sciences

ACKNOWLEDGEMENTS

First of all, I would like to express my endless thanks to my supervisor Assoc. Prof. Dr. Gülşah ŞANLI for giving me the opportunity to study with her and supporting me for every step I take during my two years at this institue. From the beginning of my academic life, her understanding, encouragement, confidence and everlasting support both have maximized my motivation and have helped me to carry out this project by keeping my tenacity of being an academist. It is a great honor to work with such a wonderful person.

I would like to thank to Prof. Dr. Oğuz BAYRAKTAR for giving me the opportunity to experiment the beginning studies of my thesis. I am also thankful to Oğuz BAYRAKTAR's students, Research Assist. İpek ERDOĞAN and Mehmet Emin USLU, for helping me whatever I needed them.

I would like to express my appreciations to Biotechnology and Bioengineering Research Center specialists, especially Özgür Yılmazer, for their kindly helps; and to Biochemistry Laboratory members. Besides, I am grateful to my dear friends Cansu ALTAY, Ayça ZEYBEK, Yıldız BAL and Gizem BOR for their good friendship, encouragements and constructive comments during my studies and being with me whenever I needed them.

My special thanks are for my parents Mustafa and Hanife ÖZDAMAR, my brothers Onur Samet ÖZDAMAR and Nurettin Uğur ÖZDAMAR and my love Abdullah GÜNGÖR for their endless support, patience, respect and faith to achive my aim during my studies.

Lastly, I owe my parents great debt of gratitude for their everlasting love and support. If they were not with me, I could not be here. So they deserve all the thanks, therefore, I dedicate my thesis to them.

ABSTRACT

IMMOBILIZATION OF OLIVE LEAF EXTRACT ON CHITOSAN NANOPARTICLES AND INVESTIGATION OF THEIR EFFECTS ON CANCER CELL LINES

Cancer incidence and mortality rates are increasing worldwide in both economically developed and developing countries. Breast cancer in females and lung cancer in males are the most common cancer types. Epidemiological research has provided increasing evidence that dietary habits, especially Mediterranean diet which has high consumption of olive oil and its products, may play an important role in lung and breast cancer.

Due to their preventive effect against cancer, olive leaf extract rich in polyphenols was immobilizied on chitosan nanoparticles which are good drug carriers because of their biocompatible and biodegradable properties with the help of capability of passing through biological barriers. For this aim, olive leaf extract loaded chitosan nanaoparticles were synthesized by ionotropic gelation mechanism. Optimum conditions to synthesize nanoparticles were determined by investigation of the effect of chitosan and tripolyphosphate mass ratio, initial pH of chitosan solution, concentration of olive leaf extract and incubation time of olive leaf extract and tripolyphosphate with chitosan solution. Characterization of nanoparticles was performed by dynamic light scattering, atomic force microscopy and infrared spectroscopy. To investigate the anticancer properties of nanoparticles, molecular biological studies were performed by in vitro cytotoxicity studies based on MTT assay, in vitro cell cycle analysis and apoptosis by flow cytometer and imaging of cells by optical microscopy.

In results, olive leaf extract loaded chitosan nanaoparticles obtained approximately 91.25 nm and showed more cytotoxicity than chitosan nanoparticles, chitosan and olive leaf extract for both lung and breast cancer cells. In contrast, there was no cytotoxicity for healthy cells. These effects were supported by cell cycle analysis. Also in optical imaging, lower number of cells and morfological differences on cancerous cells which supports the cytotoxicity results were observed. We can conclude that our results will open a new approach to use not only cytotoxic anticancer drug for cancerous cells but also biocompatible material for biomedical applications.

ÖZET

ZEYTİN YAPRAĞI EKSTRAKTININ KİTOSAN NANOPARÇACIKLARI ÜZERİNE İMMOBİLİZASYONU VE KANSER HÜCRE HATLARINDAKİ ETKİLERİNİN İNCELENMESİ

Kanser oluşum sıklığı, hem ekonomik açıdan gelişmiş hem de gelişmekte olan ülkelerde artmaktadır. Bu kanser türlerinin en yaygınları ise, kadınlarda göğüs ve erkeklerde akciğer kanseridir. Epidemiyolojik araştırmalar ise beslenme alışkanlıklarının, özellikle zeytinyağı ve ürünlerinin sıkça tüketildiği Akdeniz diyetinin, akciğer ve meme kanserinin önlenmesinde önemli bir rol oynayabileceğine dair artan kanıtlar sağlamıştır.

Çalışmamızda, kansere karşı koruyucu etkisi bilinen polifenollerce zengin zeytin yaprağı ekstraktı, biyolojik bariyerleri geçme yeteneğinin yardımı ile biyouyumlu ve biyobozunur olan ilaç taşıyıcı kitosan nanoparçacıklarına immobilize edilmiştir ve nanoparçacıklar, iyonotropik jelleşme metoduna göre sentezlenmiştir. Nanoparçacıkları sentezlemek için gerekli optimum koşullar, kitosan-sodyum tripolifosfat kütle oranının, kitosan çözeltisinin başlangıç pH'ının, zeytin yaprağı ekstraktı derişiminin ve sodyum tripolifosfat ve zeytin yaprağı ekstraktının kitosan çözeltisiyle inkübasyon süresinin araştırılması ile sağlanmıştır. Dinamik ışık saçılımı, atomik kuvvet mikroskobu ve infrared spektroskopisi ise karakterizasyon çalışmalarında lullanılmıştır. Bunun yanı sıra, nanoparçacıkların antikanser etkisinin ararştırılması için MTT testine dayalı in vitro sitotoksisite analizi, akım sitometri ile hücre döngüsü ve apoptoz analizi ve optik mikroskobu ile görüntülemeyi içeren moleküler biyolojik çalışmalar yürütülmüştür.

Sonuç olarak, zeytin yaprağı ekstraktı yüklü kitosan nanoparçacıklar yaklaşık olarak 91.25nm olarak sentezlenmiştir ve akciğer ve göğüs kanserindeki sitotoksik etkisi, kitosan nanoparçacıklar, zeytin yaprağı ekstraktı ve kitosanın sitotoksik etkisinden daha fazla bulunmuştur. Bunun yanı sıra, sağlıklı hücrelerde toksik etkilerinin olmadığı kanıtlanmıştır ve sonuçlar optik mikroskobu görüntüleriyle desteklenmiştir. Buna göre tarafımızca ilk kez sentezlenen maddeler, antikanser ilacı olmasının yanı sıra aynı zamanda biyo uyumlu bir malzeme olarak biyomedikal uygulamalarda kullanılacak yeni bir yaklaşım olacaktır.

TABLE OF CONTENTS

LIST OF FIGURES ix

LIST OF TABLES xi

CHAPTER 1. INTRODUCTION 1
1.1. Cancer 1
1.1.1. Lung Cancer 3
1.1.1.1. A549 Cell Line 4
1.1.1.2. BEAS 2B Cell Line 5
1.1.2. Breast Cancer 6
1.1.2.1. MCF-7 Cell Line 8
1.1.3. Importance of Mediterrenian Diet on Cancer 9
1.1.3.1. Olive and Olive Products in Mediterrenian Diet 10
1.1.3.2. Effect of Olive Leaf and It's Components on Cancer 12
1.2. Techniques Used In Cancer Treatment 14
1.3. Nanoparticles 15
1.4. Chitosan 18
1.5. Aim of The Study 20

CHAPTER 2. MATERIALS AND METHODS 22
2.1. Materials 22
2.2. Methods 23
2.2.1. Chemical Studies 23
2.2.1.1. Extraction of Olive Leaves 23
2.2.1.2. Characterization of Olive Leaf Extract 23
2.2.1.2.1. Determination of Total Phenolic Compound Content 23
2.2.1.2.2. Determination of Total Antioxidant Capacity 24
2.2.1.2.3. Analysis of Total Phenolic Compounds 24
2.2.1.3. Synthesizing of Chitosan Nanoparticles 25
2.2.1.4. Synthesizing of Olive Leaf Extract Loaded Chitosan Nanoparticles 25

2.2.1.5. Optimization of Olive Leaf Extract Loaded Chitosan Nanoparticles 26
2.2.1.5.1. Effect of CS-TPP Mass Ratio 26
2.2.1.5.2. Effect of pH 27
2.2.1.5.3. Effect of Incubation Time 28
2.2.1.5.3.1. Effect of Incubation Time of TPP 28
2.2.1.5.3.2. Effect of Incubation Time of OLE 28
2.2.1.5.4. Effect of Concentration of OLE 28
2.2.1.6. Characterization of Olive Leaf Extract Loaded Chitosan Nanoparticles 29
2.2.2. Molecular Biological Studies 29
2.2.2.1. Proliferation of Cancer and Healthy Cell Lines 29
2.2.2.2. Thawing the Frozen Cells 30
2.2.2.3. Freezing the Cells 30
2.2.2.4. In Vitro Cytotoxicity Study 30
2.2.2.5. Cell Cycle Analysis By Flow Cytometry 31
2.2.2.6. Apoptosis Analysis By Flow Cytometry 32
2.2.2.7. Imaging Of Optical Microscopy 33

CHAPTER 3. RESULTS and DISCUSSIONS 34
3.1. Chemical Studies 34
3.1.1. Characterization of Olive Leaf Extract 34
3.1.1.1 Determination of Total Phenolic Compound Content 34
3.1.1.2. Determination of Total Antioxidant Capacity 34
3.1.1.3. Analysis of Total Phenolic Compounds 35
3.1.2. Synthesizing of Chitosan Nanoparticles 36
3.1.2.1. Optimization of Olive Leaf Extract Loaded Chitosan Nanoparticles 36
3.1.2.1.1. Effect of CS-TPP Mass Ratio 36
3.1.2.1.2. Effect of pH 40
3.1.2.1.3. Effect of Incubation Time 43
3.1.2.1.3.1. Effect of Incubation Time of TPP 43
3.1.2.3.1.2. Effect of Incubation Time of OLE 45
3.1.2.1.4. Effect of Concentration of OLE 48

3.1.3. Characterization of Olive Leaf Extract Loaded Chitosan Nanoparticles 50
3.2. Molecular Biological Studies 55
3.2.1. In Vitro Cytotoxicity Study 55
3.2.1.1. Cytotoxicity Study on A549 Cell Lines 55
3.2.1.2. Cytotoxicity Study on MCF-7 Cell Lines 58
3.2.1.3. Cytotoxicity Study on BEAS 2B Cell Lines 61
3.2.2. Cell Cycle Analysis By Flow Cytometry 63
3.2.2.1. Cell Cycle Analysis on A549 Cell Lines 64
3.2.2.2. Cell Cycle Analysis on MCF-7 Cell Lines 66
3.2.3. Apoptosis Analysis 67
3.2.4. Imaging Of Optical Microscopy 70

CHAPTER 4. CONCLUSION 73

REFERENCES 77

APPENDICES
APPENDIX A. MEDIAS 82
APPENDIX B. CHEMICALS, REAGENTS AND SOLUTIONS 83
APPENDIX C. CALCULATIONS OF CHARACTERIZATION OF OLIVE LEAF EXTRACT 85

LIST OF FIGURES

Figure **Page**

Figure 1.1. Loss of Normal Growth Control 2
Figure 1.2. Image of A549 cell 5
Figure 1.3. Image of BEAS 2B cells 6
Figure 1.4. Image of lymphatic nodes 7
Figure 1.5. Image of MCF-7 cells 9
Figure 1.6. Image of chemical structure of phenolic compounds already identified in *O. Europaea* L. leaf extract 11
Figure 1.7. Image of the process of Enhanced Permeability and Retention effect 17
Figure 1.8. Image of chemical structure of chitosan (CS) and tripolyphosphate (TPP). 19
Figure 1.9. Image of interaction of chitosan with TPP (a) deprotonation, (b) ionic cross-linking 20
Figure 3.1. HPLC chromotogram of olive leaf extract 35
Figure 3.2. The effect of decreasing CS/TPP mass ratios on loading capacity of OLE and size of OLE-CS-NPs 38
Figure 3.3. Size distrubition graph of OLE-CS-NPs with different CS-TPP mass ratios as 1, ½, 1/3, ¼, 1/5, 1/6 38
Figure 3.4. The effect of increasing CS/TPP mass ratios on loading capacity and size of NPs 39
Figure 3.5. Size distrubition graph of OLE-CS-NPs with different CS-TPP mass ratio as 6, 5, 4, 3, 2, 1 40
Figure 3.6. Effect of initial pH value of CS solution on size of NPs and loading capacity of OLE 42
Figure 3.7. Size distrubition graph of OLE-CS-NPs with different initial pH value of CS solution 42
Figure 3.8. Effect of incubation time of TPP on loading capacity and size of nanoparticles 44
Figure 3.9. Size distribution graph of OLE-CS-NPs with different incubation time of TPP 45
Figure 3.10. Effect of incubation time of OLE with CS on loading capacity and size of NPs 47

Figure 3.11. Size distribution graph of OLE-CS-NPs with different incubation time of OLE 47
Figure 3.12. Effect of different concentrations of OLE on loading capacity of OLE into CS-NPs and size of OLE-CS-NPs 49
Figure 3.13. Size distribution graph of OLE-CS-NPs with different concentration of OLE 49
Figure 3.14. Size distrubition graph of CS-NPs and OLE-CS-NPs 50
Figure 3.15. AFM image of CS-NPs 51
Figure 3.16. AFM image of OLE-CS-NPs 52
Figure 3.17. FT-IR spectra of CS 53
Figure 3.18. FT-IR spectra of OLE 53
Figure 3.19. FT-IR spectra of OLE-CS-NPs and CS-NPs 54
Figure 3.20. The cytotoxic effect of OLE-CS-NPs on A549 cells 55
Figure 3.21. The cytotoxic effect of CS-NPs on A549 cells 56
Figure 3.22. The cytotoxic effect of OLE and CS on A549 cells 57
Figure 3.23. The cytotoxic effect of OLE-CS-NPs on MCF-7 cells 58
Figure 3.24. The cytotoxic effect of CS-NPs on MCF-7 cells 59
Figure 3.25. The cytotoxic effect of CS and OLE on MCF-7 cells 60
Figure 3.26. The cytotoxic effect of OLE-CS-NPs on BEAS 2B cells 61
Figure 3.27. The cytotoxic effect of CS-NPs on BEAS 2B cells 62
Figure 3.28. The cytotoxic effect of CS and OLE on BEAS 2B cells 63
Figure 3.29. Effects of OLE-CS-NPs on cell cycle against A549 cells 65
Figure 3.30. Effects of OLE on cell cycle against A549 cells 66
Figure 3.31. Effects of OLE-CS-NPs on cell cycle against MCF-7 cells 67
Figure 3.32. Quantification of the apoptotic effects of OLE-CS-NPs against A549 cells 68
Figure 3.33. Quantification of the apoptotic effects of OLE-CS-NPs against MCF-7 cells 69
Figure 3.34. Optical microscopy images of A549 cells as control and 1000 μg/mL CS, CS-NPs and OLE-CS-NPs applied cells 70
Figure 3.35. Optical microscopy images of MCF-7 cells as control and 1000 μg/mL CS, CS-NPs and OLE-CS-NPs applied cells 71
Figure 3.36. Optical microscopy images of BEAS-2B cells as control and 1000 μg/mL CS, CS-NPs and OLE-CS-NPs applied cells 72

LIST OF TABLES

Table **Page**

Table 2.1. Some properties of chitosan and sodium tripolyphosphate 22

Table 2.2. Different mass ratios of CS and TPP 27

Table 3.1. Effect of CS-TPP mass ratio on loading capacity of OLE and size of OLE-CS-NPs..... 37

Table 3.2. Effect of initial pH value of CS solution on loading capacity of OLE into CS-NPs and size of OLE-CS-NPs 41

Table 3.3. Effect of different incubation time of TPP on loading capacity of OLE and size of OLE-CS-NPs 44

Table 3.4. Effect of different incubation time of OLE with CS on loading capacity of OLE and size of OLE-CS-NPs 46

Table 3.5. Effect of different concentrations of OLE on loading capacity of OLE into CS-NPs and size of OLE-CS-NPs. 48

Table 3.6 Cell phase composition (%) of OLE-CS-NPs and OLE effected cells for different concentrations 64

Table 3.7 Cell phase composition (%) of OLE-CS-NPs effected cells for different concentrations 66

CHAPTER 1

INTRODUCTION

1.1. Cancer

Cancer is an umbrella word to describe a group of diseases characterized by uncontrolled growth and spread of abnormal cells. With more than 10 million new patients every year, cancer is still one of the most fatal diseases around the world (T. Lammers, 2010., D. Peer et al., 2007).

The body is made up of many types of cells. These cells grow and divide in a controlled way to produce more cells as they are needed to keep the body healthy. When cells become old or damaged, they die and are replaced with new cells.

However, sometimes this orderly process goes wrong. The genetic material (DNA) of a cell can become damaged or changed, producing mutations that affect normal cell growth and division. When this happens, cells do not die when they should and new cells form when the body does not need them. The extra cells may form a mass of tissue called a tumor. In Figure 1.1 is showed the difference between normal cells and cancer cells in terms of growth control mechanism. (NCI, accessed 2011).

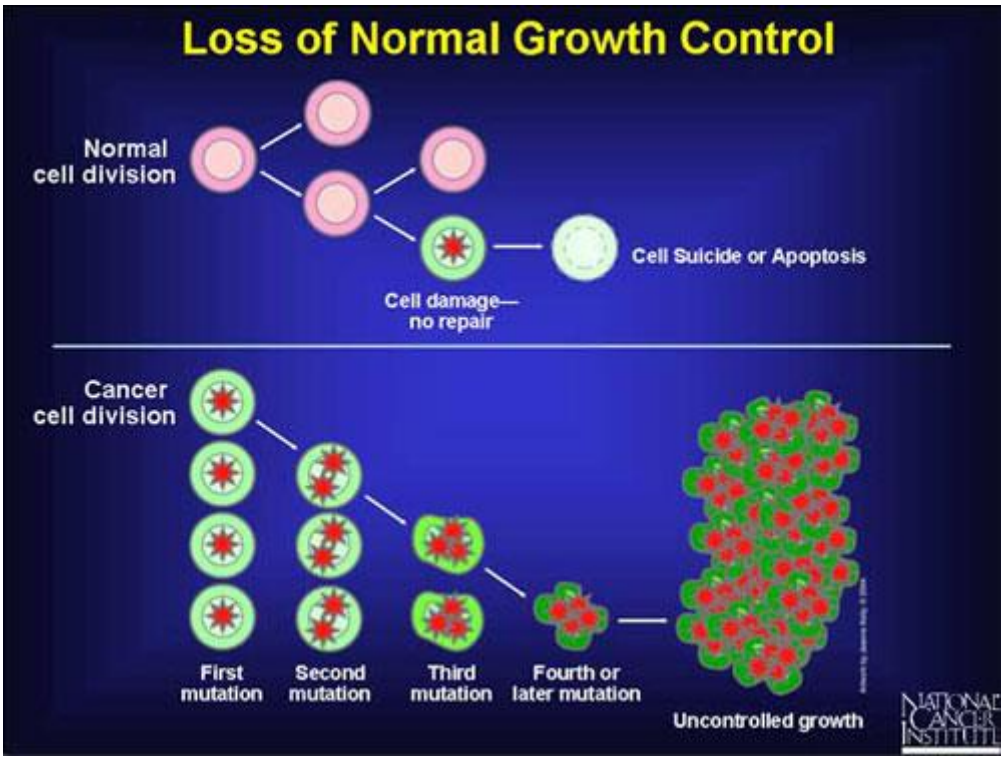

Figure 1.1. Loss of Normal Growth Control
(Source: NCI, 2011)

Cancer is not just one disease but many diseases. There are more than 100 different types of cancer. Most cancers are named for the organ or type of cell in which they start. For instance, cancer that begins in the lung is called lung cancer; cancer that begins in basal cells of the skin is called basal cell carcinoma.

Cancer types can be grouped into broader categories. The main categories of cancer include:

- Carcinoma: Cancer that begins in the skin or in tissues that line or cover internal organs.
- Sarcoma: Cancer that begins in bone, cartilage, fat, muscle, blood, vessels or other connective or supportive tissue.
- Leukemia: Cancer that starts in blood-forming tissue such as the bone marrow and causes large numbers of abnormal blood cells to be produced and enter the blood.
- Lymphoma and Myeloma: Cancers that begin in the cells of the immune system.
- Central Nervous System: Cancers that begin in the tissues of the brain and spinal cord (Anand, P. et al., 2008).

Modern molecular cancer research really began in 1975 and 1976 with the discovery of the Src proto-oncogene. And over the ensuing 30 years, we have learned an enormous amount about the molecular mechanisms that create human cancers.

An abiding theme in much of modern cancer research is the notion that many cancer causing agents, carcinogens, act through their ability to enter into the body's tissues and to damage specific genes inside previously normal cells, in other words, that carcinogens can act as mutagens to mutate genes. And through these mutations that they create, these carcinogens are able to elicit the disease of cancer. (The Biology of Cancer, by Robert A. Weinberg.)

Cancer incidence and mortality rates are increasing worldwide in both economically developed and developing countries. Breast cancer in females and lung cancer in males are the most common cancer types, followed by stomach, liver, colourectal and cervix as a result of cancer-causing effects from smoking, sedentary lifestyle and western type diets. Lifestyle-related factors, e.g. dietary habits, influence the incidence rate of diseases such as cancer (S. Isık et al., 2012).

1.1.1. Lung Cancer

Cancer of the lung is the most common type of cancer in the world. Lung cancer is the leading killer of all cancer patients. It is generally classified as small cell carcinoma and non-small cell carcinoma (Zhang P. et.al., 2003).

Lung cancer is the uncontrolled growth of abnormal cells in one or both lungs. These abnormal cells do not carry out the functions of normal lung cells and do not develop into healthy lung tissue. As they grow, the abnormal cells can form tumors and interfere with the functioning of the lung, which provides oxygen to the body via the blood.

Researchers have found that it takes a series of mutations to create a lung cancer cell. Before becoming fully cancerous, cells can be precancerous, in that they have some mutations but still function normally as lung cells. When a cell with a genetic mutation divides, it passes along its abnormal genes to the two new cells, which then divide into four cells with errors in their DNA and so on. With each new mutation, the lung tissue cell becomes more mutated and may not be as effective in carrying out its

function as a lung cell. At a later stage of disease, some cells may travel away from the original tumor and start growing in other parts of the body. This process is call metastasis and the new distant sites are referred to as metastases (http://www.lungcancer.org/find_information/publications/163-lung_cancer_101/265-what_is_lung_cancer).

There is general agreement that the incidence of lung cancer is determined mainly by active cigarette smoking followed by occupational exposures (Fortes C. et. al., 2003). Cigarette smoke contains a large number of combustion products that are inhaled into the lungs, and these agents, these chemicals, are then converted via various metabolic enzymes into chemical compounds that are capable of interacting with and forming covalent bonds with the DNA. Such structurally altered DNA molecules then may be replicated and yield ultimately altered DNA sequences which we would call mutant genes. (The Biology of Cancer, by Robert A. Weinberg.)

Treatment of lung cancer is less than optimal and the mean survival for advanced lung cancer patient is less than one year regardless what treatment regimen was used (Zhang P. et.al., 2003).

Epidemiological research has provided increasing evidence that dietary habits may play an important role in lung cancer etiology. In particular, increased vegetable and fruit intakes are associated with reduced risk, whereas alcohol, salted meat, fat and cholesterol intakes are associated with increased risk of lung cancer (Fortes C. et. al., 2003).

1.1.1.1. A549 Cell Line

The A549 cell line was first developed in 1972 (D.J Giard, et al.) through the removal and culturing of cancerous lung tissue in the explanted tumor of 58-year-old caucausian male.

A549 cells are human alveolar basal epithelial cells. These are squamous in nature and responsible for the diffusion of substances, such as water and electrolytes, across the alveoli of lungs. They grow adherently, as a monolayer, in vivo.

The squamous epithelial cells are positive for keratin, as is evidenced by immunoperoxidase staining. These cells are also able to synthesize lecithin and contain

a high percentage of desaturated fatty acids, which are utilized by the cytidine-diphospho-choline pathway and important for the maintenance of membrane phospholipids in cells. ("A549 Cell Line- Human Alveolar Adenocarcinoma Cell Line, General Information", http://a549.com/, Retrieved on 24 May 2014.)

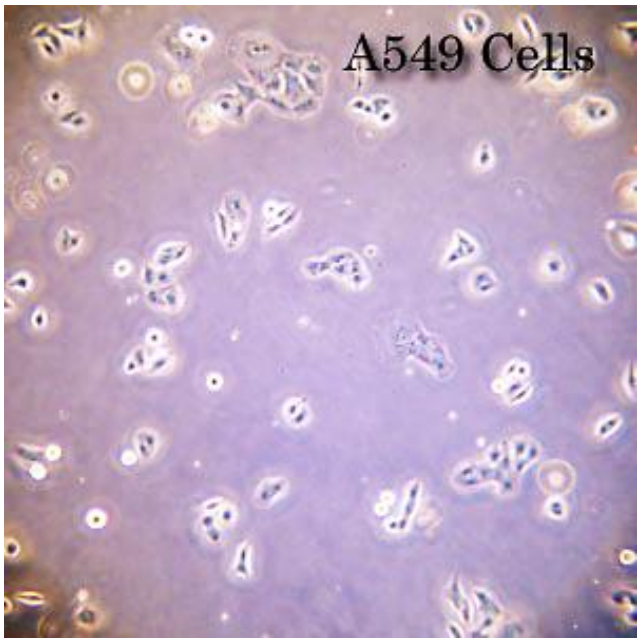

Figure 1.2. Image of A549 cell
(Source: Altogen Biosystem, 2014)

1.1.1.2. BEAS 2B Cell Line

BEAS-2B (human bronchial epithelium) cells were derived from normal bronchial epithelium obtained from autopsy of non-cancerous individuals. Cells were infected with a replication-defective SV40/adenovirus 12 hybrid and cloned. Squamous differentiation can be observed in response to serum. This ability can be used for screening chemical and biological agents inducing or affecting differentiation and/or carcinogenesis. The cell line has been applied for studies of pneumococcal infection mechanisms. BEAS-2B was described to express keratins and SV40 T antigen. (http://www.phe-culturecollections.org.uk/, General Cell Collection: BEAS-2B, Retrieved on 24 May 2014).

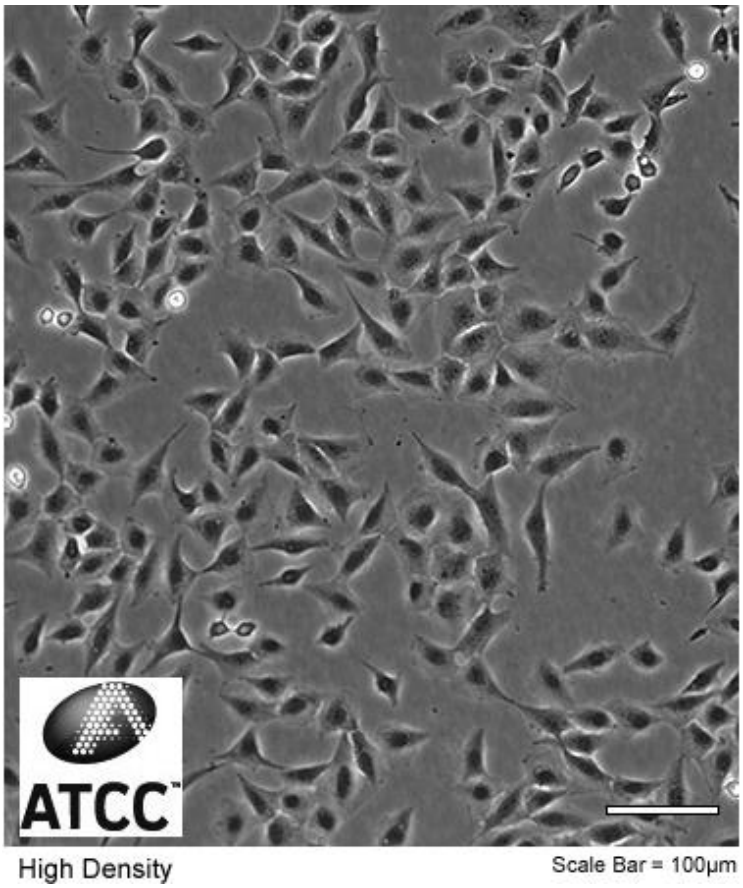

Figure 1.3. Image of BEAS 2B cells
(Source: Altogen Biosystem, 24 May 2014)

1.1.2. Breast Cancer

Breast cancer is a malignant tumor that starts in the cells of the breast. A malignant tumor is a group of cancer cells that can grow into (invade) surrounding tissues or spread (metastasize) to distant areas of the body. The disease occurs almost entirely in women, but men can get it, too.

Most breast cancers begin in the cells that line the ducts (ductal cancers). Some begin in the cells that line the lobules (lobular cancers), while a small number start in other tissues.

The lymph system is important to understand because it is one way breast cancers can spread. This system has several parts.

Lymph nodes are small, bean-shaped collections of immune system cells (cells that are important in fighting infections) that are connected by lymphatic vessels. Lymphatic vessels are like small veins, except that they carry a clear fluid called lymph (instead of blood) away from the breast. Lymph contains tissue fluid and waste

products, as well as immune system cells. Breast cancer cells can enter lymphatic vessels and begin to grow in lymph nodes.

Most lymphatic vessels in the breast connect to lymph nodes under the arm (axillary nodes). Some lymphatic vessels connect to lymph nodes inside the chest (internal mammary nodes) and those either above or below the collarbone (supraclavicular or infraclavicular nodes).

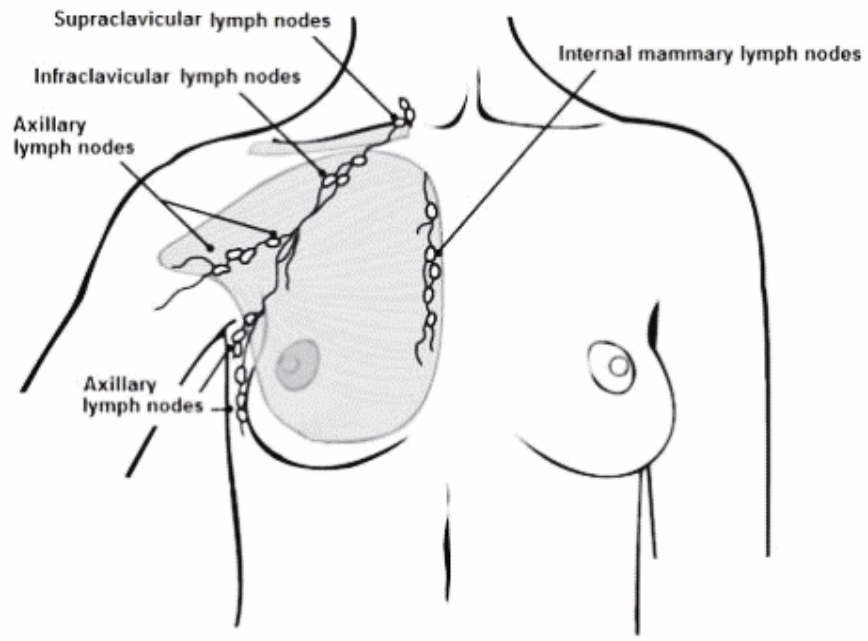

Figure 1.4 Image of lymphatic nodes
(Source: http://www.cancer.org/cancer/breastcancer, 2014)

If the cancer cells have spread to lymph nodes, there is a higher chance that the cells could have also gotten into the bloodstream and spread (metastasized) to other sites in the body. The more lymph nodes with breast cancer cells, the more likely it is that the cancer may be found in other organs as well. Because of this, finding cancer in one or more lymph nodes often affects the treatment plan.

Studies continue to uncover lifestyle factors and habits that alter breast cancer risk. Ongoing studies are looking at the effect of exercise, weight gain or loss, and diet on breast cancer risk. Studies on the best use of genetic testing for BRCA1 and BRCA2 mutations continue at a rapid pace. Scientists are also exploring how common gene variations may affect breast cancer risk. Each gene variant has only a modest effect in risk (10 to 20%), but when taken together they may potentially have a large impact.

Fenretinide, a retinoid, is also being studied as a way to reduce the risk of breast cancer (retinoids are drugs related to vitamin A). In a small study, this drug reduced breast cancer risk as much as tamoxifen. Other drugs, such as aromatase inhibitors, are also being studied to reduce the risk of breast cancer. (http://www.cancer.org/cancer/breastcancer/, Retrieved on 24 May 2014.)

1.1.2.1. MCF-7 Cell Line

MCF-7 is a cell line that was first isolated in 1970 from the breast tissue of a 69-year old Caucasian woman. Of the two mastectomies she received, the first revealed the removed tissue to be benign. Five years later, a second operation revealed malignant adenocarcinoma in a pleural effusion from which was taken cells for MCF-7. The woman was treated for breast cancer with radiotheraphy and hormonotherapy.

MCF-7 cells are useful for in vitro breast cancer studies because the cell line has retained several ideal characteristics particular to the mammary epithelium. These include the ability for MCF-7 cells to process estrogen, in the form of estradiol, via estrogen receptors in the cell cytoplasm. This makes the MCF-7 cell line an estrogen receptor (ER) positive control cell line. ("MCF-7 Cells, human breast adenocarcinoma cell line, General Information", http://www.mcf7.com/, Retrieved on 24 May 2014.)

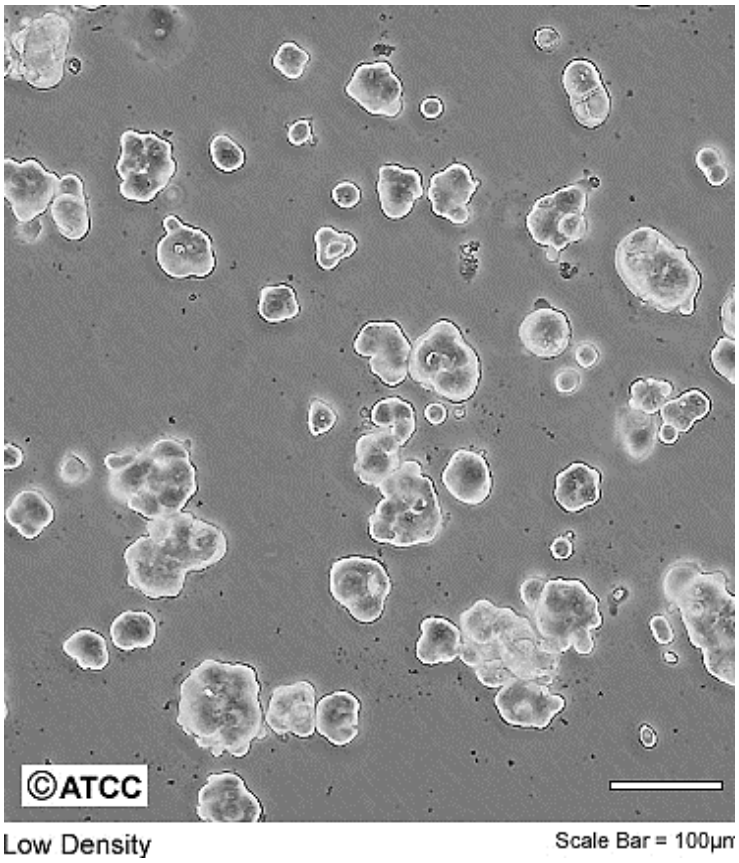

Figure 1.5 Image of MCF-7 cells
(Source: http://www.lgcstandardsatcc.org, 2014)

1.1.3. Importance of Mediterrenian Diet on Cancer

The Mediterranean diet contains a great variety of natural antioxidants, such as carotenoids, vitamins C and E, phenols and flavonoids (Fortes C. et al., 2003).

Among the generally accepted correlations between dietary habits and disease risk, the Mediterranean diet has been recognized as a healthful dietary pattern with preventive effect against chronic diseases, including cancer and cardiovascular diseases (M.P. Carrera-Gonzalez et al., 2013).

The incidence of cancer in Mediterranean countries is lower than in the rest of European countries and the United States. This is mostly described by the lower rate of the large bowel, breast, endometrial, and prostate cancers by a number of epidemiological studies, and the major reason for this, apart from possible genetic factors, is attributed to the dietary practices. The traditional Mediterranean diet is characterized by high consumption of foods of plant origin, relatively low consumption of red meat, and high consumption of olive oil and its products. There are a number of

studies on health beneficial effects of olive oil. Several studies have been reported that olive oil is more favorable against cancer than other forms of added lipids due to its high content of monounsaturated fatty acids (Han, J. et. al., 2009).

1.1.3.1. Olive and Olive Products in Mediterrenian Diet

References to the olive tree date back to Biblical and Roman times and to Greek mythology. Historically, the products of *Olea europaea* have been used as aphrodisiacs, emollients, laxatives, nutritives, sedatives, and tonics. Specific conditions traditionally treated include colic, alopecia, paralysis, rheumatic pain, sciatica, and hypertension.

Although there are dietary variations among Mediterranean countries, a common feature is the high consumption of extra-virgin olive oil.

Extra-virgin olive oil is a functional food, which in addition to contain multiple minor components also has a high level of monounsaturated fatty acids (MUFA). Minor components are present in about 2% of extra-virgin olive oil weight and include >230 chemical compounds. It is difficult to quantify the dietary intake of these components but Mediterranean countries tend to consume extra-virgin olive oil, which is much richer in phenolic compounds than refined oils (M.P. Carrera-Gonzalez et al., 2013).

The olive fruit is a drupe, oval in shape and consisting of two main parts: the pericarp and the endocarp (the pit or kernel, which contains the seeds). The pericarp is composed of the epicarp (skin) and the mesocarp (pulp). The pericarp contains 96% to 98% of the total amount of oil, with the remaining 2% to 4% in the kernel. Edible olive oil constituents can be divided into saponifiable (98.5% to 99.5% of the oil) and unsaponifiable (0.5% to 1.5% of the oil) fractions. The saponifiable fraction includes fatty acids and triacylglycerols; the unsaponifiable fractions include hydrocarbons (squalene and carotenoids), chlorophylls, tocopherols, aliphatic alcohols, sterols, phenolic compounds, and volatile compounds (Yumi Z. et. al., 2005).

The major phenolic compounds identified and quantified in olive and olive oil belong to three different classes: simple phenols (hydroxytyrosol, tyrosol); secoiridoids (oleuropein, the aglycone of ligstroside and their respective decarboxylated dialdehyde derivatives) and the lignans [(+)-1-acetoxypinoresinol & (+)- pinoresinol]. All three classes have potent antioxidant properties (Çınar A. et al., 2011).

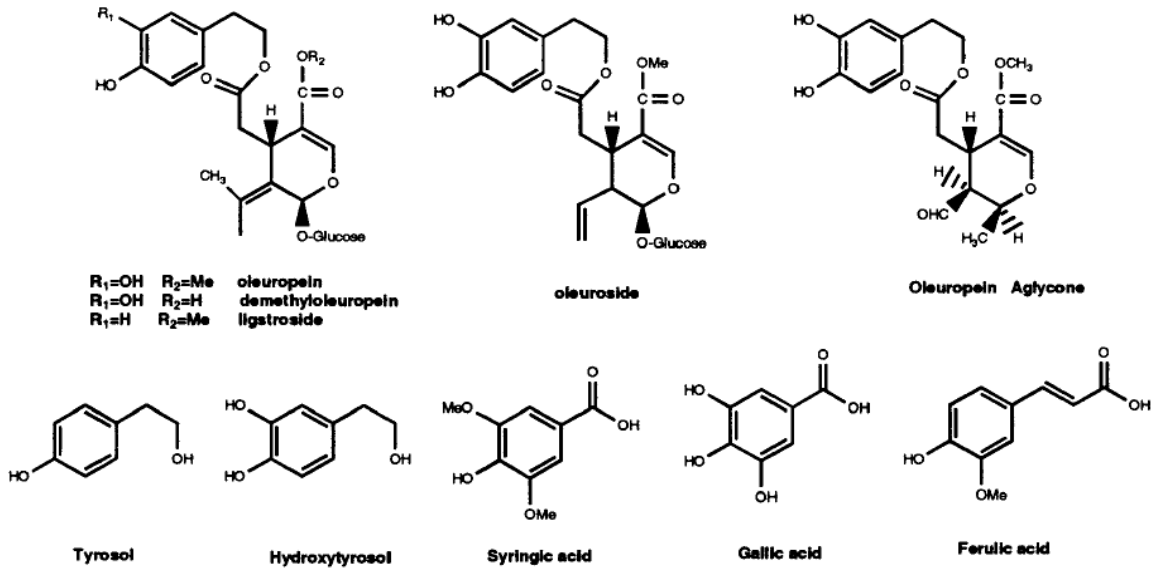

Figure 1.6. Image of chemical structure of phenolic compounds already identified in *O. Europaea* L. leaf extract

The main antioxidants of virgin olive oil are carotenoids and phenolic compounds, which are both lipophilic and hydrophilic. The lipophilics include tocopherols, while the hydrophilics include flavonoids, phenolic alcohols and acids, secoiridoids and their metabolites (E, Tripoli., 2005).

Mediterranean diet's health benefit effects are attributed to the high consumption rate of olive and olive products in these areas. Dietary agents present in olive products, such as polyphenols, are responsible for these protective effects. The main polyphenols, that function in olives and olive products, are hydroxytyrosol, tyrosol, secoiridoids and lignans, and squalene (S. Isık et al., 2012).

Studies conducted thus far (including human, animal, in vivo and in vitro) have demonstrated that olive oil phenolic compounds have positive effects on various physiological biomarkers, implicating phenolic compounds as partially responsible for health benefits associated with the Mediterranean diet. Furthermore, olive oil phenolic compounds have been shown to be highly bioavailable, reinforcing their potential health promoting properties.

The metabolism of olive oil phenolic compounds is important in determining their availability. If phenolics are broken down and converted to other phenolics this may have a notable effect on their bioavailability. Phenolic compounds, oleuropein-

glycoside and oleuropein and ligstroside-aglycones are converted to hydroxytyrosol or tyrosol and excreted in urine. Hydroxytyrosol and tyrosol themselves are sometimes conjugated to glucuronic acid and excreted in urine as glucuronides.

Research has shown that the phenolic compounds, hydroxytyrosol and tyrosol are absorbed after ingestion in a dose-dependent manner (S. Cicerale et al., 2010). The metabolic fate of hydroxytyrosol and tyrosol in vivo has also been evaluated by administration to rats, both by mouth and intravenously, of the radiolabelled polyphenols. Also in this case, hydroxytyrosol appeared in the plasma, at maximum levels, as soon as 10 min after oral administration. Hydroxytyrosol is quickly eliminated from the plasma and excreted in the urine, as a free compound, and bound to glucuronic acid; to a smaller extent (5 %) it is also eliminated in the faeces (E, Tripoli., 2005).

Tuck and colleagues demonstrated increased bioavailability of hydroxytyrosol and tyrosol when administered as an olive oil solution compared to an aqueous solution. The differences in bioavailability have been suggested to be due to the high antioxidant content of virgin olive oil compared to water and this high antioxidant content may have protected the breakdown of phenolics in the gastrointestinal tract prior to absorption (Tuck K.L. et al., 2001).

1.1.3.2. Effect of Olive Leaf and It's Components on Cancer

Cancer incidence in Mediterranean countries is lower than that in Scandinavian countries and the United States. This situation has been attributed to the Mediterranean style diet, characterised by high and regular consumption of olives and olive products, fruits, vegetables and legumes. Studies demonstrate that there is a correlation between the Mediterranean-style diet and the incidence of some degenerative diseases associated with oxidative damage, such as cardiovascular diseases and cancer (S. Isık et al., 2012).

Recently, olive compounds have shown significant anti-carcinogenic effects by directly modulating the activities of various types of receptor tyrosine kinases, including the human epidermal growth factor receptor (HER2) (Amani T. et al., 2012). Mainly, studies have revolved around the effects of these compounds against some types of cancers, such as breast, colon, stomach and human leukemia (S. Isık et al., 2012).

The biological effects of polyphenols present in extra-virgin olive oil have been further investigated. In particular it has been found that oleuropein is a potent scavenger

of the free radicals and nitrogen species as well inducing the production of nitric oxide in macrophages. In addition, it plays an important role in the prevention of DNA damage, thus impairing mutagenesis and carcinogenesis. In this sense, Hamdi and Castellon (2005) demonstrated that antitumoral effect of oleuropein exerted by the disruption of actin filament in tumor cells (M.P. Carrera-Gonzalez et al., 2013).

Oxidative damage to DNA is a precursor for human carcinogenesis and it is well known that oxygen radicals continually attack human cells. Unless damage to these cells is counteracted, DNA damage may result, and such damage can lead to cancer development. A randomized crossover intervention trial has shown that intake of phenol rich virgin olive oil decreases oxidative DNA damage by up to 30% compared to a low phenol virgin olive oil (S. Cicerale et al., 2010).

Researchs to date have shown that phenolic compounds mostly hydroxytyrosol, tyrosol and oleuropein can be used in prevention of tumor formation and cell proliferation. There are lots of experiments in different cell lines for these features.

Oleuropein was found to cause cell rounding, which disrupts the cell actin cytoskeleton. Moreover, oleuropein affects and disrupts purified actin filaments, providing direct antitumor effects due to cell disruption (Hamdi H.K., 2005).

Fabriani et al. demonstrated that hydroxytyrosol inhibits cell proliferation, blocking the G1 phase of the cell cycle, with a proportional increase of cells in the G0/G1 phase and a concomitant decline in the S and G2/M phases. Moreover they observed that phenols extract, obtained from virgin olive oil, was more potent that hydroxytyrosol alone in both inhibiting proliferation and inducing apoptosis, suggesting a synergistic effect of other phenols in this process (Fabriani R. et al., 2002).

Han J. et al. have showed that oleuropein or hydroxytyrosol decreased cell viability, inhibited cell proliferation, and induced cell apoptosis in MCF-7 cells. Also hydroxytyrosol and oleuropein exhibited statistically significant block of G1 to S phase transition manifested by the increase of cell number in G0/G1 phase (Han J. et al., 2009).

Olive oil phenols are capable of scavenging free radicals produced in the fecal matrix, which is thought to explain the epidemiological data suggesting a colonic chemoprotective effect of olive oil (Waterman E. et al., 2007).

Antiproliferative effect of hydroxytyrosol was investigated on human colon adenocarcinoma by Corona et al. They found that this compound inhibited proliferation by inducing a cell cycle block in G2/M (Corona et al., 2009).

Furthermore, Gill et al. (2005) and later Hashim et al. (2008) demonstrated that treatment of human colon adenocarcinoma cells with OO-phenols resulted in the inhibition of all colon carcinogenetic processes such as initiation, promotion, and metastasis, triggering cell death by apoptosis (Ivan, C. et al., 2013).

1.2. Techniques Used In Cancer Treatment

Surgery, radiotherapy and chemotherapy or their combinations are the most widely applied cancer treatments. However, they have their restrictions. For instance, chemotherapeutic drugs are often of low molecular weight, which entitles them a short half-life in the blood circulation. Also, small drug molecules diffuse rapidly and distribute evenly in human bodies which cause damages to the healthy cells and adverse systematic toxicity to patients (Haag R. et al., 2006).

From this perspective, innovative drug delivery systems with functions of targeting anti-tumor drugs, eliminating solubility and resistance problems are urgently needed. Nanoparticles (NPs) have been a fascinating part of this field (Parveen S. et. al., 2012).

The treatment of disseminated cancer has become increasingly aimed at molecular targets derived from studies of the oncogenes and tumor suppressors known to be involved in the development of human cancers. This increase in specificity of cancer treatment, from the use of general cytotoxic agents such as nitrogen mustard in the 1940s, to the development of natural-product anticancer drugs in the 1960s such as Vinca alkaloids and anthracyclines, which are more cytotoxic to cancer cells than normal cells, to the use of specific monoclonal antibodies and immunotoxins targeted to cell surface receptors and specific agents that inactivate kinases in growth-promoting pathways, has improved the response rate in cancer and reduced side effects of anticancer treatment but has not yet resulted in cure of the majority of patients with metastatic disease (Michael, M., 2002).

1.3. Nanoparticles

Nanoparticles are the most promising of the delivery systems showing potential for the mucosal delivery of drugs and antigens. First described for pharmaceutical applications by Birrenbach and Speiser (1976), nanostructured carriers of appropriate size and surface charge should be able to protect drugs from enzymatic degradation to improve their penetration across the mucosal epithelium and to modulate drug pharmacokinetics, thus improving efficacy and reducing drug toxicity (Parveen S. et al., 2012).

Nanoparticles have been investigated in order to minimize side effects of anticancer drugs and enhance the antitumoral drug efficacy in cancer therapy (Jong-Ho Kim et. al., 2008). There is a wealth literature display significantly improved therapeutic efficacy of nano-sized drug carriers against different tumor model, due to the tumor targeting ability of nanosized drug careers, compared to the free drugs.

A wide range of materials, such as natural and synthetic polymers, lipids, and surfactants have been employed to prepare drug-containing nanocarriers. Among the materials proposed for mucosal delivery, polysaccharides have received increasing attention because of their outstanding physical and biological properties (T. López-León et al., 2005).

In vitro and in vivo evaluation of the delivery systems that have been studied include polymeric nanoparticles (NPs), has enabled identification of some of the favorable properties for protein and peptide delivery systems. For example, it has been found that delivery systems with mean diameters in the range of hundreds of nanometers have a greater ability to penetrate the epithelia when compared to particles in the micrometer size range (Hong, Z et. al., 2004).

The potential use of polymeric nanoparticles as drug carriers has led to the development of many different colloidal delivery vehicles. The main advantages of this kind of systems lie in their capacity to cross biological barriers, to protect macromolecules, such as peptides, proteins, oligonucleotides and genes from degradation in biological media, and to deliver drugs or macromolecules to a target site with following controlled release. In the last years several synthetic as well as natural

polymers have been examined for pharmaceutical applications (T. López-León et al., 2005).

Particularly, polymeric nano-sized carriers have shown a high tumor targeting ability at tumor tissue and the nano-sized drug carriers were minimally found at normal tissue sites (Jong-Ho Kim et. al., 2008) because the disorganised vasculature and absence of effective lymphatic drainage in solid tumours allows nanoparticles to leak from the blood stream and accumulate in the cancer, a phenomenon known as the Enhanced Permeability and Retention (EPR) effect. This allows nanoparticles to target tumours passively, reducing uptake into healthy cells (Amelia J. et. al., 2012.).

Nanomaterials may offer a way to treat cancer without doing too much damage to healthy tissue. The weakness isn't really a property of the tumors themselves but of the blood vessels that feed them. The pores in normal blood vessels are just 2–6 nm in size. Nanoparticles between about 10 and 300 nm in diameter are just the right size to pass through the gaps in the blood vessels supplying tumors but don't significantly penetrate healthy tissue. By loading the particles with chemotherapy drugs -established cancer killers- one can, at least in principle, deliver the drugs to tumor cells without damaging healthy cells. Figure 1.7 illustrates the process.

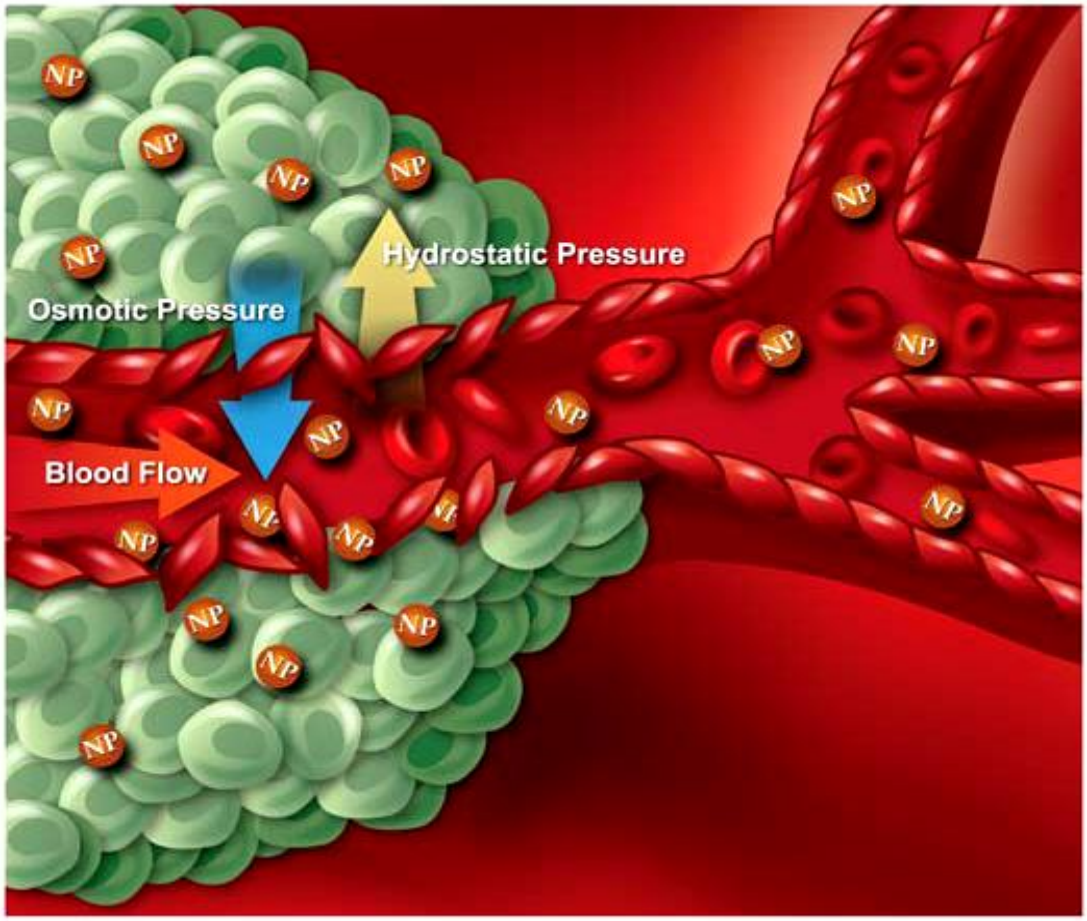

Figure 1.7. Image of the process of Enhanced Permeability and Retention effect

Beyond size, one has to consider the surface properties of a cancer nanomedicine. Surfaces are extremely important at the nanoscale because surface-to-volume ratios are so high. It's convenient to think about nanoparticles in terms of two fundamental components: the core, which doesn't interact with the environment, and the surface layer or "corona," which does. Most cell membranes have a net negative charge, so nanoparticles with cationic coronas may have an easier time getting into cells to deliver their payload.

Nanomedicines must be thoroughly characterized because their properties can vary from batch to batch even when they're made under carefully controlled conditions. Preclinical physicochemical characterization of a nanomedicine includes measurement of size and shape, surface chemistry, and state of aggregation or agglomeration. Nanomedicine characterization is often complicated by the polydispersity of samples, so

it can be necessary to measure the same quantity with multiple methods, such as electron microscopy and light scattering for size, to gain a detailed understanding.

To help get nanotech cancer treatments ready for clinical trials, the National Cancer Institute makes the services of its Nanotechnology Characterization Laboratory (NCL) available to anyone who has developed a nanotech cancer treatment and has demonstrated preliminary proof of concept. The NCL conducts physicochemical characterization and performs nanomaterial safety and toxicity testing in vitro and in laboratory animals. It works closely with the FDA and NIST to devise experiments that are relevant to nanomaterials, validate the tests on a variety of nanomaterial types, and disseminate its methods to the nanotech and cancer research communities. To date, the NCL has evaluated more than 250 nanoparticles intended for medical applications. (Jennifer, H. G., 2012).

1.4. Chitosan

Chitosan, a material of choice for developing micro or nanoparticles, is a natural biopolymer consisting of β-1 → 4 linked 2-amino-2-deoxy-glucopyranose(GlcN) and 2-acetamido-2-deoxy- β -d-glucopyranose (GlcNAc) residues, manufactured commercially on a large scale by alkaline N-deacetylation of chitin, an abundant biopolymer isolated from the exoskeleton of crustaceans, such as crabs and shrimps (Antonio, R. et al., 2013).

Chitosan has many advantages, namely: it has the ability to control the release of active agents; it allows synthesis without the use of hazardous organic solvents since it is soluble in aqueous acidic solution; it is a linear polyamine containing a number of free amine groups that are readily available for cross linking; its cationic nature allows for ionic cross linking with multivalent anions; it has muco-adhesive character, which increases the residual time at the site of absorption; and so on. Chitosan is known to have a low toxicity and immunogenicity and be biocompatible and degradable by enzymes (Hıtesh, J. et al., 2013).

Chitosan nanoparticles are drug carriers with wide development potential and have the advantage of slow/controlled drug release, which improves drug solubility and stability, enhances efficacy and reduces toxicity (Shi, X. Y., Fan, X. G., 2002). As a

new drug delivery system, they have attracted increasing attention for their wide applications in, for example, loading protein drugs, gene drugs, and anticancer chemical drugs, and via various routes of administration including oral, nasal, intravenous and ocular (Wang et al., 2011). Hydrophilic nanoparticles based on CS receive currently increasing interest as they could control the rate of drug release, prolonging the duration of the therapeutic effect, and deliver the drug to specific sites in the body (S. Papadimitriou et al., 2008).

To date, there have been a variety of reports on the preparation of CS particles. Ohya et al. prepared CS particles with mean dimensions from 250 to 300 nm using a water-in-oil emulsion method. This method involved ultrasonication of a solution of CS in acetic acid mixed with toluene followed by chemical cross-linking of the CS particles with glutaraldehyde. Ultrasonication and emulsification techniques have also been employed to prepare CS-alginate particulate systems. The mean diameter of the particles varied from 450 nm to 8 μm.

Alonso et al. reported the use of an ionic gelation method to prepare CS-NPs. (Hong, Z., 2004). This procedure is based on reversible crosslinking by electrostatic interaction (between protonized NH_3 and an anion such as tripolyphosphate), (D. R. Nogueira et al., 2013) when it comes in contact with specific polyanions due to the formation of inter and intra-molecular cross-linkages mediated by these poly-anions, (S. Papadimitriou., 2008) instead of chemical crosslinking. It avoids the potential toxicity of reagents and the possibility of damaging the drugs, especially with biological agents (D. R. Nogueira et al., 2013) and permits a satisfactory encapsulation capacity, mass production, and easy control of particle size (C-W. Chou et al., 2013).

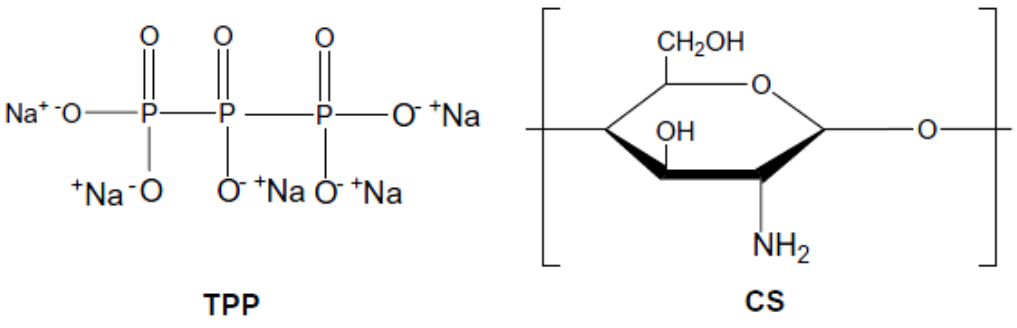

Figure 1.8 Image of chemical structure of chitosan (CS) and tripolyphosphate (TPP)

Bodmeier et al. (Bodmeier, Chen, & Paeratakul, 1989) was the first to report the ionotropic gelation of CS with tripolyphosphate (TPP) for drug encapsulation while Alonso et al. developed CS nanoparticles with the addition of a solution containing TPP into an acidic phase (pH 4–6) containing CS (S. Papadimitriou., 2008).

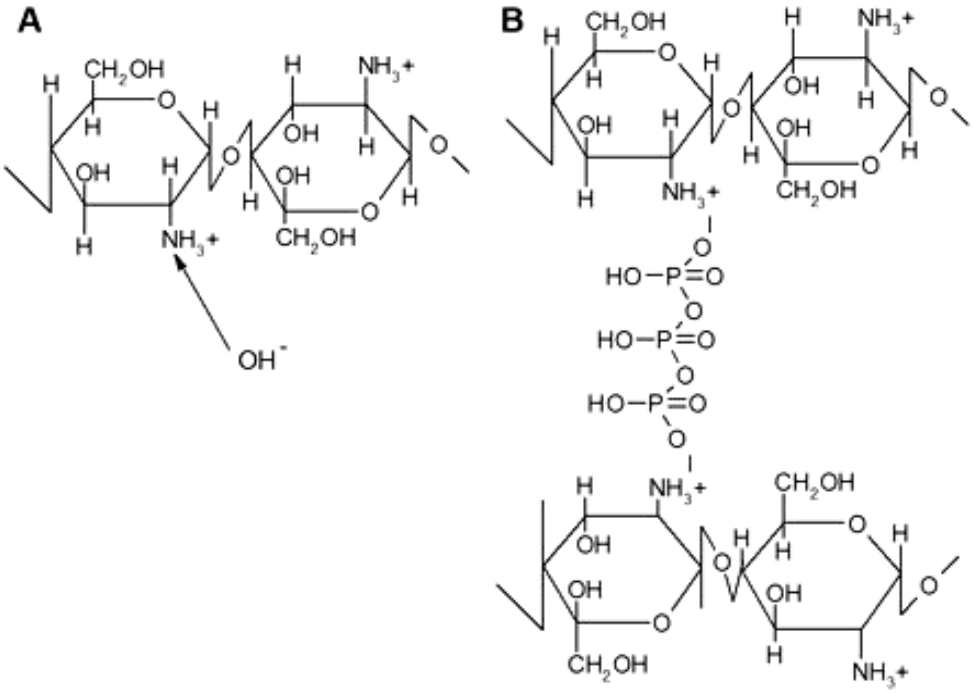

Figure 1.9 Image of interaction of chitosan with TPP (a) deprotonation, (b) ionic cross-linking (D. R. Bhumkar et al., 2002)

The nanoscopic size of this carrier system allows interactions with cellular membranes, subcellular organelles, passing through microvasculature, and may reduce immunogenicity by avoiding reticuloendothelial uptake (C-W. Chou et al., 2013).

1.5. Aim of The Study

Mediterranean diet's health benefit effects are attributed to the high consumption rate of olive and olive products in these areas. Dietary agents present in olive products, such as polyphenols, are responsible for these protective effects due to

their antioxidant activity, which is related to the development of atherosclerosis and cancer.

From this perspective, aim of our study is to investigate the anticancer effect of olive leaf extract, rich in polyphenols, loaded nanoparticles against lung and breast cancer and to synthesize not only cytotoxic anticancer drug for cancerous cells but also biocompatible material for biomedical applications. Thus, extraction of olive leaf was performed firstly. After characterization studies, extract was immobilized to chitosan and olive leaf extract loaded chitosan nanoparticles were synthesized by ionotropic gelation mechanism.

Chitosan was used as drug carrier in our study to synthesize nanoparticles that enhance the effect of olive leaf extract on cancerous cells. The reason of using chitosan is related to its strong potential for application in such areas with its advantage of slow/controlled drug release, being capable of passing through biological barriers in vivo (such as the blood–brain barrier) and delivering drugs to the lesion site to enhance their efficacy.

Investigation of anticancer effects of olive leaf extract loaded chitosan nanoparticles was performed by measuring the IC_{50} value using MTT assay against MCF-7 and A549 cell lines. To determine if the olive leaf extract loaded chitosan nanoparticles have cytotoxic effect on healthy cells or not, MTT assay was performed on BEAS 2B cells, too. Apoptosis rate and cell cycle analysis were performed to determine the effect of different concentration of olive leaf extract loaded chitosan nanoparticles, chitosan nanoparticles and olive leaf extract.

Besides this, each of two cell lines were compared with the effect of olive leaf extract loaded chitosan nanoparticles. Additionally, to take cell images, optical microscopy was used. With this method, images of MCF-7 and A549 as a control and applied with olive leaf extract loaded chitosan nanoparticles, chitosan nanoparticles, olive leaf extract and chitosan were obtained.

CHAPTER 2

MATERIALS AND METHODS

2.1. Materials

Olive leaves used for extraction in our study were obtained from *"Zeytincilik Araştırma Enstitüsü, İzmir"* and extraction studies were performed at laboratory of Oğuz BAYRAKTAR in Chemical Engineering Depertment, Izmir Institue of Technology.

Chitosan (CS) and sodium tripolyphosphate (TPP) used for nanoparticle synthesis were obtained from Sigma-Aldrich. Some important properties of compounds can be seen in Table 2.1.

Table 2.1. Some properties of chitosan and sodium tripolyphosphate

	CHITOSAN	**TPP**
Molecular Formula		$Na_5P_3O_{10}$
Molar Mass	Medium Molecular Weight, 480,000 Da	367.864 g/mol
Solubility	Soluble in dilute aqueous acid	14.5 g/100 mL (25 °C) in water
Appearence	Powder and/or Chips	White powder

Chemicals, solutions and some materials that are necessary in cell culture studies were obtained from Biotechnology and Bioengineering Research and Application Centre, Izmir Institue of Technology.

Throughout this study, all the analyses were carried out at least duplicate and mean values are reported. Detailed list of used chemicals, buffers, solutions and their compositions are presented in Appendix A and Appendix B.

2.2. Methods

Extraction and characterization of olive leaf extract were carried out according to D. Bayçın et al. (2007) procedures.

Synthesizing and characterization of chitosan nanoparticles (CS-NPs) and olive leaf extract loaded chitosan nanoparticles (OLE-CS-NPs) were carried out according to the B. Hu et. al. (2008) procedures with some modifications.

Proliferation of cell lines and in vitro cytotoxicity studies were carried out according to the Mosmann T. (1983) procedures. Cell cycle and cell apoptosis studies were carried out according to the Çakmak, Ö.Y (2011) procedures.

2.2.1. Chemical Studies

2.2.1.1. Extraction of Olive Leaves

Collected olive leaves were washed with deionized water and then dried at 37 °C for 3 consecutive days. The dried leaves were powdered and extracted in 70% ethanol aqueous solution for 2 h at 25 °C. The solvent of the extracted medium was removed by using rotary evaporator at 38 °C, 120 rpm rotation under vacuum. Then, the solvent-free olive leaf extract was dried using a freeze-dryer system at -52 °C and 0.2 mbar, and it was stored in light-protected glasses until further use in adsorption studies.

2.2.1.2. Characterization of Olive Leaf Extract

2.2.1.2.1. Determination of Total Phenolic Compound Content

Total phenolic compound content in olive leaf extract was determined using the Folin-Ciocalteus method (Bayçın et al. (2007). Folin reagent was diluted from the stock solution at 1:10 ratio. Spectrometric analysis was repeated three times for olive leaf extract. The extract containing phenolic compounds was diluted with distilled water.

Diluted solutions were vortexed and 20 µL sample were plated in 96-well plate. 100 µL of Folin reagent was added into each well. After 2.5 min., 80 µL of 7% Na_2CO_3 was added into each solution and mixed. After 1 h., the intensity of green color of each solution was measured by spectrometer (Thermo, Varioskan Flash, U.S.A.) at 725 nm. The results are expressed as miligrams of gallic acid equavelents per gram of dry olive cake (mg of GAE/g).

2.2.1.2.2. Determination of Total Antioxidant Capacity

To obtain total antioxidant capacity, Trolox Equivalent Antioxidant Capacity (TEAC) assay was performed. The method is based on the ability of antioxidant molecules to quench the long-lived $ABTS^{\cdot+}$, a blue-green chromophore with characteristic absorption at 734 nm, compared with that of Trolox, a water-soluble vitamin E analog. The addition of antioxidants to the preformed radical cation reduces it to ABTS, determining a decolorization.

A stable stock solution of $ABTS^{\cdot+}$ was produced by reacting aqueous solution of ABTS with $K_2S_2O_8$ solution at 1:1 ratio and allowing the mixture to stand in the dark at room temperature for 12–16 h before use. At the beginning of the analysis day, an $ABTS^{\cdot+}$ working solution was obtained by the dilution in ethanol of the stock solution to an absorbance of 0.70±0.02 AU at 734 nm, verified by spectrometer (Thermo, Varioskan Flash, U.S.A.), and used as mobile phase in a flow-injection system, according to Pellegrini et al. (2003) Results were expressed as TEAC in mmol of Trolox per kg (solid foods and oils) or per L (beverages) of sample.

2.2.1.2.3. Analysis of Total Phenolic Compounds

To obtain percent amount of phenolic compounds found in olive leaf extract, HPLC analysis was performed. The HPLC equipment used was a Hewlett-Packard Series HP 1100 equipped with a diode array detector. The stationary phase was a C18 LiChrospher 100 analytical column (250 mm×4 mm i.d.) with a particle size of 5 mm thermostated at 30 ºC. The flow rate was 1 mL/min and the absorbance changes were monitored at 280 nm. The mobile phases for chromatographic analysis were: (A) acetic

acid/water (2.5:97.5) and (B) acetonitrile. A linear gradient was run from 95% (A) and 5% (B) to 75% (A) and 25% (B) during 20 min; it changed to 50% (A) and (B) in 20 min (40 min, total time); in 10 min it changed to 20% (A) and 80% (B) (50 min, total time), after reequilibration in 10 min (60 min, total time) to initial composition. Oleuropein in OLE was identified by comparing its retention times with the corresponding standards. Coumarin was used as an internal standard for the quantification of oleuropein and rutin. Other standards were used only for identification of these compounds in OLE.

2.2.1.3. Synthesizing of Chitosan Nanoparticles

0.5% CS was dissolved in 1% (w/v) acetic acid solution with shaker at 115 rpm until the solution was transparent. The pH of solution was adjusted to 5.0 with 3M NaOH. The aqueous solution of TPP was obtained as 0.1%. As a consequence of the addition of TPP solution to CS solution with stirring at room temperature by shaker, the formation of CS-TPP nanoparticles started spontaneously via the TPP-initiated ionic gelation mechanism. TPP solution was mixed with CS solution for 1h. After stirring with TPP, the solution was centrifugated for 30 min. at 13500 rpm. The nanoparticle suspensions were immediately subjected to further analysis and applications and the supernatant was used for further characterization analysis. Freeze-dried nanoparticles were stored at 4^{o}C.

2.2.1.4. Synthesizing of Olive Leaf Extract Loaded Chitosan Nanoparticles

For the preparation of CS-NPs loaded with olive leaf extract (OLE-CS-NPs), the aqueous solution of 0.25% olive leaf extract was added into CS solution 30 min. before the addition of TPP solution. Then, the same procedure with the synthesizing of CS-NPs was performed.

2.2.1.5. Optimization of Olive Leaf Extract Loaded Chitosan Nanoparticles

During the experiments, optimum conditions were choosen with the result of loading capacity of OLE into CS-NPs and the size of OLE-CS-NPs. Loading capacity of NPs was calculated as explained below:

$$\%LC=(A-B)/A\times100$$

Where, "A" is the total amount of OLE; "B" is the free amount of OLE.

2.2.1.5.1. Effect of CS-TPP Mass Ratio

To obtain the effect of CS-TPP mass ratio on synthesizing NPs, 10 different mass ratio were choosen. For this purpose, 0.5% CS was dissolved in 1% (w/v) acetic acid solution with shaker at 115 rpm until the solution was transparent. The pH of solution was adjusted to 4.3 with 3M NaOH. Then, the aqueous solution of 0.25% olive leaf extract was added into CS solution. After 30 min., the aqueous solution of TPP that has different concentration according to the choosen ratio was added into solution. Then, the same procedure with the synthesizing of CS-NPs was performed. The CS-TPP mass ratio can be seen in Table 2.2.

Table 2.2. Different mass ratios of CS and TPP

MASS RATIO	CHITOSAN	TPP
1:1	0.5%	0.5%
1:2	0.5%	1.0%
1:3	0.5%	1.5%
1:4	0.5%	2.0%
1:5	0.5%	2.5%
1:6	0.5%	3.0%
2:1	0.5%	0.25%
3:1	0.5%	0.17%
4:1	0.5%	0.125%
5:1	0.5%	0.1%
6:1	0.5%	0.08%

2.2.1.5.2. Effect of pH

To study the effect of the initial pH value of the CS solution on particle size and zeta potential, CS-TPP nanoparticles prepared with a fixed CS-TPP mass ratio of 5:1 and 5 different pH value were choosen. For this purpose, 0.5% CS solution was prepeared with 1.0% acetic acid and pH was adjusted to 4.0, 4.3, 4.6, 4.7, 5.0 with 3.0 M NaOH. Then, the aqueous solution of 0.25% olive leaf extract was added into CS solution. After 30 min., the aqueous solution of TPP was added in each solution and stirred at shaker at 115 rpm for an hour. The solution was centrifugated for 30 min. at 13500 rpm. Supernatant of the solution was used for determination of loading capacity and pellet was used for determination of nanoparticle size.

2.2.1.5.3. Effect of Incubation Time

2.2.1.5.3.1. Effect of Incubation Time of TPP

To study the effect of incubation time of TPP on particle size and zeta potential, CS-TPP nanoparticles prepared with a fixed CS-TPP mass ratio of 5:1 and pH of 0.5% CS solution was adjusted to 5.0. 0.25% OLE was added into CS solution and stirred for 30 min. Then, the aqueus solution of TPP was added into solution and stirred at shaker at 115 rpm for 15, 30, 60, 90, 120 min. The solution was centrifugated for 30 min. at 13500 rpm. Supernatant of the solution was used for determination of loading capacity and pellet was used for determination of nanoparticle size.

2.2.1.5.3.2. Effect of Incubation Time of OLE

To study the effect of incubation time of OLE on particle size and zeta potential, CS-TPP nanoparticles prepared with a fixed CS-TPP mass ratio of 5:1 and pH of 0.5% CS solution was adjusted to 5.0. 0.25% OLE was added into CS solution and stirred at shaker at 115 rpm for 15, 30, 60, 90 and 120 min. Then, the aqueus solution of TPP was added into solution and stirred at shaker at 115 rpm for 60 min. The solution was centrifugated for 30 min. at 13500 rpm. Supernatant of the solution was used for determination of loading capacity and pellet was used for determination of nanoparticle size.

2.2.1.5.4. Effect of Concentration of OLE

To study the effect of concentration of OLE on particle size and zeta potential, CS-TPP nanoparticles prepared with a fixed CS-TPP mass ratio of 5:1 and pH of 0.5% CS solution was adjusted to 5.0. Then, the aqueous solution of OLE with the amount of 0.10%, 0.25%, 0.50%, 1.00%, 1.50% and 2.00% was added into CS solution. After 30 min., the aqueous solution of TPP was added in each solution and stirred at shaker at 115 rpm for an hour. The solution was centrifugated for 30 min. at 13500 rpm.

Supernatant of the solution was used for determination of loading capacity and pellet was used for determination of nanoparticle size.

2.2.1.6. Characterization of Olive Leaf Extract Loaded Chitosan Nanoparticles

The loading capacity of nanoparticles were examined with Folin-Ciocalteu method by spectrometric analysis with Thermo, Varioskan Flash, U.S.A. The morphological characteristics of nanoparticles were examined by Nanomagnetic Instruments ezAFM on Tapping mode. The measurements of particle size of nanoparticles were performed on a Zetasizer Nano-ZS (Malvern Instruments) on the basis of dynamic light scattering (DLS) techniques. FT-IR was carried out according to the Miracle Zn-Se ATR method on a Spectrum-100 FT-IR Spectrometer (Perkin Elmer) in the range of 650-4000 cm^{-1}.

2.2.2. Molecular Biological Studies

2.2.2.1. Proliferation of Cancer and Healthy Cell Lines

MCF-7 (Michigan Cancer Foundation-7) breast cell line, BEAS 2B (human bronchial epithelial cell line) and A-549 (adenocarcinomic human alveolar basal epithelial cells) cells line were obtained from Biotechnology and Bioengineering Research and Application Centre, IZTECH. The cells were grown in Roswell Park Memorial Institute-1640 (RPMI-1640) growth medium containing 10% fetal bovine serum (FBS) and 1% gentamicine sufate in a humidified atmosphere containing 5% CO_2 at 37°C. The cells were refreshed twice a week. In order to passage these cells, whole cell suspension was taken from tissue culture flask (75 cm^2 or 150 cm^2) into a sterile falcon tube (50 mL) and then centrifuged at 800 rpm for 5 minutes at room temperature. After centrifugation, the supernatant was removed from the tube and for solving the pellet 2 mL RPMI-1640 (10% FBS and 1% Gentamicine sulfate) was addedto falcon tube. After solving, it was transferred (1 mL) into a sterile 75 cm^2 or 150

cm^2 filtered tissue culture flask and added 14 mL for 75 cm^2 flask, 24mL for 150 cm^2 flask. Then it was incubated in humidified incubator 5% CO_2 at 37°C.

2.2.2.2. Thawing the Frozen Cells

Cells (2 mL) were removed from frozen storage at -80°C and quickly thawed in a water bath at 37°C so as to acquire the highest percentage of viable cells. When the ice crystals melted, the content was immediately transferred into a sterile filtered tissue culture flask (25cm^2) containing 5-6 mL of RPMI-1640 growth medium and incubated overnight at 37°C in 5% CO_2. After incubation, cells were passaged as mentioned before.

2.2.2.3. Freezing the Cells

Cells taken from tissue culture flask were centrifuged at 800 rpm for 5 minutes at room temperature. After centrifugation, the supernatant was carefully removed and the pellet was resuspended by the addition of RPMI-1640 and 0.5 mL dimethyl sulfoxide (DMSO). Then, gentle pipetting was applied and the cell suspension was transferred to the cryogenic vials (2 mL) by labelling. At the following step, these cryogenic vials were incubated at +4°C for 1 hour and then at -20°C for 1 hour and finally lifted to freezing compartment -80°C for long-term storage.

2.2.2.4. In Vitro Cytotoxicity Study

The cytotoxicity of various concentrations of the OLE-CS-NPs, CS-NPs, OLE and CS were measured using the MTT Assay. The MTT assay measures the cell metabolic activity whereby the mitochondrial dehydrogenase enzyme of viable cells reduces the yellow tetrazolium salt, 3-[4,5-dimethylthiazol-2-yl]-3,5-diphenyl tetrazolium bromide dye (MTT), to a purple formazan crystals (Nasti et al., 2009). The absorbance of this solution can be quantified by spectrophotometer. This reduction only occurs if mitochondrial reductase enzymes are active, thus conversion is directly related to the number of viable cells.

To investigate the cytotoxic effects of OLE-CS-NPs, CS-NPs, OLE and CS against A549, MCF-7 and BEAS 2B cells, 95 µg/mL of cells were seeded in 96-well plates at a density of 1 x 10^4 cells/mL and incubated for 24h. OLE-CS-NPs and CS-NPs were dissolved in dimethyl sulfoxide (DMSO) and dilute at appropriate concentrations with the culture medium and OLE and CS were dissolved in culture medium. After 24 h, 5 µL of these compounds were added into each cell and final concentrations were 5.0, 10.0, 100.0, 400.0, 500.0, 750.0 and 1000.0 µg/mL for A549 and BEAS 2B and 25.0, 50.0, 100.0, 300.0, 500.0, 750.0 and 1000.0 µg/mL for MCF-7 cells. After incubation, 100 µg/mL of MTT (5.0 mg/mL in PBS) was added to each cell. Untreated cells were used as a control groups and cells were incubated further for 72 h in CO_2 incubator at 37 °C. After the incubation, the medium was removed and cells washed with phosphate-buffered saline (PBS). %10 MTT solution (5.0mg/ml in PBS) was prepared with RPMI respectively and after removing the growth medium from plates, 100 µL MTT solution was added to each well. After adding MTT solution, plates were incubated at 37 °C for 4 h in dark and then plates were centrifuged at 1800 rpm for 10 minutes at room temperature to avoid accidental removal of formazan crystals. After removing MTT, 100 µL DMSO was added to each well to dissolve the formazan crystals and than 96-well plates put in shaker for 15 min. Finally, the absorbance was determined using plate reader at a wavelength of 540 nm.

Cell viability was expressed as the ratio between the absorbance of cells treated with the different nanoparticles and non-treated cells as a control. The concentration inhibiting cell viability by 50% (IC_{50}) was obtained by interpolation of the cell viability curves. Three independent assays were repeated (n=3).

2.2.2.5. Cell Cycle Analysis By Flow Cytometry

In order to determine the effects of the OLE and OLE-CS-NPs on MCF-7 and A549 cell cycle, these drugs were tested by flow cytometer based on propidium iodide staining.

A549 and MCF-7 cells were cultured for the analysis and seeded onto 6-well plates in 1,98 mL growth medium at 1 x 10^5 cells/well and incubated overnight. After incubation, 20 µL OLE and OLE-CS-NPs were added to the concentration of drug

ranging from 300.0, 500, 750 and 1000.0 µg/mL for A-549 and 100, 500, 1000 µg/mL for MCF-7 cell lines. Then, these treated cells and untreated cells used as a control were continually fostered in the medium at 37°C with 5% CO_2 for 72h. After 72h, the cells were washed with PBS and treated with 500 µL trypsin. Then, cells were transferred to a falcon tube and then centrifuged at 1200×g for 10.0 min. After centrifugation, supernatants were removed and the cell pellet were solved in 1mL cold PBS and than 4mL PBS was added on ice. The cell suspension was centrifuged again and the pellet resuspended in 1mL PBS and fixed by adding 4mL -20^{o}C ethanol was added slowly during vortex and kept on ice. Fixed cells were kept at -20 ^{o}C until the analysis day.

Before analysis by flow cytometer, the cells were dyed with propidium iodide (PI). For this purpose, kept cells were centrifuged at 1200xg for 10 min at 4 ^{o}C. After removing of supernatants, cell pellets were solved in 1 mL 4 ^{o}C PBS and added 4 mL 4 ^{o}C PBS and centrifuged again at 4 ^{o}C. After centrifugation the cell pellets were solved in 200 µl 0,1 % Triton X-100 in PBS. 20µL RNase A (200 µg/ml) was added to cell suspension and cells were incubated in 37°C in 5% CO_2 for 30 min. After 30 minutes 20 µl PI (1mg/mL) was added and incubated at room temperature for 15 min. The cell cycle distribution was determined by flow cytometer (FACSCANTO, BD), and data were analyzed by ModFit software. It were collected at least 10,000 events for each sample.

2.2.2.6. Apoptosis Analysis By Flow Cytometry

Also called programmed cell death or cell suicide, apoptosis is an integral and necessary part of life cycle of organisms. In the human body, about a hundred thousand cells are produced every second by mitosis and a similar number of them die by apoptosis (Vaux, 1999). The apoptotic mode of cell death can be described as a process which plays an important role in the improvement and homeostasis of multicellular organism and in the regulation and maintenance of the cell populations in tissues upon pathological and physiological conditions (Hengartner, 2000; Jacobson, Weil, & Raff, 1997; Leist & Jaattela, 2001; Meier, Finch, & Evan, 2000).

To investigate the apoptotic effect of OLE and OLE-CS-NPs on A549 and MCF-7 cells, these drugs were tested by using Annexin V- FITC Detection Kit. 1x10^{5} cells/well

were seeded in a 6-well plate in 1,98 mL growth medium and incubated at 37°C in 5% CO_2 for 24h. After incubation, 20 µL OLE and OLE-CS-NPs were added to the concentration of drug ranging from 100, 300, 500 and 1000.0 µg/mL for both A-549 and MCF-7 cell lines. Then, these treated cells were continually fostered in the medium at 37°C with 5% CO_2 for 72h. Untreated cells were used as control groups. After incubation, the cells were taken to a falcon tube and centrifugated at 800 rpm for 5 minutes. When centrifugation finished, the pellet was dissolved in 5 mL of PBS and centrifuged again. After that, the pellet was resuspended in 200 µL of binding buffer. 2 µL of Annexin V-FITC and PI were added. The stained cells were incubated for 15 minutes at room temperature. Finally, the mixture was determined by flow cytometer (FACSCANTO, BD).

2.2.2.7. Imaging Of Optical Microscopy

A549, BEAS 2B and MCF-7 cells were seeded onto 96-well plates for imaged of optical microscopy. After waiting overnight, OLE-CS-NPs, CS-NPs, OLE and CS were added at cytotoxic concentration and incubated for 72h. And also it was prepared as control which was not given any drug. After incubation, cells were imaged by using optical microscopy (OLYMPUS-CKX41).

CHAPTER 3

RESULTS AND DISCUSSIONS

3.1. Chemical Studies

3.1.1. Characterization of Olive Leaf Extract

3.1.1.1 Determination of Total Phenolic Compound Content

Total phenol content of OLE was determined by Folin-Ciocalteu assay and results were expressed as mg gallic acid equivalent per g of extract (mg GAEq./g). Total phenol content calculations of OLE were carried out by the gallic acid calibration curve shown in Appendix. C.1. The concentration of total phenolic compounds is 0.26 mg/mL according to the absorbance of OLE at 725nm in UV-Visible Spectrophotometer. Total phenolic compound content of OLE was calculated as 260 mg GAEq/g extract.

3.1.1.2. Determination of Total Antioxidant Capacity

Olive leaf antioxidants are able to scavenge or inhibit the ABTS radical cations. This inhibition can be observed as a decrease in the absorbance values at 734 nm in UV-Visible Spectrophotometer. The percentage inhibitions of absorbance at different concentrations were calculated to be represented in Appendix C. The TEAC values of olive leaves were calculated by comparing the slope of these curves with the slope of Trolox dose-response curve given in Appendix C.

Antioxidant capacity was determined as 2.18 mmol of TEAC /g olive leaf extract. The antioxidant capacity of olive leaf extracts was calculated in many of the studies but they were not reported in terms of mmol of TEAC /gr olive leaf extract, for this reason, it was difficult to compare this result with the literature. However, Laporta

et al. (2006) reported that the antioxidant capacity of olive leaf extract and green tea extract were nearly the same and Arts et al. (2002) reported the antioxidant capacity of green tea extract as 7.3 mmol of TEAC/g of freeze dried green tea. These statements proved that our result was consistent with the literature.

3.1.1.3. Analysis of Total Phenolic Compounds

After extracting the olive leaf, sample was injected to HPLC and the chromotogram was obtained. The amount of oleuropein was calculated using the calibration curves (Appendix C.3.).

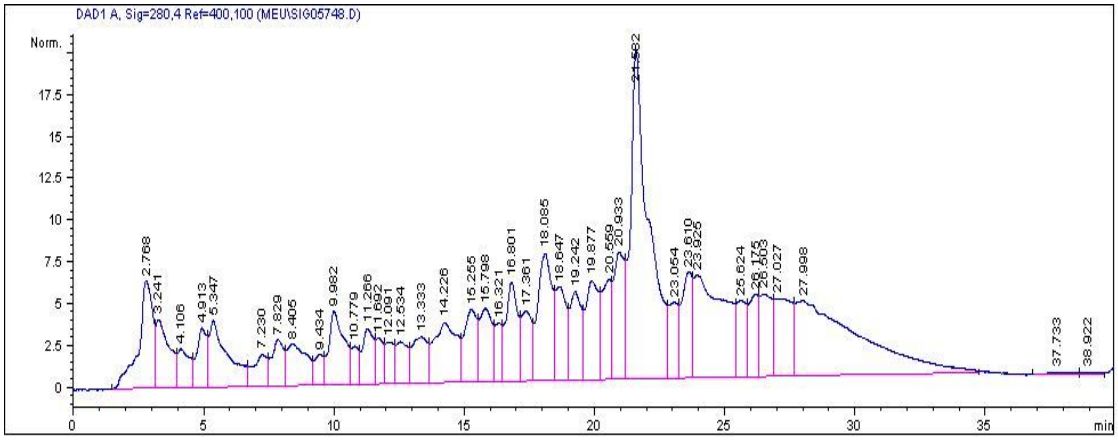

Figure 3.1. HPLC chromotogram of olive leaf extract

Figure 3.1. shows the retention time of polyphenols during the elution. The chromotogram demonstrates that the amount of other polyphenols is not as much as the oleuropein. Also, this chromatogram shows that the retention time of oleuropein is 21.592 min., respectively. Elution time of polyphenols is directly proportional to their polarity in reversed phase columns.

The area of oleuropein pick is obtained as 944.4 from the chromotogram analysis. The amount of oleuropein is 0.23 µg/mL and the percentages of oleuropein in olive leaf extract were 2.3 %, respectively.

3.1.2. Synthesizing of Chitosan Nanoparticles

The formation of particles using ionic gelation is advantageous because the process is relatively simple and mild and also avoids the use of organic solvents and high temperatures, thus allowing the successful encapsulation of fragile molecules, such as proteins (Al-Qadiet al., 2012; Berger et al., 2004; Nasti et al., 2009; Xu and Du,2003). In particular, many researchers have explored the potential pharmaceutical usage of tripolyphosphate (TPP)-chitosan complexes after Bodmeier and Pramar reported the preparation of beads by dropping chitosan into a TPP solution (Bodmeier, Chen, & Paeratakul, 1989) (Antonio R. et. al., 2013). It is important that these characteristic properties be predictably produced and easily modulated in a flexible and reliable nano fabrication process with high yield and particle stability (Q. Gan et. al., 2005). Therefore, we investigated the effects of CS-TPP mass ratio, initial pH value of CS solution, incubation time of TPP and OLE with CS solution and concentration of OLE incubated with CS solution on particle size.

3.1.2.1. Optimization of Olive Leaf Extract Loaded Chitosan Nanoparticles

3.1.2.1.1. Effect of CS-TPP Mass Ratio

To study the effects of CS-TPP mass ratio on size of OLE-CS-NPs and loading capacity of OLE into NPs, parameters are fixed as chitosan concentration 0.5%, OLE concentration 0.25%, pH of 5.0, 30 min incubation of OLE, 60 min incubation of TPP and 25^{o}C. Results are presented in Table 3.1.

Table 3.1. Effect of CS-TPP mass ratio on loading capacity of OLE and size of OLE-CS-NPs

Mass Ratio	**Loading Capacity %**	**Size (nm)**
1:1	99.52	115.5
1:2	88.34	945.2
1:3	82.65	1000.0
1:4	106.17	1730.0
1:5	81.87	751.4
1:6	62.66	2238.0
2:1	86.68	78.82
3:1	88.22	75.10
4:1	84.09	80.90
5:1	97.55	91.30
6:1	82.10	57.85

Fig 3.2. shows that there is a decrease from 99.52% to 62.66% in loading capacity of OLE into CS-NPs with the increasing amount of TPP.

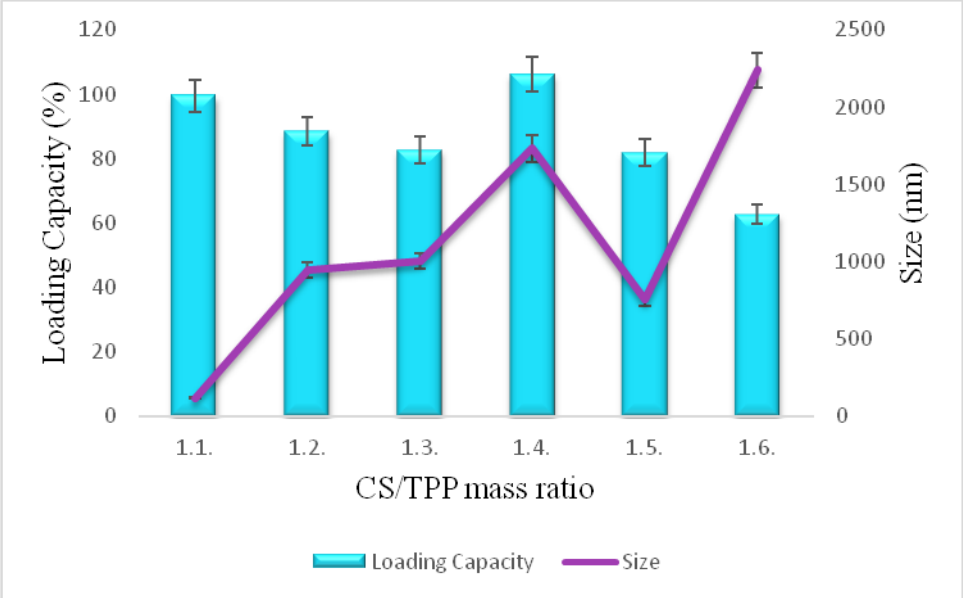

Figure 3.2. The effect of decreasing CS/TPP mass ratios on loading capacity of OLE and size of OLE-CS-NPs

Also in increasing amount of TPP conditions, the size of NPs are bigger than 10^3 nm and the aggregation is observed which is supported with the size distrubition results obtained by DLS measurements (Fig. 3.3).

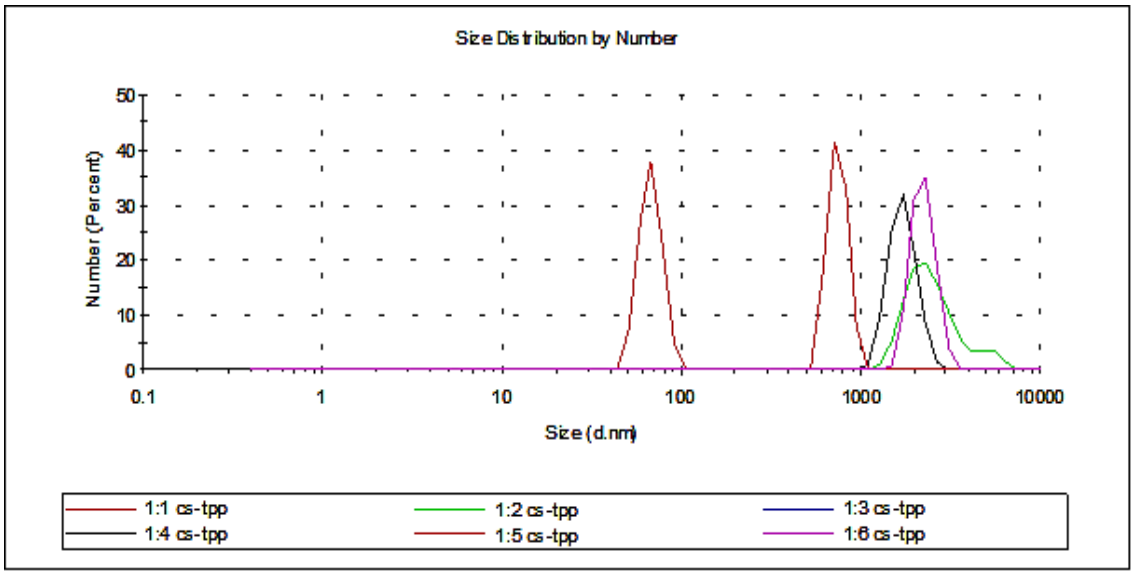

Figure 3.3. Size distrubition graph of OLE-CS-NPs with different CS-TPP mass ratios as 1, ½, 1/3, ¼, 1/5, 1/6

In addition, an increase in size of NPs is observed with the increased mass ratio of CS-TPP as seen Fig. 3.4. A similar result was reported by Gan et.al. (2005) which indicated that the particle size is increased with the increasing CS-TPP mass ratio.

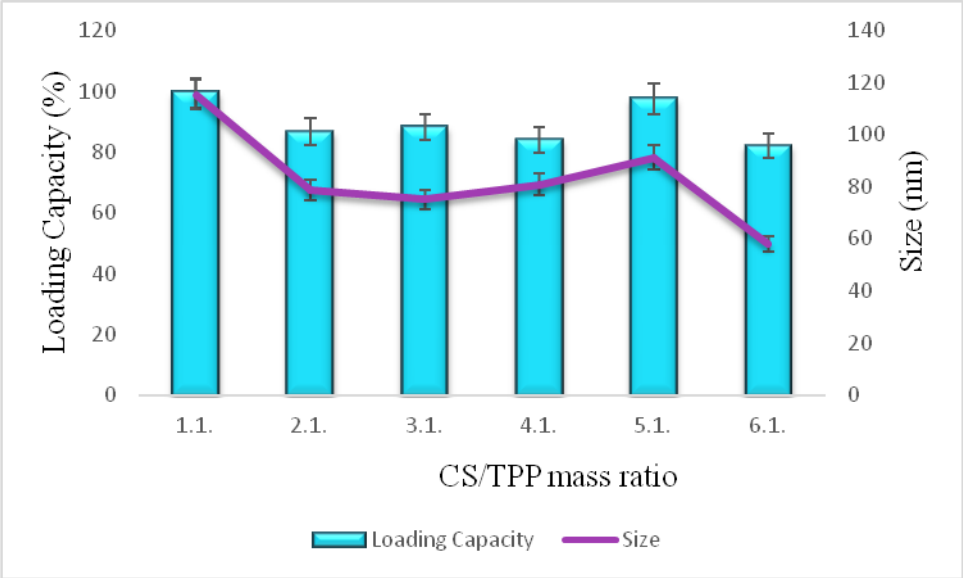

Figure 3.4. The effect of increasing CS/TPP mass ratios on loading capacity and size of NPs

In these conditions, there is no sharp difference with the loading capacity of OLE into CS-NPs.

Results are supported with the size distrubition graph obtained by DLS measurements (Fig. 3.5).

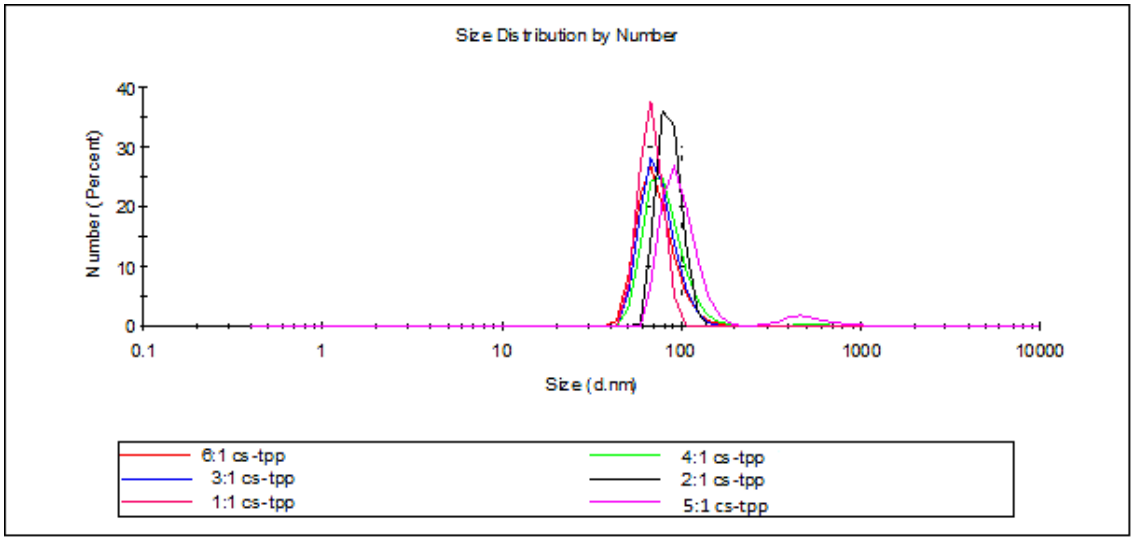

Figure 3.5. Size distrubition graph of OLE-CS-NPs with different CS-TPP mass ratio as 6, 5, 4, 3, 2, 1

By increasing the amount of TPP, the nanoparticle suspension became more and more turbid but particle aggregation occurred rapidly and drastically. It was reported that when the available quantity of TPP was high, the dominantly inter- and intra molecular crosslinks were associated with TPP which enabled NPs to form larger particles and large flocculating aggregates (chitosan/TPP mass ratio lower than 4:1) (Antonio R. et. al., 2013).

The results of these preparations and characterizations indicate that NPs prepared with a CS/TPP ratio of 5:1 turned out to be the best formulations according to the loading capacity of OLE into CS-NPs and size of OLE-CS-NPs results. Our results fit with the study of Wu et al. which showed that the formation of nanoparticles is only possible within specific, moderate concentrations of CS and TPP range of 4:1–6:1 in order to obtain a high yield of nanoparticles (Wu, Yang,Wang, Hu, & Fu, 2005; Zhang, Oh, Allen, & Kumacheva, 2004) (S. Papadimitriou., 2008).

3.1.2.1.2. Effect of pH

Chitosan is a weak base polysaccharide, having an average amino group density of 0.837 per disaccharide unit, and insoluble at neutral and alkaline pH values. In an acidic medium, the amine groups will be positively charged, conferring to the polysaccharide a

high charge density. Therefore, the surface charge density of chitosan molecules is strongly dependent on solution pH, and the ionic cross-linking process for the formation of CS–TPP nanoparticles is pH-responsive, providing opportunities to modulate the formulation and properties of the CS–TPP nanoparticles (Q. Gan et. al., 2005). Therefore, effect of pH of initial CS solution was investigated in our study.

To investigate the effect of initial pH value of CS solution on size of NPs and loading capacity of OLE, parameters are fixed as chitosan concentration 0.5% , OLE concentration 0.25%, CS-TPP mass ratio of 5:1, 30 min incubation of OLE, 60 min incubation of TPP and 25^{o}C. Results are presented in Table 3.2.

Table 3.2. Effect of initial pH value of CS solution on loading capacity of OLE into CS-NPs and size of OLE-CS-NPs

pH	**Loading Capacity (%)**	**Size (nm)**
4.0	80.05	116.5
4.3	81.87	85.54
4.6	50.77	66.90
4.7	59.00	85.08
5.0	97.55	91.3

According to the results, there is a decrease both in loading capacity of OLE into CS-NPs from 80.05% to 50.77% and size of NPs from 116.5 to 66.90 up to the pH 4.6. After pH 4.6, loading capacity is increasing up to 99.7% and size of NP is increasing up to 91.3 nm as seen in Fig 3.6. Also, there is a direct proportion between the loading capacity and size of nanoparticles during the increasing of pH value.

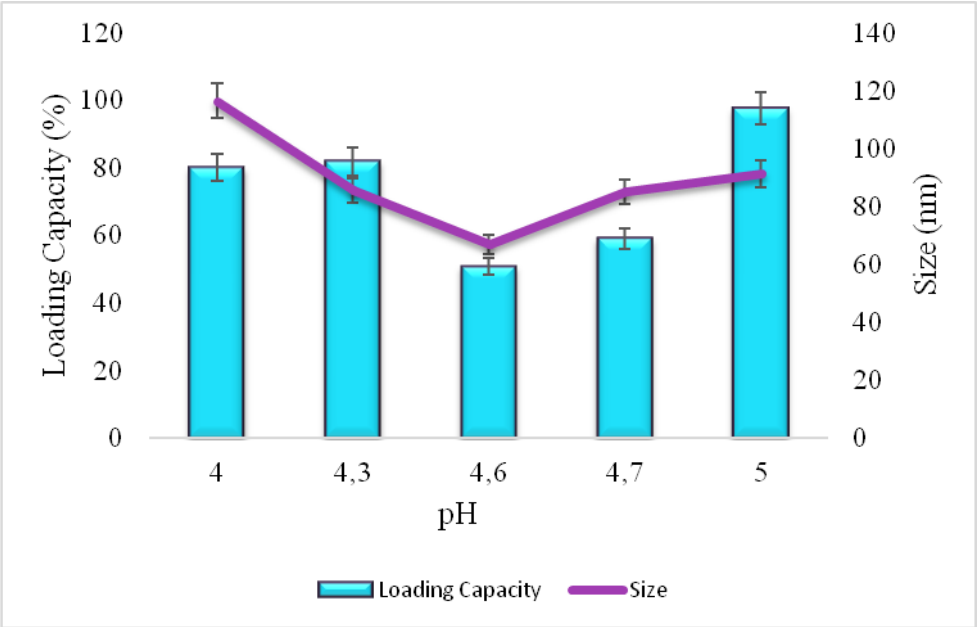

Figure 3.6. Effect of initial pH value of CS solution on size of NPs and loading capacity of OLE

The results of the effect of initial pH value of CS solution on size of nanoparticles are supported by the size distrubition graph seen in Fig. 3.7. There is an increase up to the pH 4.6 and a decrease down to the pH 5.0.

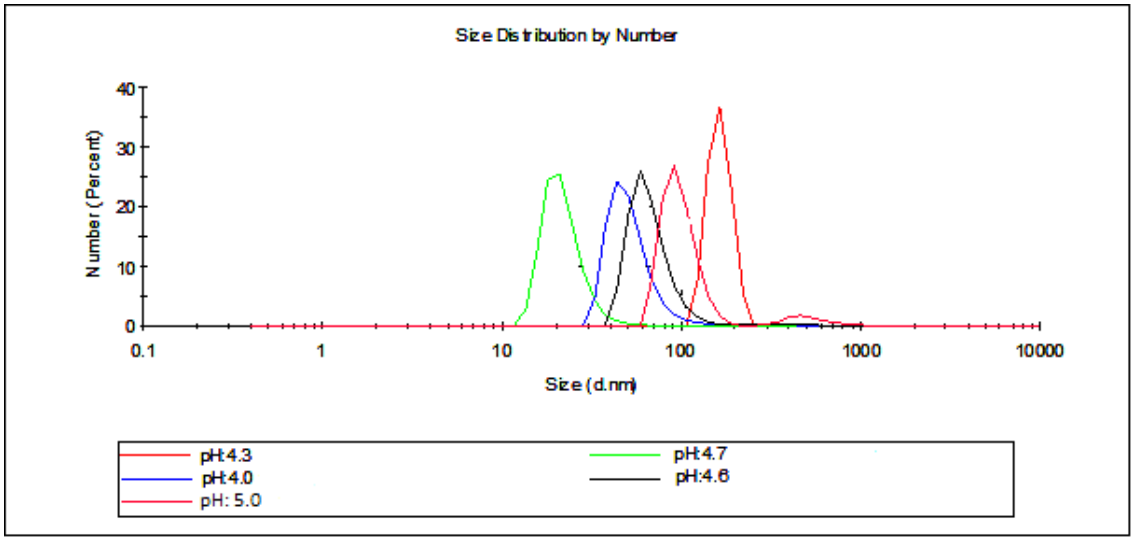

Figure 3.7. Size distrubition graph of OLE-CS-NPs with different initial pH value of CS solution

Similar results are reported by B. Hu et. al. (2008) which indicates that the particle size decreased as the pH value increased from 3.6 to 4.5. Afterward, the particle size increased as the pH value rose from 4.5 to 5.5. Also, Zhang, L et. al. indicated that below pH 4.5, the stronger protonation of the $-NH_2$ moiety led to a stronger intra molecular repulsion, making the CS chain stretch and resulting in larger nanoparticles. Up to pH 4.5, the comparatively weak interaction between CS and TPP led to the formation of larger nanoparticles (Zhang, L., Kosaraju, S. L. 2007).

3.1.2.1.3. Effect of Incubation Time

To study the effect of incubation time of OLE and TPP with CS solution on loading capacity of OLE and size of OLE-CS-NPs, parameters are fixed as chitosan concentration 0.5%, OLE concentration 0.25%, CS-TPP mass ratio of 5:1, 5.0 of pH and 25^{o}C.

3.1.2.1.3.1. Effect of Incubation Time of TPP

The most popular way to produce chitosan nanoparticles is through ionotropic gelation of chitosan with sodium tripolyphosphate (TPP), a small ion with a triple negative charge throughout the physiologically acceptable pH range. Thus, incubation time of TPP with CS solution could be an important parameter through the nanoparticle formation because of the interactions of two solutions.

To study the effect of incubation time of TPP with CS solution on loading capacity of OLE and size of OLE-CS-NPs, parameters are fixed as chitosan concentration 0.5% , OLE concentration 0.25%, CS-TPP mass ratio of 5:1, pH of 5.0, 30 min incubation of OLE and 25^{o}C. Results are presented in Table 3.3.

Table 3.3. Effect of different incubation time of TPP on loading capacity of OLE and size of OLE-CS-NPs

Time (min)	Loading Capacity (%)	Size (nm)
15'	74.66	31.74
30'	78.51	86.47
60'	97.55	91.3
90'	81.20	79.92
120'	82.44	77.10

As seen in Fig 3.8., there is an increase both in loading capacity of OLE into CS-NPs from 74.66% to 97.55% and size of OLE-CS-NPs up to 60 min incubation of TPP with CS solution. Above 60 min incubation of TPP with CS solution, there is a decrease both in loading capacity of OLE from into CS-NPs 97.55% to 82.44% and size of OLE-CS-NPs from 91.3 to 77.10 nm.

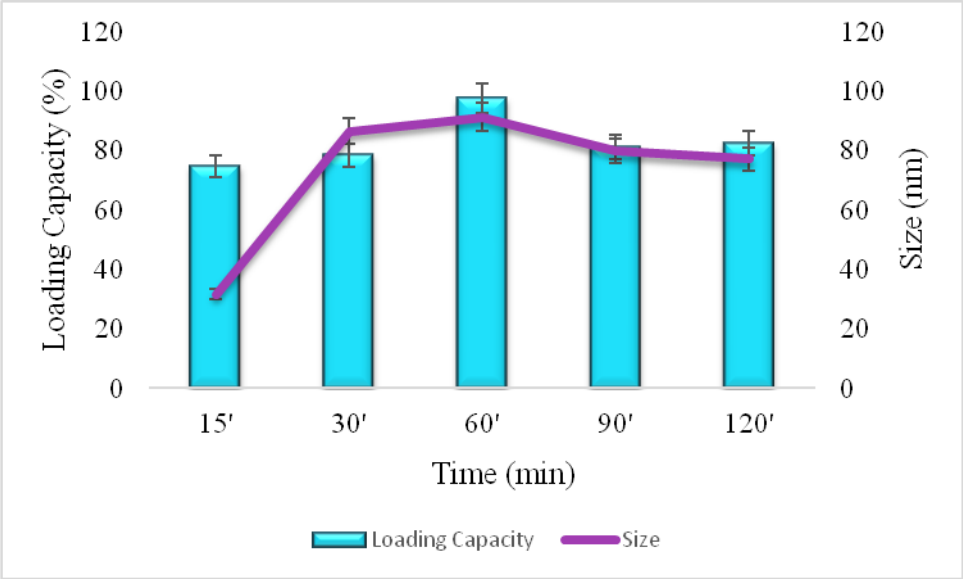

Figure 3.8. Effect of incubation time of TPP on loading capacity and size of nanoparticles

The effect of incubation time of TPP on size of OLE-CS-NPs is supported by size distribution graph obtained by DLS measurement as seen in Fig. 3.9.

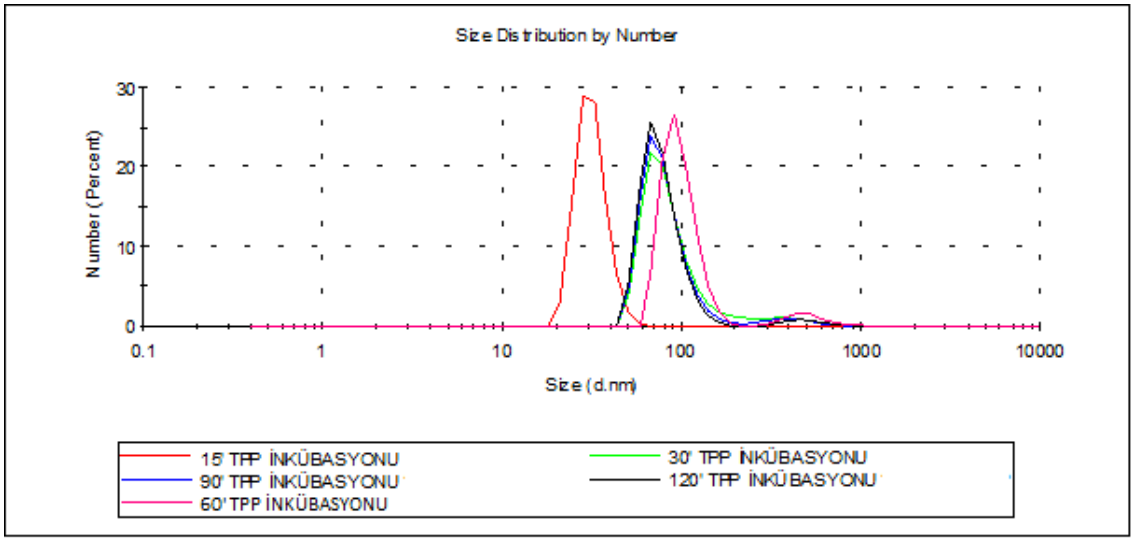

Figure 3.9. Size distribution graph of OLE-CS-NPs with different incubation time of TPP

According to the results, it can be presumed that the formation of OLE-CS-NPs should be time-dependent for the full interaction between TPP and CS. Also, it was decided that solutions of OLE and CS for studying loading capacity were gently stirred for 60 min with TPP solution to synthesize OLE-CS-NPs that has the best properties for the further studies.

3.1.2.3.1.2. Effect of Incubation Time of OLE

Chitosan is a non-toxic biodegradable polycationic polymer with low immunogenicity. It has been extensively investigated for formulating carrier and delivery systems for therapeutic macrosolutes, particularly genes and protein molecules primarily because positively charged chitosan can be easily complexed with negatively charged DNAs and proteins (Quan G. et. al., 2005). The positive charge of CS caused by the primary amino groups in its structure is responsible for its mucoadhesive properties and therefore prolonging the residual time at the absorption site (Hosseinzadeh et al., 2012). Also, it is known that the main antioxidants of virgin olive

oil are both lipophilic and hydrophilic (E, Tripoli., 2005). In the light of these information, it can be thought that the interaction time of positively CS solution and negatively OLE solution which is rich in polyphenols could be important parameter for immobilization of OLE into CS-NPs through the synthesis of NPs.

To study the effect of incubation time of OLE with CS solution on loading capacity of OLE and size of OLE-CS-NPs, parameters are fixed as chitosan concentration 0.5% , OLE concentration 0.25%, CS-TPP mass ratio of 5:1, 5.0 of pH and 25^{o}C. Results are presented in Table 3.4.

Table 3.4. Effect of different incubation time of OLE with CS on loading capacity of OLE and size of OLE-CS-NPs

Time (min)	**Loading Capacity (%)**	**Size (nm)**
15'	82.63	81.56
30'	97.55	91.3
60'	81.31	44.58
90'	79.20	51.31
120'	88.73	35.53

The highest loading capacity of OLE into CS solution obtained after the mixture of OLE and CS was gently stirred for 30 min before the addition of TPP solution. Although the size of nanoparticles are decreased, the loading capacity of OLE into CS-NPs has variability after 30 min as seen in Fig. 3.10.

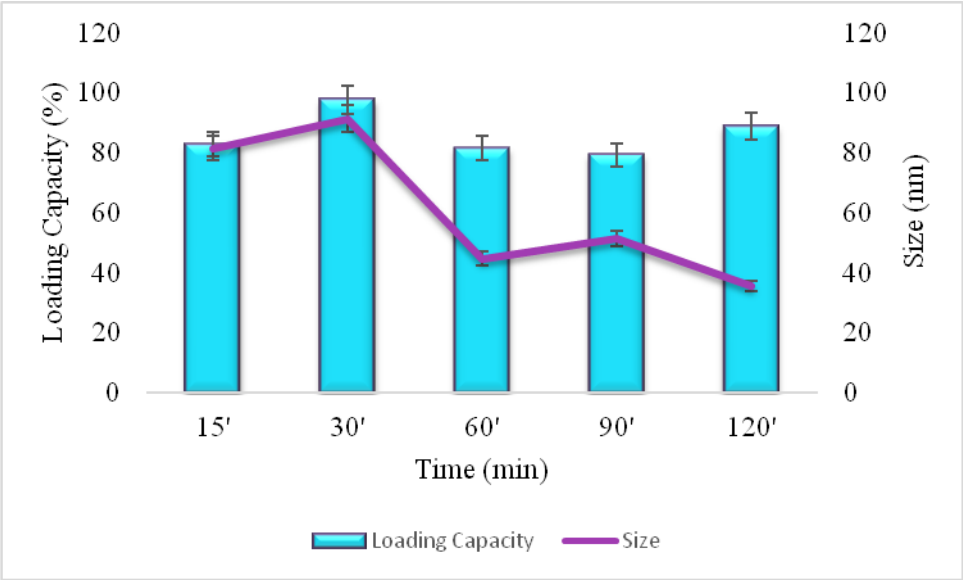

Figure 3.10. Effect of incubation time of OLE with CS on loading capacity and size of NPs

Also, a decrease in size of nanoparticles with the increasing incubation time supported by size distribution graph observed by DLS measurement (Fig. 3.11.).

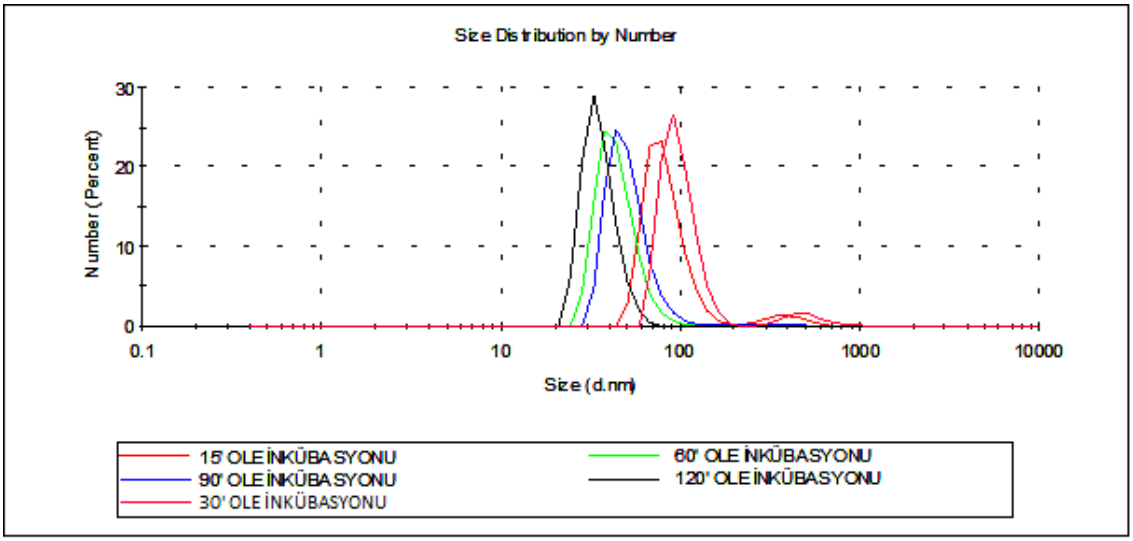

Figure 3.11. Size distribution graph of OLE-CS-NPs with different incubation time of OLE

According to these results, it can be presumed that the loading capacity of OLE is time-dependent for the full interaction between OLE and CS. All of the following

mixtures of OLE and CS for studying loading capacity were gently stirred for 30 min before the addition of TPP solution.

3.1.2.1.4. Effect of Concentration of OLE

To study the effect of concentration of OLE on loading capacity of OLE into CS solution and size of OLE-CS-NPs, parameters are fixed as chitosan concentration 0.5%, CS-TPP mass ratio of 5:1, 5.0 of pH, 30 min incubation of OLE, 60 min incubation of TPP and 25^{o}C. Results are presented in Table 3.5.

Table 3.5. Effect of different concentrations of OLE on loading capacity of OLE into CS-NPs and size of OLE-CS-NPs.

Mass of OLE (%)	**Loading Capacity (%)**	**Size (nm)**
0.10%	60.76	35.12
0.25%	97.55	91.3
0.50%	23.49	87.56
1.00%	30.47	111.0
1.50%	28.88	343.0

The loading capacity of OLE into CS solution is only increased up to 0.25% of OLE solution from 60.76% to 97.55%. Above this concentration, there is a variabile decreasing on loading capacity of OLE into CS solution as seen in Fig.3.12. It can be concluded from this result that there is an inverse proportion between the increasing concentrations of OLE and loading capacity of OLE-CS-NPs.

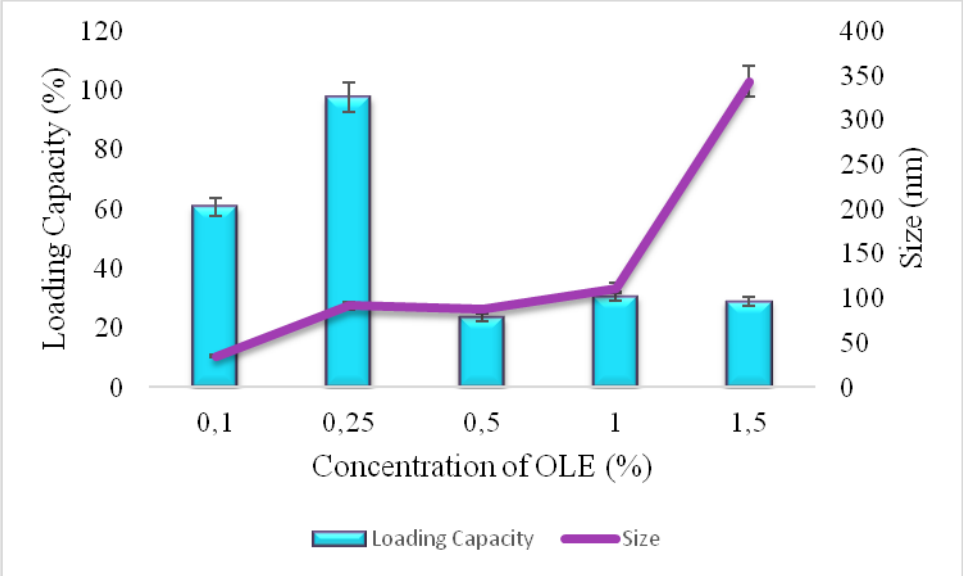

Figure 3.12. Effect of different concentrations of OLE on loading capacity of OLE into CS-NPs and size of OLE-CS-NPs

When the concentation of OLE is increased from 0.10% to 1.50%, size of OLE-CS-NPs increases from 35.12 to 343.0 nm as seen in Fig. 3.12. It can be concluded from this result that there is a direct proportion between the increasing concentrations of OLE and size of OLE-CS-NPs. This result is also supported by size distribution graph observed by DLS measurement as seen in Fig. 3.13.

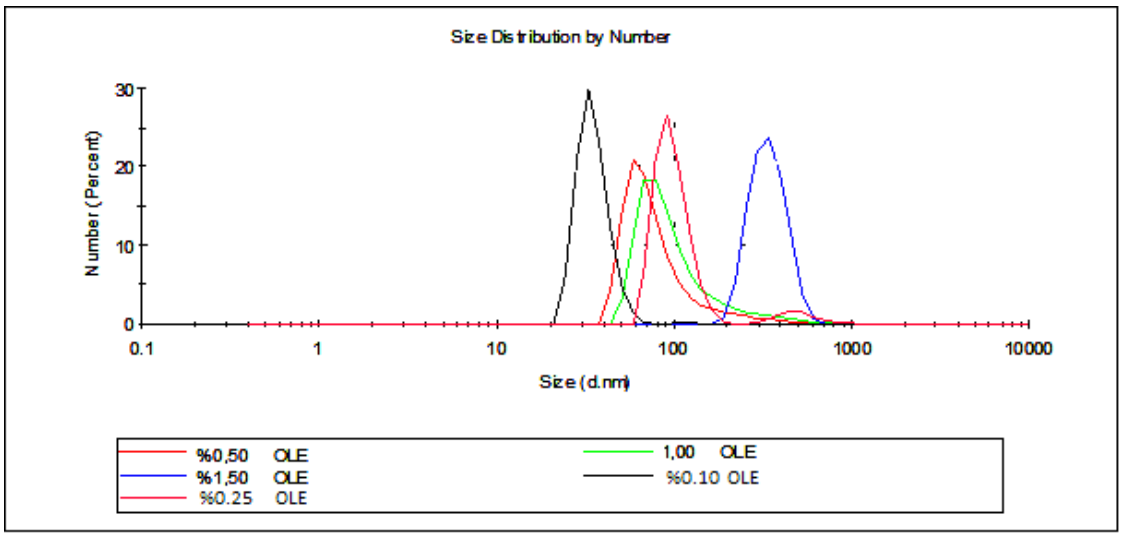

Figure 3.13. Size distribution graph of OLE-CS-NPs with different concentration of OLE

According to these results, it can be presumed that different concentration of OLE is an effective parameter on synthesizing OLE-CS-NPs. Thus, the best concentration of OLE is defined as 0.25% on synthesizing OLE-CS-NPs.

A similar result was reported by B. Hu et. al. (2008), which indicates that there is a direct proportion between the concentration of tea catechins, structure are nearly similar with olive oil polyphenols, and the size of the formed nanoparticles.

3.1.3. Characterization of Olive Leaf Extract Loaded Chitosan Nanoparticles

The measurements of particle size of nanoparticles were performed on a Zetasizer Nano-ZS (Malvern Instruments) on the basis of dynamic light scattering (DLS) techniques. Differences between OLE-CS-NPs and CS-NPs were investigated after synthesizing of nanoparticles at optimum conditions.

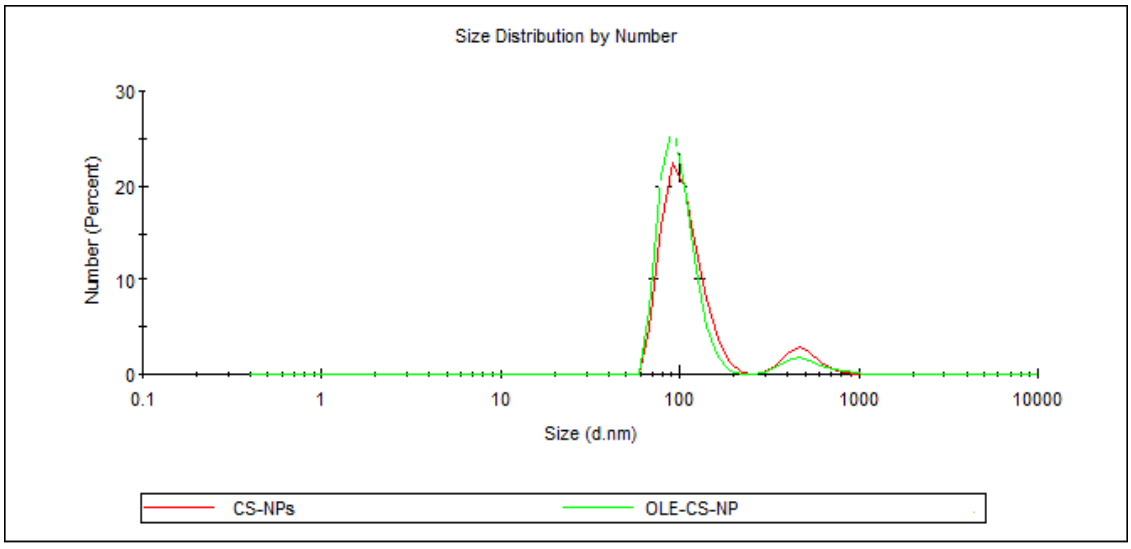

Figure 3.14. Size distrubition graph of CS-NPs and OLE-CS-NPs

Fig 3.14 indicates the differences of size distrubition between CS-NPs and OLE-CS-NPs. Interestingly, the mean diameter of the CS-TPP nanoparticles loaded with OLE was smaller than that of the corresponding CS-TPP nanoparticles, which may be attributable to a greater cross-linking density of the OLE-CS-NPs caused by the

interactions between the CS matrix and polyphenols in OLE. The same result was obtained by B. Hu et. al. (2008).

The morphological characteristics of nanoparticles were examined by Nanomagnetic Instruments ezAFM on Tapping mode. 10 µl of 0.1mM diluted nanoparticles suspension was evenly placed on a freshly cleaved silicon substrate; the surface was then air-dried at room temperature.

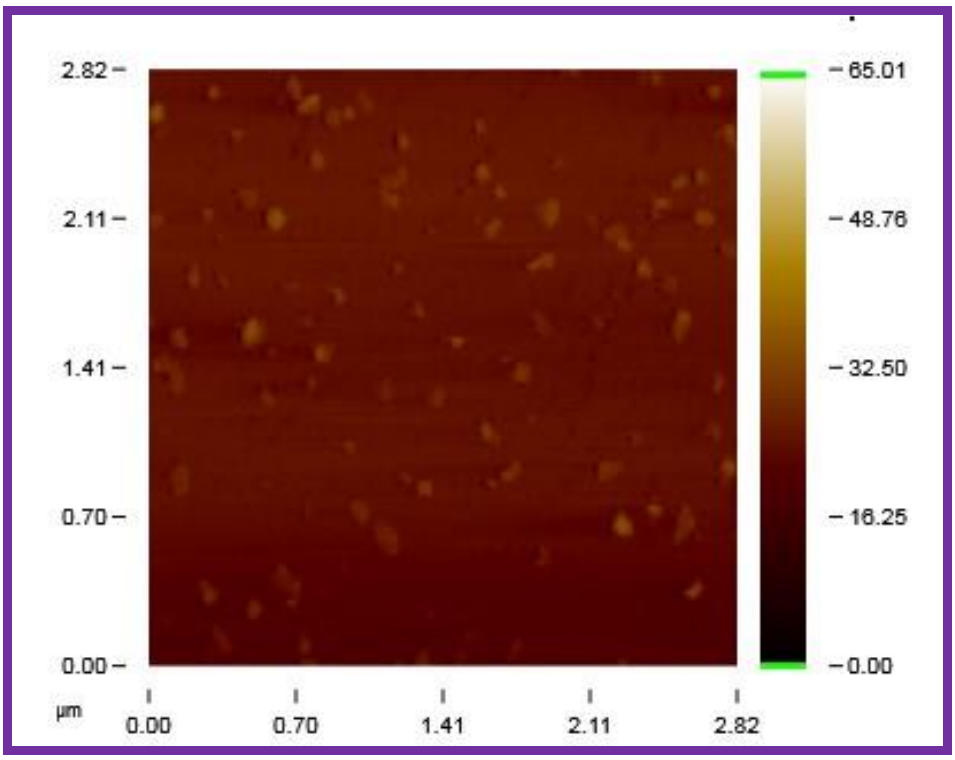

Figure 3.15. AFM image of CS-NPs

AFM image of chitosan nanoparticles is shown in Fig. 3.15. All nanoparticles were observed to be of spherical or ellipsoidal shape. Similar result was reported by J. Liu et al. (2010).

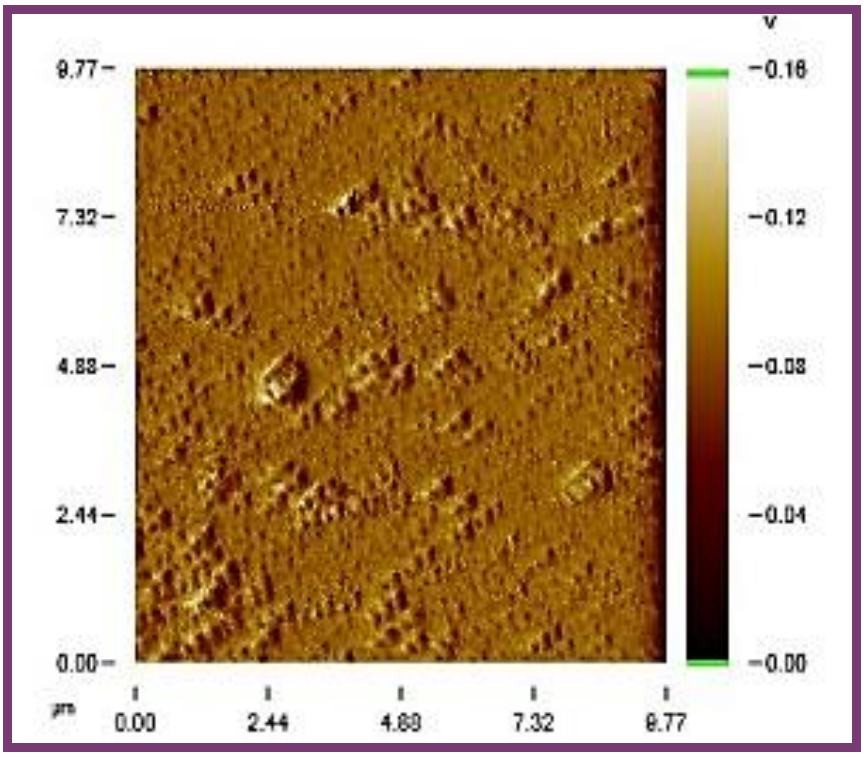

Figure 3.16. AFM image of OLE-CS-NPs

AFM image of OLE-CS-NPs is shown in Fig 3.16. According to the result, OLE-CS-NPs were spherical and when the result were compared with the AFM image of CS-NPs, lack of morfological differences on NPs is the proof of immobilization of OLE into CS solution. This result was obtained firstly by us.

FT-IR was carried out according to the Miracle Zn-Se ATR method on a Spectrum-100 FT-IR Spectrometer (Perkin Elmer) in the range of 650-4000 cm^{-1}.

FT-IR spectra of CS and OLE was shown in Figure 3.17 and 3.18.

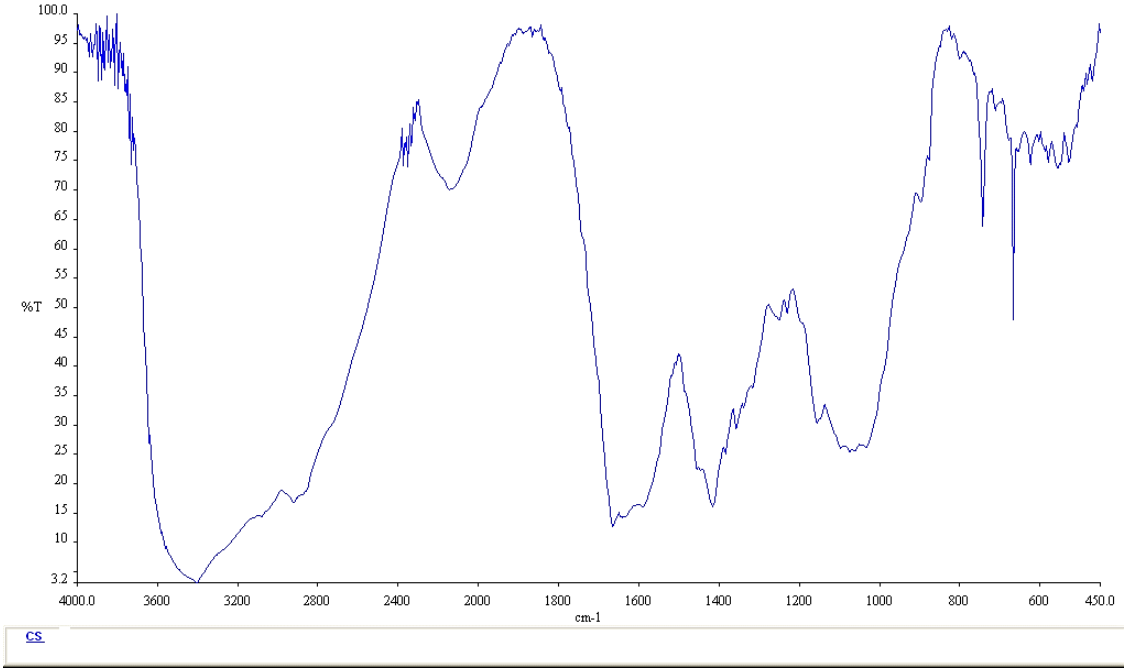

Figure 3.17. FT-IR spectra of CS

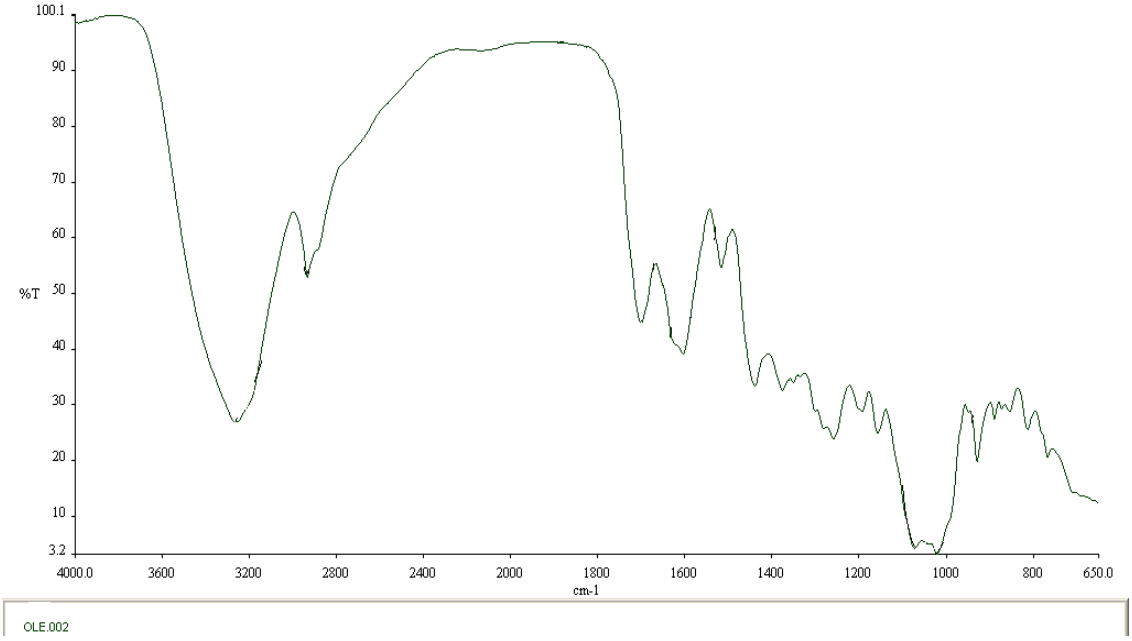

Figure 3.18. FT-IR spectra of OLE

Whereas in the FT-IR spectra of cross-linked chitosan the peak of 1655 cm^{-1} disappears, two new peaks at 1630 cm^{-1} and 1547 cm^{-1} appears when CS was incubated with OLE and TPP. The disappearance of the band could be attributed to the linkage between the phosphoric and ammonium ions. The crosslinked chitosan also showed a

peak for P = O at 1150 cm^{-1}. Xu et al, Knaul J.Z et al. (1999) and Wang X. et al. (2001) observed similar results in their study of formation of chitosan nanoparticles and chitosan film treated with phosphate.

Also, when spectra of OLE was compered with the spectra of OLE-CS-NPs, disappearence of characteristic peaks of phenolic groups of OLE was the proof of immobilization of OLE into CS matrix.

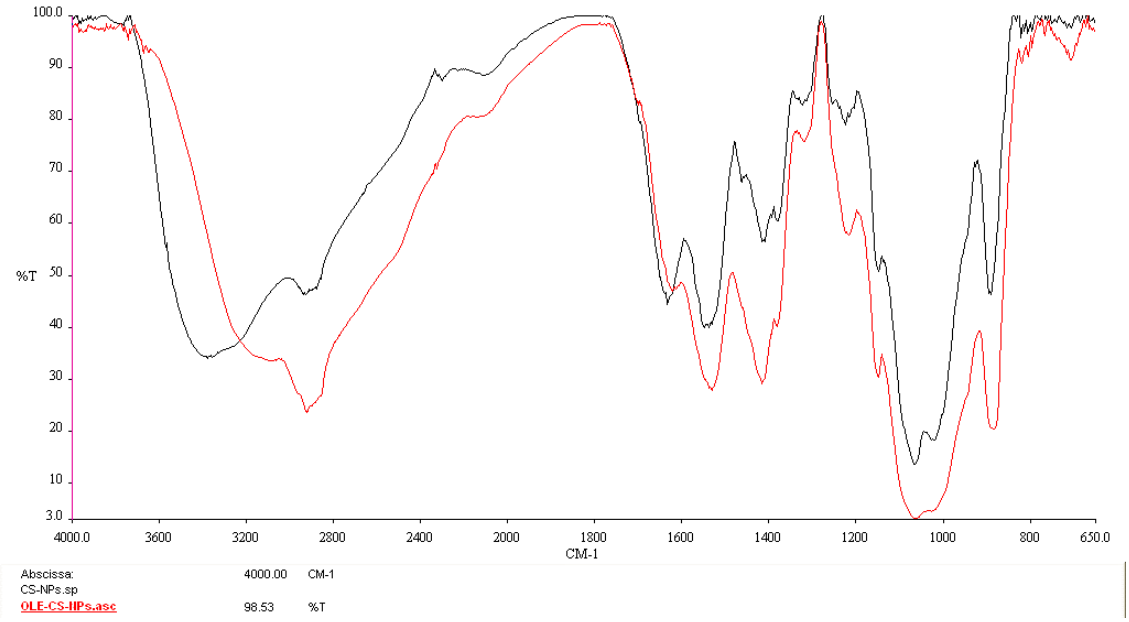

Figure 3.19. FT-IR spectra of OLE-CS-NPs and CS-NPs

The FT-IR spectra of OLE-CS-NPs and cross-linked chitosan (CS-NPs) was shown in Figure 3.19. A characteristic band at 3449 cm^{-1} was attributed to $–NH_2$ and –OH groups stretching vibration and the band for amide I at 1655 cm^{-1} was seen in the infrared spectrum of chitosan.

When the OLE-CS-NPs spectra was compared with spectra of CS-NPs, shifted bands were observed from 3449 cm^{-1} to 3336.7 cm^{-1} as a result of H-bonding that occures between the OLE and CS matrix. Stretching vibration of $–NH_2$ and –OH groups were shifted to 3154.4 cm^{-1} In addition to this situation, characteristic $–NH_2$ band disappeared. The disappearance of the band could be attributed to the linkage between the –OH groups of TPP and ammonium ions of chitosan. At 1200 cm^{-1} wavenumber, there was a new peak that belongs to the C-O streching bonds that only occures in

esters. This linkage could also be the reason of shifting through smaller frequences for whole bands when OLE was immobilized on CS-NPs.

3.2. Molecular Biological Studies

3.2.1. In Vitro Cytotoxicity Study

3.2.1.1. Cytotoxicity Study on A549 Cell Lines

The cytotoxicity of various concentrations of the OLE-CS-NPs, CS-NPs, OLE and CS were measured using the MTT Assay. Concentrations of compounds were 5.0, 10.0, 100.0, 400.0, 500.0, 750.0 and 1000.0 µg/mL and results are represented as Log[C]-Cell Viability graph.

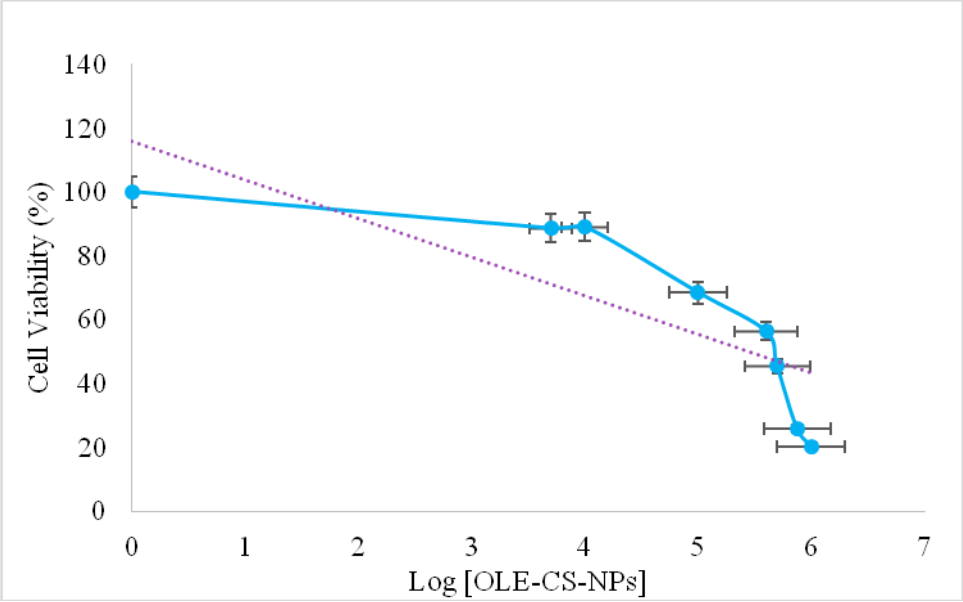

Figure 3.20. The cytotoxic effect of OLE-CS-NPs on A549 cells

To determine the cytotoxic effect of OLE-CS-NPs on A549 cells, IC_{50} value of compound was calculated from the Log [OLE-CS-NPs]-Cell Viability graph as seen in Fig 3.20. IC_{50} value of OLE-CS-NPs was found 285.0 µg/mL for A549 cells. It can be

concluded from this result that OLE-CS-NPs are very effective on A549 cell proliferation in lower doses.

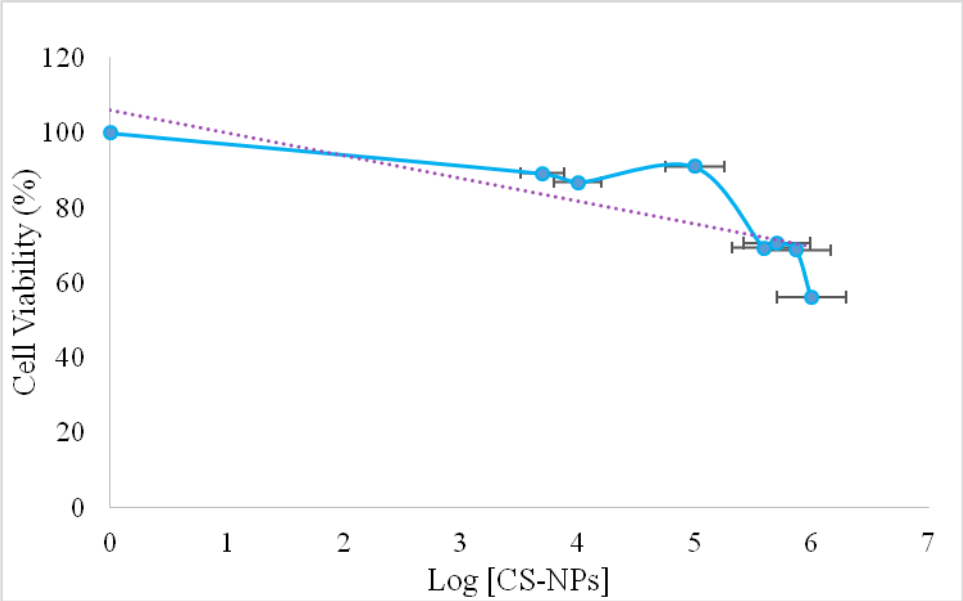

Figure 3.21. The cytotoxic effect of CS-NPs on A549 cells

To determine the cytotoxic effect of CS-NPs on A549 cells, IC_{50} value of compound was calculated from the Log [OLE-CS-NPs]-Cell Viability graph as seen in Fig 3.21. This result indicates that IC_{50} value of CS-NPs is 2146.2 µg/mL for A549 cells. Thus, it can be concluded from this result that CS-NPs are not very effective on A549 cell proliferation.

When we compare the effect of CS-NPs and OLE-CS-NPs on A549 cell proliferation, it can be said that NPs have cytotoxic effect on cells when they are loaded with OLE as we expected. Also, since CS-NPs are nontoxic for cells, they can be used as a drug carrier.

The effect of nanoparticles with OLE as a free drug and CS as a carrier are compered in Fig 3.22.

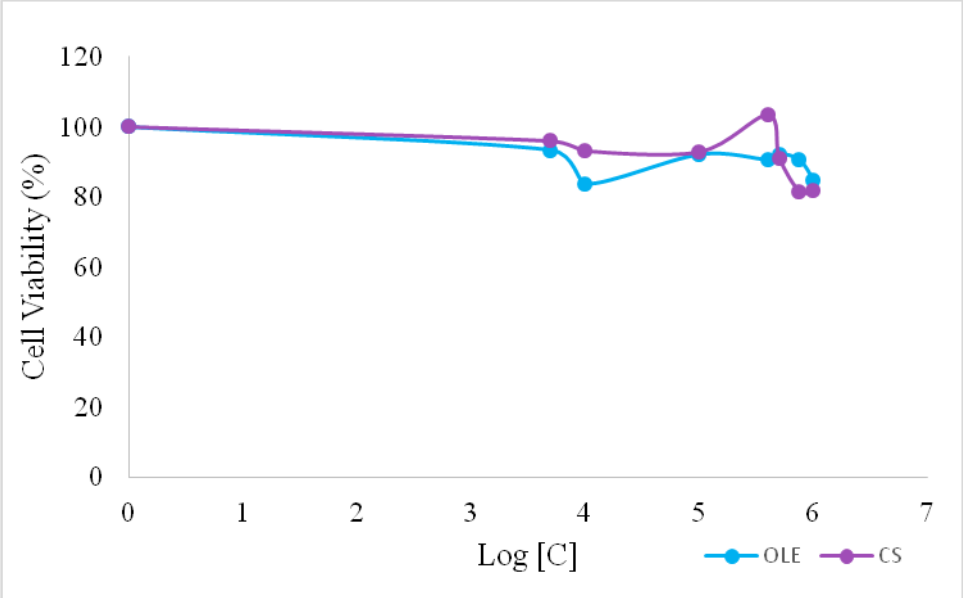

Figure 3.22. The cytotoxic effect of OLE and CS on A549 cells

According to Figure 3.22., neither OLE nor CS have cytotoxic effect on A549 cells. Cell viability is approximately 90-100 %. These results show us that olive leaf extract and chitosan have no toxic effects, as we expected.

The results indicate that OLE-CS-NPs are the most cytotoxic compounds and also these results suggested that the CS-NPs could be used for enhancing the bioavailability of OLE.

Beside this, when it was looked at previous studies, it was explained that the cytotoxicity of cationic polymers, such as poly-L-lysine, poly-L-arginine, and protamine, was directly related to their surface charge density. Although the number of primary amino groups was important, the charge density resulting from the number of groups and the three-dimensional arrangement of the cationic residues were also important contributors of cytotoxicity for a material. Chitosans with high degrees of deacetylation have extended conformation because of charge repulsion, which might allow them to bind more readily to cell membranes than coiled chitosans of lower degrees of deacetylation (Huang et al., 2004).

Up to date, not only there is no data about synthesis of olive leaf extract loaded nanoparticles but also there is no analytical epidemiological study that has evaluated the association between the components of the Mediterranean diet and lung cancer (Fortes, C. et al., 2003). Thus, the results were obtained for the first time in both studies.

3.2.1.2. Cytotoxicity Study on MCF-7 Cell Lines

The cytotoxicity of various concentrations of the OLE-CS-NPs, CS-NPs, OLE and CS were measured using the MTT Assay. Concentrations of compounds were 100.0, 200.0, 300.0, 400.0, 500.0, 750.0 and 1000.0 µg/mL for MCF-7 cells. Results are represented as Log[C]-Cell Viability graph.

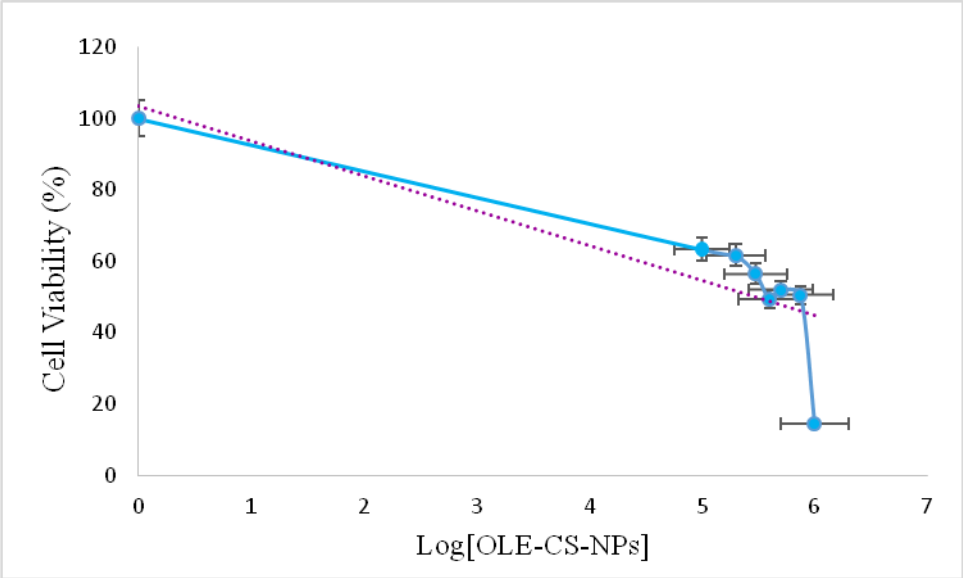

Figure 3.23. The cytotoxic effect of OLE-CS-NPs on MCF-7 cells

To determine the cytotoxic effect of OLE-CS-NPs on MCF-7 cells, IC_{50} value of compound was calculated from the Log [OLE-CS-NPs]-Cell Viability graph as seen in Fig 3.23. IC_{50} value of OLE-CS-NPs was found as 298.8 µg/mL for MCF-7 cells. It can be concluded from this result that OLE-CS-NPs are very effective on MCF-7 cell proliferation in lower doses.

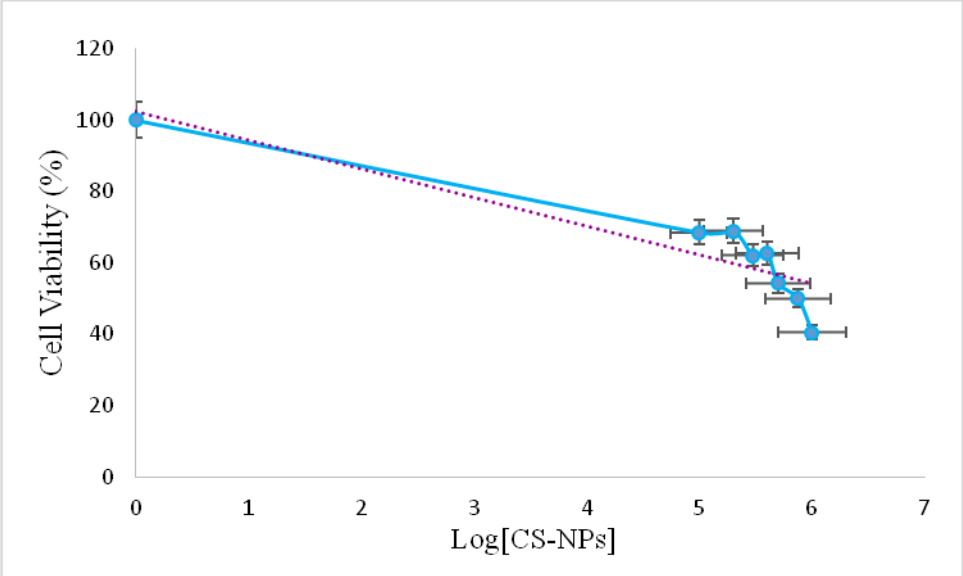

Figure 3.24. The cytotoxic effect of CS-NPs on MCF-7 cells

To determine the cytotoxic effect of CS-NPs on MCF-7 cells, IC_{50} value of compound was calculated from the Log [OLE-CS-NPs]-Cell Viability graph as seen in Fig 3.24. This result indicates that IC_{50} value of CS-NPs is 3325.0 µg/mL for MCF-7 cells. Thus, it can be concluded from this result that CS-NPs are not very effective on MCF-7 cell proliferation.

When we compare the effect of CS-NPs and OLE-CS-NPs on MCF-7 cell proliferation, it can be said that NPs have cytotoxic effect on cells when they are loaded with OLE as we expected. Also, since CS-NPs are nontoxic for cells, they can be used as a drug carrier.

The effect of nanoparticles with OLE as a free drug and CS as a carrier are compered in Fig 3.25.

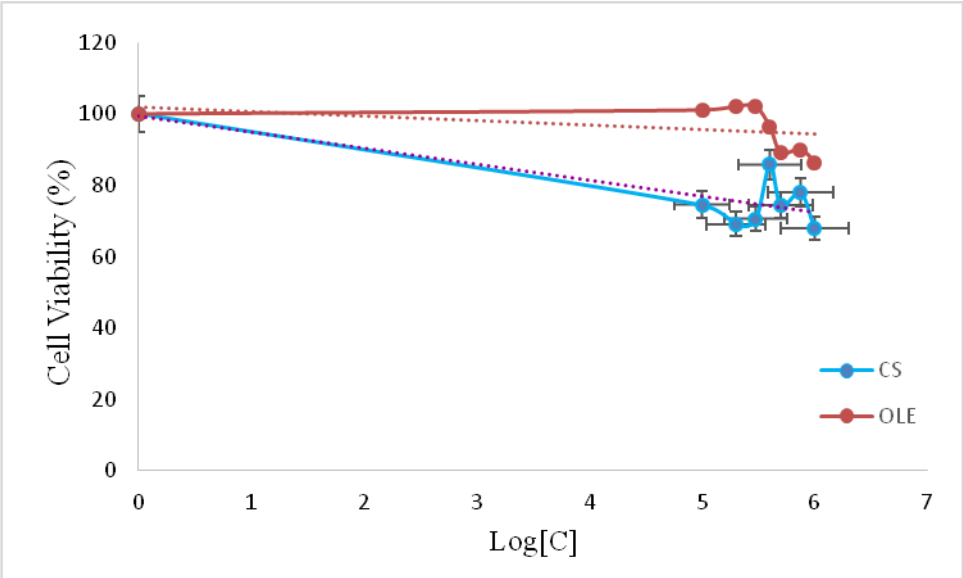

Figure 3.25. The cytotoxic effect of CS and OLE on MCF-7 cells

According to Figure 3.25., neither OLE nor CS have cytotoxic effect on MCF-7 cells. Cell viability is approximately 90-100 %. These results show us that olive leaf extract and chitosan have no toxic effects on MCF-7 cells.

It was expected that both in low concentrations of OLE (0.25%) and CS (0.50%) are not cytotoxic against MCF-7 cells. On the other hand, OLE-CS-NPs were found cytotoxic on MCF-7 cells. This result can be explained with the same reasons as mentioned in 3.2.1.1. The results indicate that OLE-CS-NPs are the most cytotoxic compounds and also these results suggested that the CS-NPs could be used for enhancing the bioavailability of OLE.

Beside this, previous studies demonstrate that there is no study that investigates the cytotoxic effect of olive leaf extract loaded chitosan nanoparticles. Chitosan is a suitable material for delivering as explained by Huang et al. (2004).

Also, our results show that OLE-CS-NPs are more effective on MCF-7 cells than olive leaf extract polyphenols. For example, Han J. et al. (2009) have showed that oleuropein or hydroxytyrosol decreased cell viability, inhibited cell proliferation, and induced cell apoptosis in MCF-7 cells for 200 µg/mL of oleuropein or 50 µg/mL of hydroxytyrosol. In addition, according to the study of Z. Bouallagui et al., it was reported that a concentration of 3000 µg/mL olive leaf extract leading to 38.4% inhibition in the MTT assay on MCF-7 cells (Z. Bouallagui et al., 2011). In the light of

these results, we can conclude that OLE is more cytotoxic when it was immobilized on CS-NPs.

3.2.1.3. Cytotoxicity Study on BEAS 2B Cell Lines

The cytotoxicity of various concentrations of the OLE-CS-NPs, CS-NPs, OLE and CS were measured using the MTT Assay. Concentrations of compounds were 5.0, 10.0, 100.0, 400.0, 500.0, 750.0 and 1000.0 µg/mL for BEAS 2B cells. Results are represented as Log[C]-Cell Viability graph.

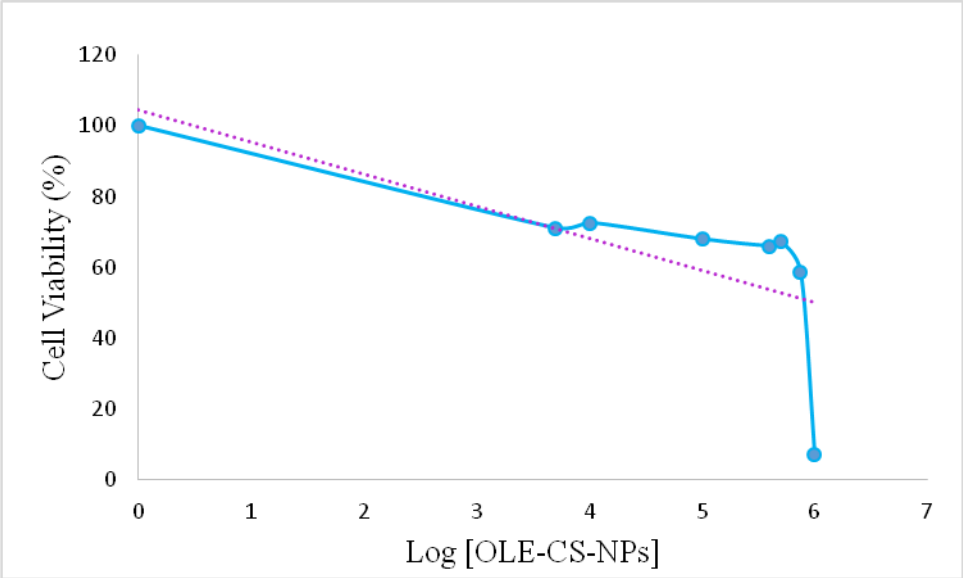

Figure 3.26. The cytotoxic effect of OLE-CS-NPs on BEAS 2B cells

To determine the cytotoxic effect of OLE-CS-NPs on BEAS 2B cells, IC_{50} value of compound was calculated from the Log [OLE-CS-NPs]-Cell Viability graph as seen in Fig 3.26. IC_{50} value of OLE-CS-NPs was found as 1015.0 µg/mL for BEAS 2B cells. It can be concluded from this result that OLE-CS-NPs are not effective on BEAS 2B cell proliferation at lower doses. Also, cytotoxic doses of OLE-CS-NPs for A549 cells are not cytotoxic for BEAS 2B cells.

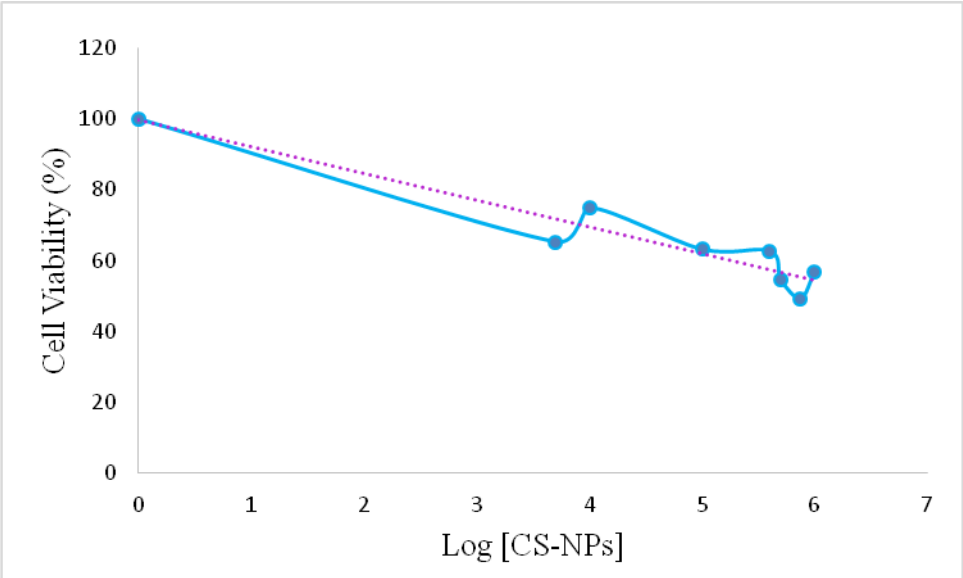

Figure 3.27 The cytotoxic effect of CS-NPs on BEAS 2B cells

To determine the cytotoxic effect of CS-NPs on BEAS 2B cells, IC_{50} value of compound was calculated from the Log [OLE-CS-NPs]-Cell Viability graph as seen in Fig 3.27. This result indicate that IC_{50} value of CS-NPs is 3745.5 µg/mL for BEAS 2B cells. Thus, it can be concluded from this result that CS-NPs are not effective on BEAS 2B cell proliferation.

When we compare the effect of CS-NPs and OLE-CS-NPs on BEAS 2B cell proliferation, it can be said that compounds have no cytotoxic effect on cells as we expected.

The effect of nanoparticles with OLE as a free drug and CS as a carrier are compered in Fig 3.28.

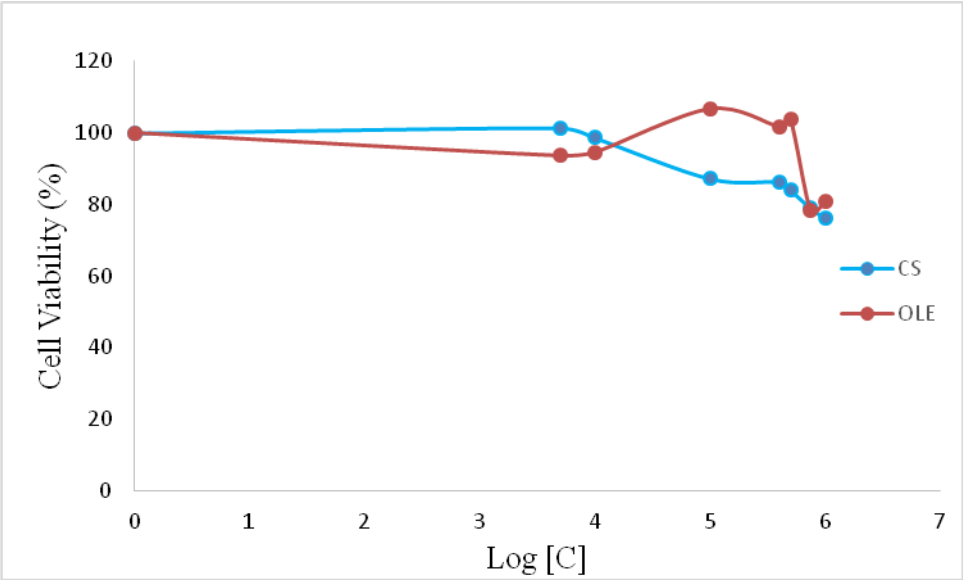

Figure 3.28. The cytotoxic effect of CS and OLE on BEAS 2B cells

According to Figure 3.28., neither OLE nor CS have cytotoxic effect on BEAS 2B cells. Cell viability is approximately 90-100 % for OLE while it is 75-85 % for CS. These results show us that olive leaf extract and chitosan have no toxic effects on BEAS 2B cells both at lowest and highest concentrations which is cytotoxic for cancerous cells.

As a result of being no cytotoxic for healthy cells, we can conclude that our compounds can be used for cancerous cells as a new therapeutic drug.

3.2.2. Cell Cycle Analysis By Flow Cytometry

The division cycle of most cells consists of four coordinated processes: cell growth, DNA replication, distribution of the duplicated chromosomes to daughter cells, and cell division. Although cell growth is usually a continuous process, DNA is synthesized during only one phase of the cell cycle, and the replicated chromosomes are then distributed to daughter nuclei by a complex series of events preceding cell division.

The M phase of the cycle corresponds to mitosis, which is usually followed by cytokinesis. This phase is followed by the G1 phase (gap 1), which corresponds to the interval (gap) between mitosis and initiation of DNA replication. During G1, the cell is metabolically active and continuously grows but does not replicate its DNA. G1 is

followed by S phase (synthesis), during which DNA replication takes place. The completion of DNA synthesis is followed by the G2 phase (gap 2), during which cell growth continues and proteins are synthesized in preparation for mitosis.

Progression between these stages of the cell cycle is controlled by a conserved regulatory apparatus, which not only coordinates the different events of the cell cycle but also links the cell cycle with extracellular signals that control cell proliferation (NCBI can be accessed, http://www.ncbi.nlm.nih.gov/books/NBK9876/).

3.2.2.1. Cell Cycle Analysis on A549 Cell Lines

To investigate the effects of free OLE and OLE-CS-NPs on cell cycle against A549 cells, the cells were treated with OLE and OLE-CS-NPs for different concentrations (10, 100, 500, 1000 μM) and untreated cells were performed as control group by using flow cytometry based on propidium iodide (PI) staining as explained in Chapter 2.2.2.5. The results are listed in Table 3.6.

Table 3.6 Cell phase composition (%) of OLE-CS-NPs and OLE effected cells for different concentrations

	OLE-CS-NPs			**OLE**		
Concentration (μM)	**G0/G1**	**S**	**G2/M**	**G0/G1**	**S**	**G2/M**
0	72.20	11.90	15.90	72.20	11.90	15.90
10	61.17	24.88	13.95	72.26	12.68	15.06
100	53.8	35.32	10.88	72.98	11.02	16
500	60.01	25.94	14.05	58.73	25.69	15.58
1000	39.03	55.3	5.67	71.47	12.69	15.84

Effects of OLE-CS-NPs on cell phase composition (%) against A549 cells are seen in Fig. 3.29. When the results were compered with cell phase composition (%) of control cells, it was seen that there was an increase in S phase from 11.90% to 55.3% with the increasing concentration of OLE-CS-NPs. With the increasing of S phase

composition, the composition of G2/M phase was decreased from 15.90% to 5.67% as expected. As a result of this decreasing, transition to the G2/M phase was blocked with OLE-CS-NPs and thus, cell growth and protein synthesis for mitosis are blocked.

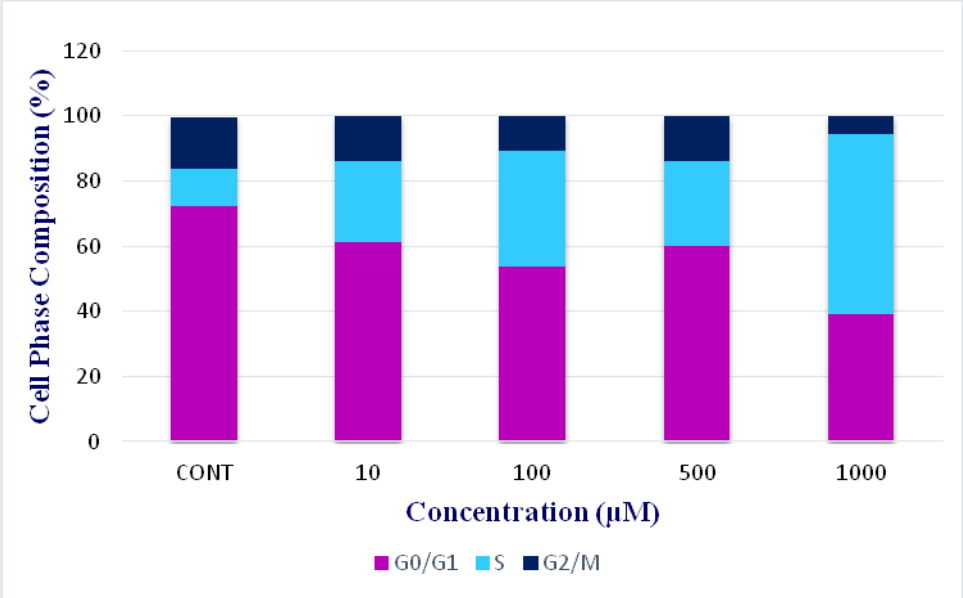

Figure 3.29. Effects of OLE-CS-NPs on cell cycle against A549 cells

Effects of OLE on cell phase composition (%) against A549 cells are seen in Fig. 3.30. When the results were compered with cell phase composition (%) of control cells, it was seen that there were no differences on cell phase composition (%) of OLE effected cells. The results were found nearly the same with control cells. It can be concluded from this result that free OLE is not effected on cell cycle of A549 cells.

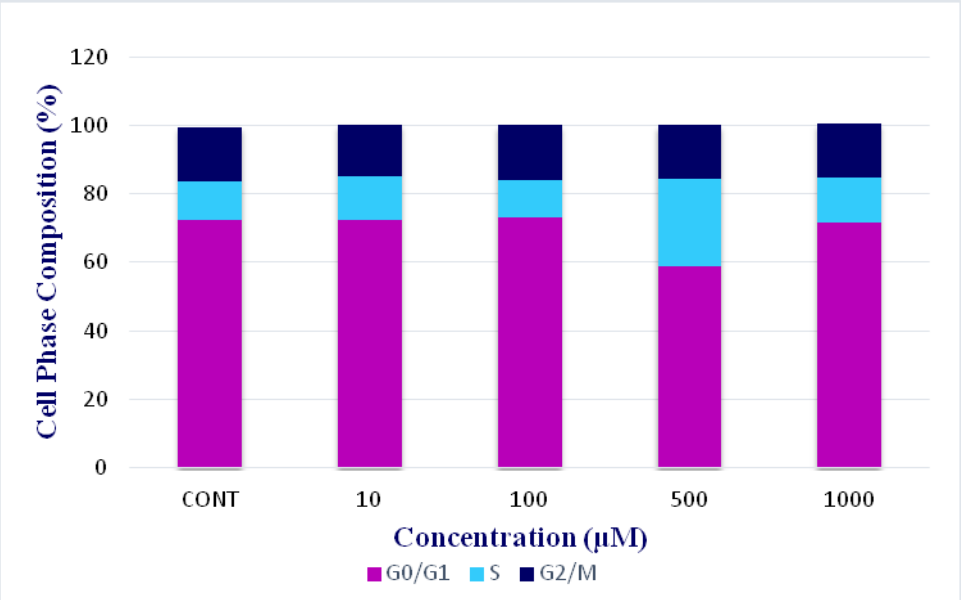

Figure 3.30. Effects of OLE on cell cycle against A549 cells

3.2.2.2. Cell Cycle Analysis on MCF-7 Cell Lines

To investigate the effects of OLE-CS-NPs on cell cycle against MCF-7 cells, the cells were treated with OLE-CS-NPs for different concentrations (100, 500, 1000 µM) and untreated cells were performed as control group by using flow cytometry based on propidium iodide (PI) staining as explained in Chapter 2.2.2.5. The results are listed in Table 3.7.

Table 3.7 Cell phase composition (%) of OLE-CS-NPs effected cells for different concentrations

Concentration (mM)	G0/G1	S	G2/M
0	54.23	28.9	16.565
100	58.35	27.96	13.68
500	53.88	30.29	15.005
1000	56.41	28.34	15.25

Effects of OLE-CS-NPs on cell phase composition (%) against MCF-7 cells are seen in Fig. 3.31. When the results were compered with cell phase composition (%) of

control cells, it was seen that there was an increase in G0/G1 phase from 54.23% to 58.35% at the lowest concentration of OLE-CS-NPs. Thus, a slight decrease in S phase from 28.90% to 27.96% and 16.57% to 13.68% in G2/M phase as expected. Because, OLE-CS-NPs were effective on G0/G1 phase and inhibited the initiation of DNA replication and metabolic activity and growth of cells so the transition to the S phase was blocked.

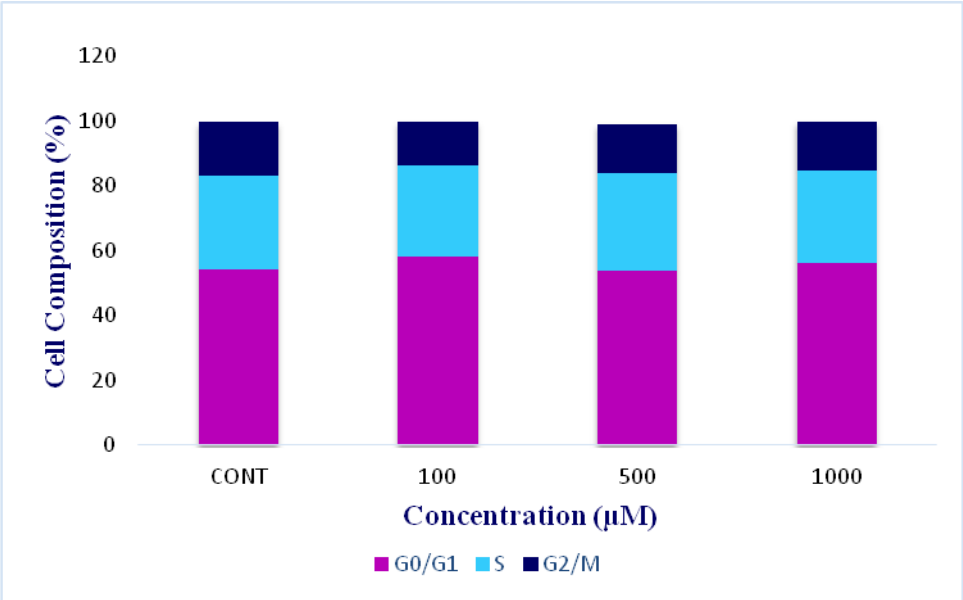

Figure 3.31. Effects of OLE-CS-NPs on cell cycle against MCF-7 cells

Although the effect of OLE-CS-NPs on cell phase composition (%) against MCF-7 cells was observed at the lowest concentration, there was nearly no differences at higher concentrations when compered with control cells.

Similar result was reported by Junkyu H. et al. that the effect of oleuropein which has highest amount in olive leaf extract on MCF-7 cell cycle distrubition as inhibition the G0/G1 phase at 100 mM of oleuropein (Junkyu H. et al., 2009).

3.2.3. Apoptosis Analysis

To investigate the apoptotic effects of OLE-CS-NPs against A549 and MCF-7 cells, this compound was applied with different concentrations (100, 300, 500 and 1000

μg/mL) to these cells and untreated cells were used as control group by using flow cytometry based Annexin V-FITC and PI staining.

In this method, the early apoptotic cells were detected. It is ideal for the detection of cell apoptosis quantitatively with the characteristics of simplicity, sensitivity and specificity with this staining. The propidium iodide (PI) is a non-specific DNA intercalating agent, which can be used to distinguish necrotic cells from apoptotic and living cells. If the cell membrane has an injury, the DNA of the cell may emit red fluorescence when stained with PI, while the intact cell membrane does emit no red fluorescence. Therefore, the early apoptotic cells and living cells have exhibited no red fluorescence signal (Liang J. et al., 2014). The percentage of cell phase composition was calculated as a result.

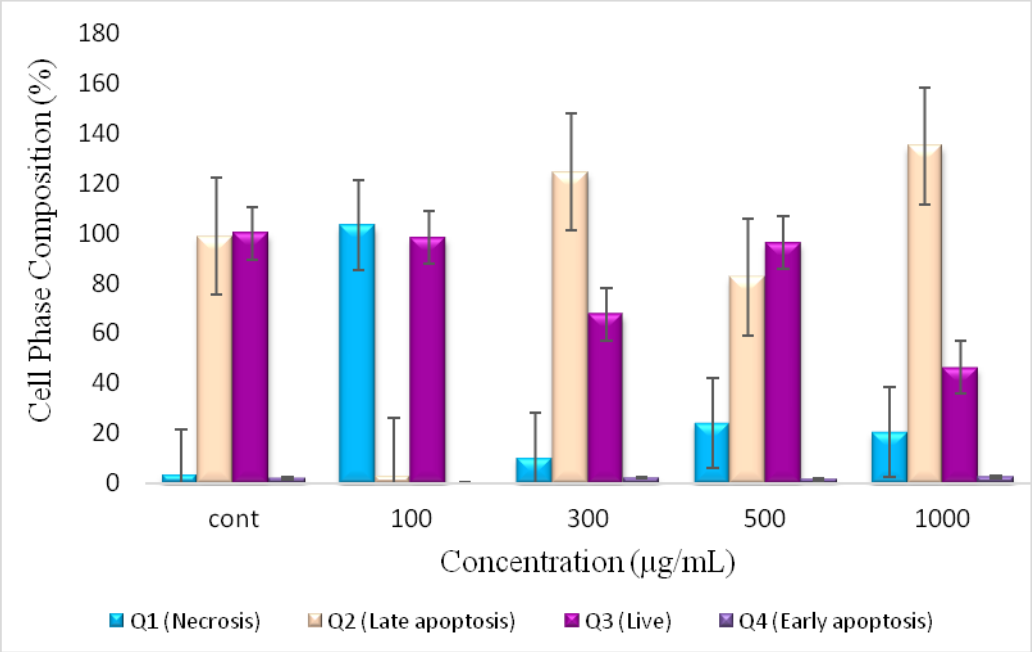

Figure 3.32. Quantification of the apoptotic effects of OLE-CS-NPs against A549 cells

The apoptotic effects of OLE-CS-NPs against A549 cells was shown in Figure 3.32. According to this result, when cell phase composition of control cells was compared with OLE-CS-NPs treated cells it was observed that there was an decrease at the amount of living cells (Q3 phase) with the increasing concentrations. Also, going through late apoptosis phase (Q2 phase which is a naturally occurring programmed and targeted cause of cellular death, (Proskuryakov et al., 2003)) was observed, too. Decreasing at the amount of living cells was fit with the results of MTT assay as

expected. At lowest concentration, amount of living cells were nearly similar with the amount of control cells.

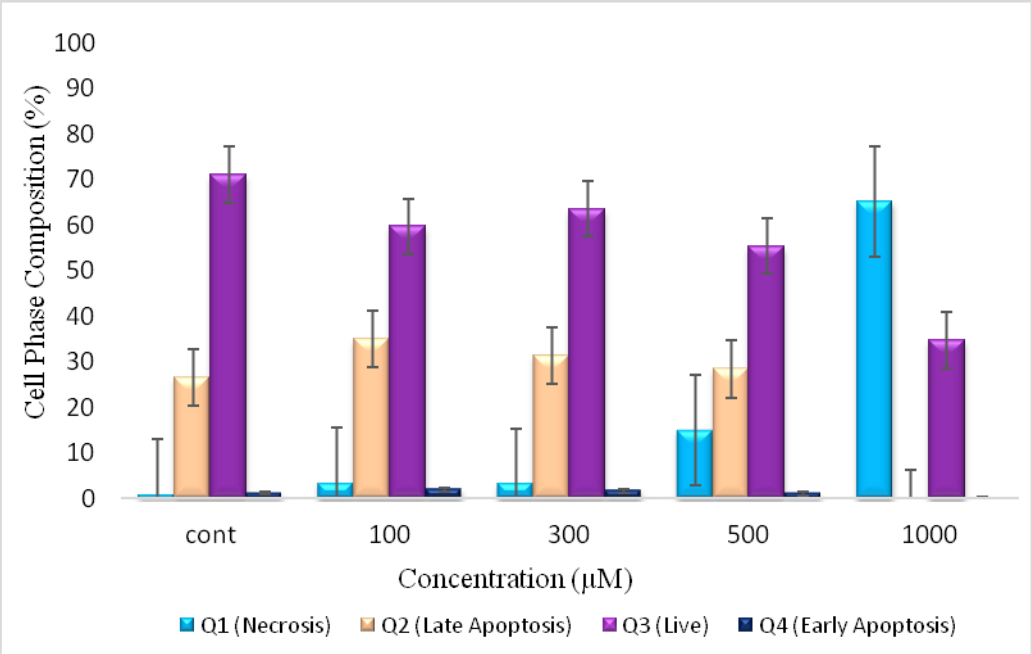

Figure 3.33. Quantification of the apoptotic effects of OLE-CS-NPs against MCF-7 cells

The apoptotic effects of OLE-CS-NPs against MCF-7 cells was shown in Figure 3.33. According to this result, when cell phase composition of control cells was compared with OLE-CS-NPs treated cells it was observed that there was an decrease at the amount of living cells (Q3 phase) with the increasing concentrations. Also, going through necrosis phase (Q1 phase which is a form of cell injury that results in the premature death of cells in living tissue, (Proskuryakov, Konoplyannikov, & Gabai, 2003)) was observed, too. Decreasing at the amount of living cells was fit with the results of MTT assay as expected. At lowest concentrations, amount of living cells and apoptotic cells were nearly similar with the amount of control cells.

3.2.4. Imaging Of Optical Microscopy

In order to understand the appearance of cancer cells before and after given OLE, CS, CS-NPs and OLE-CS-NPs, optical microscopy was used.

According to the Fig 3.34, there were nearly no differences between the CS and CS-NPs applied cells and control cells of A549.

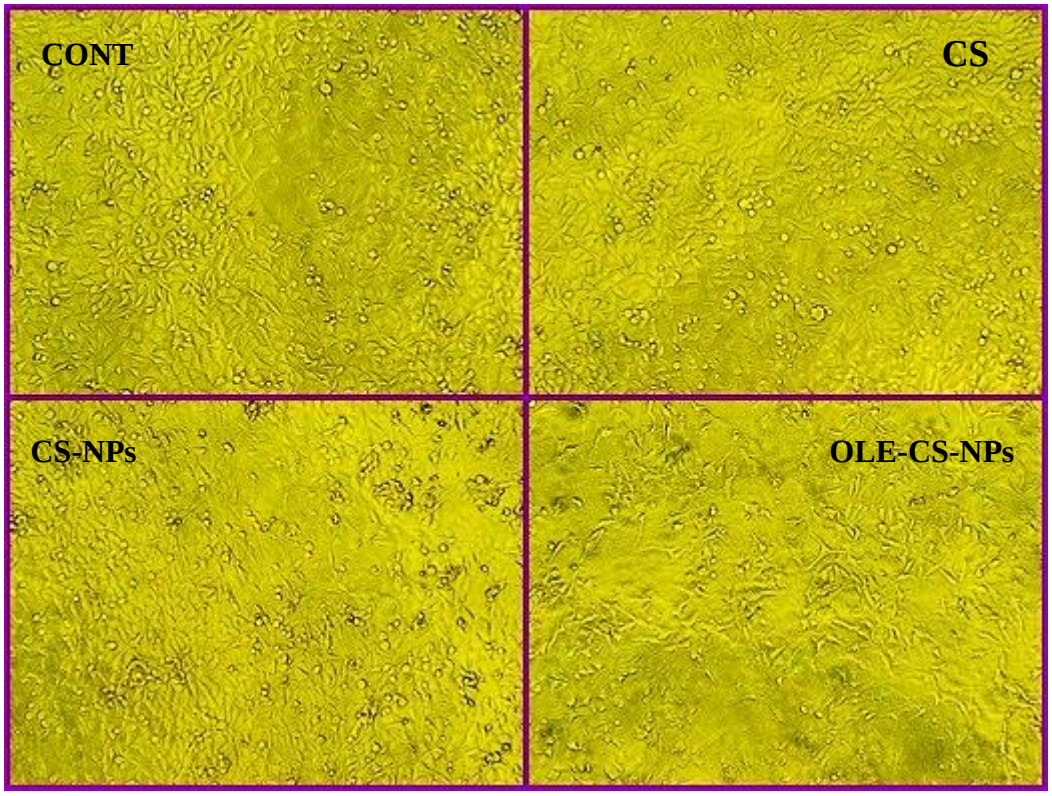

Figure 3.34. Optical microscopy images of A549 cells as control and 1000 μg/mL CS, CS-NPs and OLE-CS-NPs applied cells

While there were no differences on CS and CS-NPs applied cells morphology, there was significant difference on OLE-CS-NPs applied cells compared with control group. Also, it was clearly observed that there was apoptotic body organism on OLE-CS-NPs applied cells.

These result was expected according to the results of cytotoxic effect of compounds on A549 cells so it was fit with MTT results.

According to the Fig 3.35, there were nearly no differences between the CS and CS-NPs applied cells and control cells of MCF-7 cells.

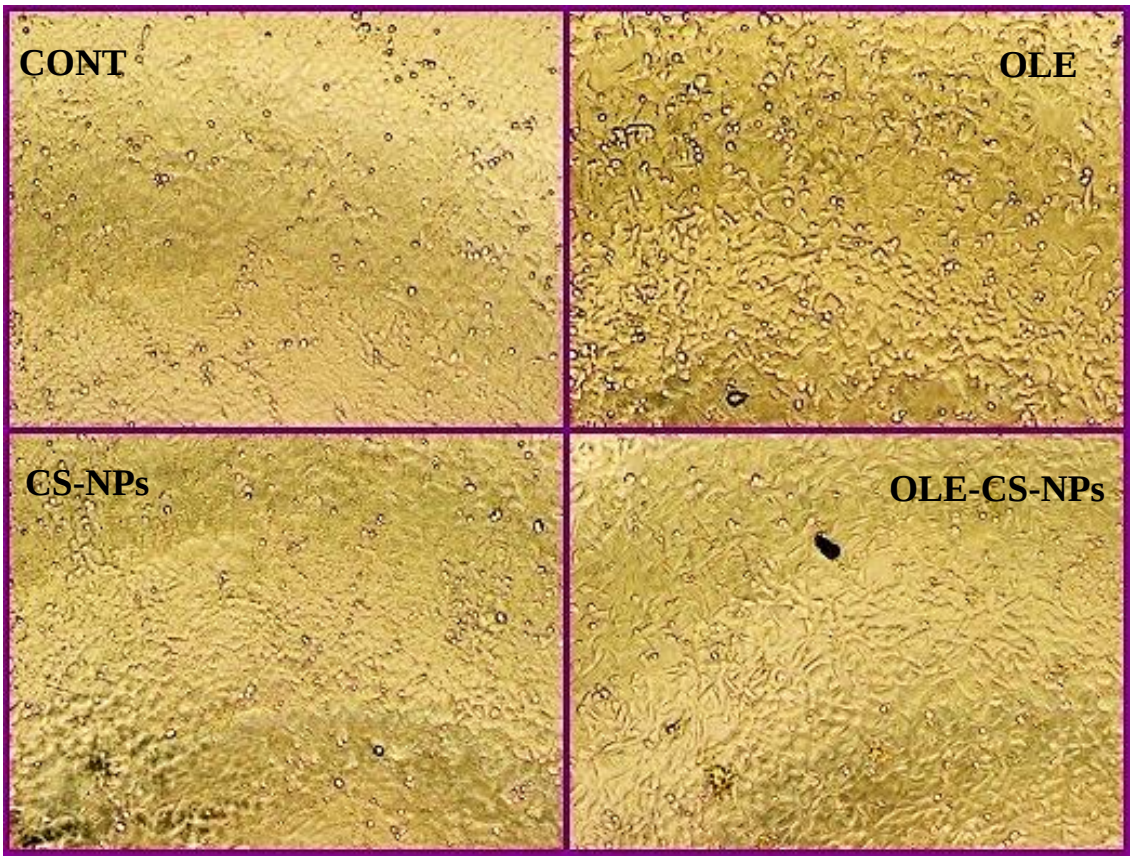

Figure 3.35. Optical microscopy images of MCF-7 cells as control and 1000 μg/mL CS, CS-NPs and OLE-CS-NPs applied cells

While there were no differences on CS and CS-NPs applied cells morphology, there was significant difference on OLE-CS-NPs applied cells compared with control group. Also, it was clearly observed that there was apoptotic body organism on OLE-CS-NPs applied cells.

These result was expected according to the results of cytotoxic effect of compounds on MCF-7 cells so it was fit with MTT results.

To support the bioavailable usage of OLE-CS-NPs on cancerous cells it was expected that there were no morfological differences on BEAS-2B cell lines when they were treated with each compounds, too. The results were illustrated in Figure 3.36.

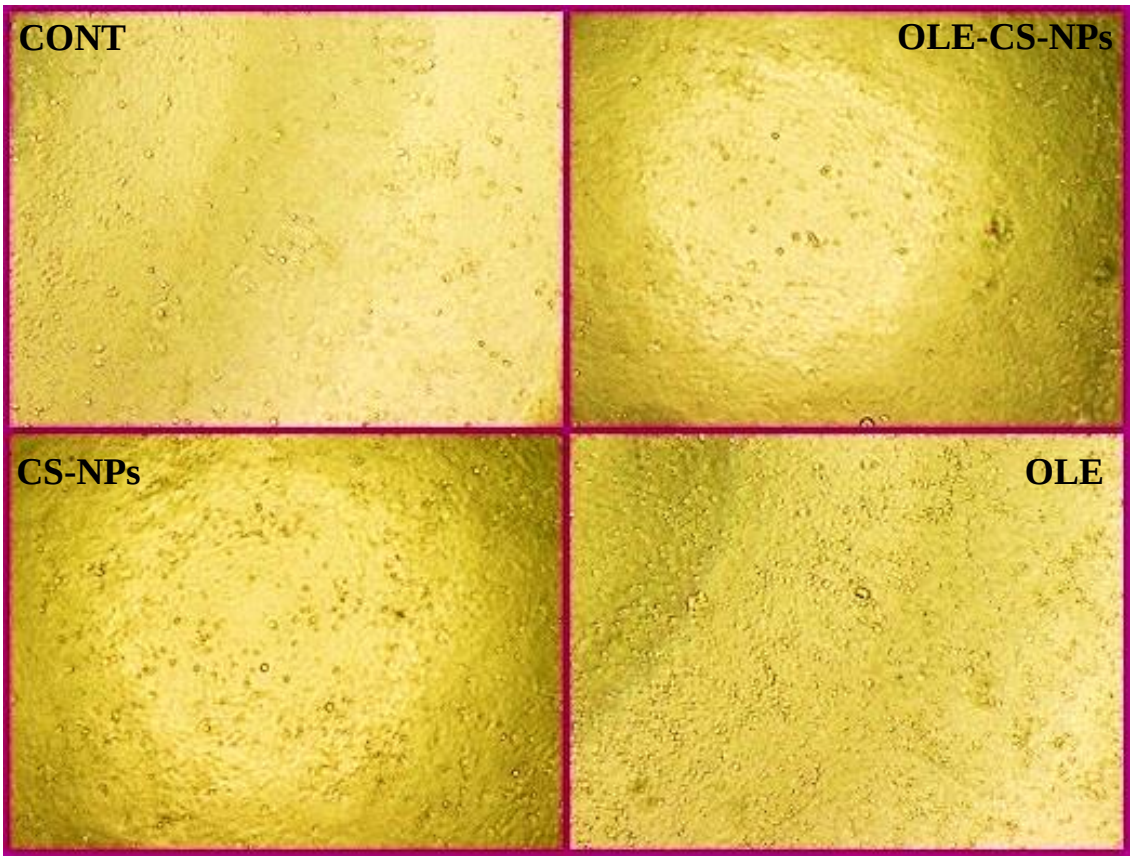

Figure 3.36. Optical microscopy images of BEAS-2B cells as control and 1000 µg/mL CS, CS-NPs and OLE-CS-NPs applied cells

According to the result, there were no morfological differences on BEAS-2B cells when they were treated with each compounds as expected. Also, increasing amount of OLE treated cells was supported the cell viability results. These results were fit with the MTT results and also support the bioavailabile usuage of compounds on cells.

CHAPTER 4

CONCLUSION

Cancer incidence and mortality rates are increasing worldwide in both economically developed and developing countries. Lifestyle-related factors, e.g. dietary habits, influence the incidence rate of diseases such as cancer (S. Isık et al., 2012). Epidemiological research has provided increasing evidence that dietary habits, especially Mediterranean diet which has high consumption of olive oil and its products, may play an important role in lung and breast cancer.

When the treatment methods of cancer is thought, it can be said that they have their restrictions. From this perspective, innovative drug delivery systems with functions of targeting anti-tumor drugs, eliminating solubility and resistance problems are urgently needed. Nanoparticles (NPs) have been a fascinating part of this field (Parveen S. et. al., 2012). The biocompatibility and non-toxicity of the chitosan makes it attractive as a neutral agent as nanoparticle for delivery of active agents.

In this study, to investigate the effect of olive leaf extract rich in polyphenols loaded nanoparticles against cancer cells, the nanoparticles were synthesized, firstly. For this aim, olive leaf was extracted and characterized to obtain their phenol content and antioxidant properties. Then, olive leaf extract was immobilized on chitosan nanoparticles. During the synthesis, characterization of optimum conditions were demonstrated. After synthesizing of nanoparticles at optimum conditions, characterization studies were performed by dynamic light scattering, atomic force microscopy and infrared spectroscopy.

According to the optimization studies, it can be concluded that nanoparticles have the best loading capacity and size distribution properties when they were synthesized at 5/1 CS:TPP mass ratio when the pH of CS solution was 5.0 and incubated with TPP for 60 min after adding 0.25% OLE to CS solution at the end of 30 min. In these conditions, the loading capacity of OLE-CS-NPs was 97.55% and 91.30 nm in size which was supported by DLS measurements and FT-IR results.

CS-NPs were observed to be of spherical or ellipsoidal shape and OLE-CS-NPs was smaller than that of the corresponding CS-TPP nanoparticles, which may be

attributable to a greater cross-linking density of the OLE-CS-NPs caused by the interactions between the CS matrix and polyphenols in OLE. Also, disappearing of characteristic peaks of CS-TPP was the proof of forming OLE-CS-NPs and immobilizing of OLE into CS-NPs.

Our results fit with the study of Wu et al. (2005), B. Hu et. al. (2008), Zhang, L., Kosaraju, S. L. (2007), J. Liu et al. (2010), Xu et al, Knaul J.Z et al (1999) and Wang X. et al. (2001) as disscused in results and discussion part of the text.

Demonstration of cancer preventive effect (both cytotoxic, apoptotic and cell cycle effects) of olive leaf extract loaded nanoparticles was investigated against lung (A549) and breast (MCF-7) cancer and the effect of nanoparticles was compared with free olive leaf extract, chitosan and chitosan nanoparticles. Also, the cytotoxic effect of compounds was investigated against healthy lung cells (BEAS 2B) to determine their biocompatibility and if they damage the healthy cells or not. In addition, morfological differences of cells were scanned after and before treated with these compounds for A549, MCF-7 and BEAS 2B cells by using optical microscopy.

The cytotoxic effect against A549, MCF-7 and BEAS 2B cells was determined by measuring the IC_{50} value of free OLE, CS, CS-NPs and OLE-CS-NPs based on MTT assay.

IC_{50} value of OLE-CS-NPs was found 285.0 μg/mL whereas IC_{50} value of CS-NPs is 2146.2 μg/mL for A549 cells. In addition, neither OLE nor CS have cytotoxic effect on A549 cells and cell viability was approximately 90-100 %. It can be concluded from this result that OLE-CS-NPs are very effective on A549 cell proliferation in lower doses in contrast to CS-NPs and NPs have cytotoxic effect on cells when they are loaded with OLE. Thus, CS-NPs are nontoxic for cells, they can be used as a drug carrier.

Up to date, not only there is no data about synthesis of olive leaf extract loaded nanoparticles but also there is no analytical epidemiological study that has evaluated the association between the components of the Mediterranean diet and lung cancer (Fortes, C. et al., 2003). Thus, the results were obtained for the first time in both studies.

IC_{50} value of OLE-CS-NPs was found as 298.8 μg/mL whereas IC_{50} value of CS-NPs is 3325.0 μg/mL for MCF-7 cells. In addition, neither OLE nor CS have

cytotoxic effect on MCF-7 cells and cell viability was approximately 90-100 %. It can be concluded from this result that OLE-CS-NPs are very effective on MCF-7 cell proliferation in lower doses in contrast to CS-NPs and CS-NPs could be used for enhancing the bioavailability of OLE.

When we compare our results with previous studies, our results show that OLE-CS-NPs are more effective on MCF-7 cells than olive leaf extract polyphenols. According to the study of Z. Bouallagui et al., it was reported that a concentration of 3000 μg/mL olive leaf extract leading to 38.4% inhibition in the MTT assay on MCF-7 cells (Z. Bouallagui et al., 2011).

IC_{50} value of OLE-CS-NPs was found as 1015.0 μg/mL and IC_{50} value of CS-NPs was 3745.5 μg/mL for BEAS 2B cells. Thus, it can be concluded from this result that both OLE-CS-NPs and CS-NPs are not effective on BEAS 2B cell proliferation in lower doses and cytotoxic doses of OLE-CS-NPs for A549 cells are not cytotoxic for BEAS 2B cells. As a result of being no cytotoxic for healthy cells, we can conclude that our compounds can be used for cancerous cells as a new therapeutic drug.

After cytotoxic effect of compounds were demonstrated, it was investigated that in which step of cell cycle the compounds were effective. According to the results of cell cycle analysis based on PI staining by flow cytometer, it was seen that there was an increase in S phase composition with the increasing concentration of OLE-CS-NPs against A549 cells when it was compared with control cells. Therefore, cell growth and protein synthesis for mitosis were blocked. Also, it was seen that there were no differences on cell phase composition (%) of OLE treated cells. The results were found nearly the same with control cells. It can be concluded from this result that free OLE is not effected on cell cycle of A549 cells.

When the results were compered with cell phase composition (%) of control cells, it was seen that there was an increase in G0/G1 phase at the lowest concentration of OLE-CS-NPs against MCF-7 cells. Therefore, initiation of DNA replication and metabolic activity and growth of cells were inhibited.

Similar result was reported by Junkyu H. et al. that the effect of oleuropein, highest amount in olive leaf extract, was demonstrated as inhibition of the G0/G1 phase at 100 mM on MCF-7 cell cycle distrubition (Junkyu H. et al., 2009).

Apoptosis analysis were performed to support the cytotoxicity results in our study. According to apoptosis analysis, when cell phase composition of control cells was compared with OLE-CS-NPs treated A549 and MCF-7 cells it was observed that there was an decrease at the amount of living cells (Q3 phase) with the increasing concentrations. This decreasing amount of living cells was fit with the results of MTT assay as expected. Also, going through late apoptosis phase (Q2 phase) for A549 cells and going through necrosis phase for MCF-7 cells was observed.

According to the optical imaging results, while there was no differences on CS and CS-NPs applied cells morphology, there was significant difference on OLE-CS-NPs applied cells compared with control group. It was clearly observed that there was an apoptotic body organism on OLE-CS-NPs applied A549 and MCF-7 cells. Also, there was no morfological differences on BEAS-2B cells when they were treated with OLE-CS-NPs. These results was expected according to the results of cytotoxic effect of compounds on A549 and MCF-7 cells and the results were fit with cytotoxicity results.

Previous studies demonstrate that there is no study that investigates the cytotoxic effect of olive leaf extract loaded chitosan nanoparticles. Chitosan is a suitable material for delivering as explained by Huang et al. (2004). As our results were fit with the literature, we can conclude that OLE-CS-NPs have cytotoxic effect against cancerous cells at lower doses and as being nontoxic for both cancerous and healthy cells, CS-NPs can be used as drug delivery system.

For the further steps, protein profiling studies may be performed to provide much better understanding of OLE-CS-NPs action on cancerous cells.

REFERENCES

Al-Qadi, S., Grenha, A., Carrión-Recio, D., Seijo, B., Remu˜nán-López, C., 2012. Microencapsulated chitosan nanoparticles for pulmonary protein delivery: in vivoevaluation of insulin-loaded formulations. J. Control. Release 157, 383–390.

Amani T., David A-R., Enrique B-C., Verónica R-T., Almudena P-S., Miguel H., Elena I., Vicente M., Mokhtar Z., Antonio S-C., Alberto F-G. 2012. Use of advanced techniques for the extraction of phenolic compounds from Tunisian olive leaves: Phenolic composition and cytotoxicity against human breast cancer cells, Food and Chemical Toxicology, 50, 1817–1825.

Amelia, J. W., Sarah, D. B., Megan, R. H., Gemma E. C., Jane A. P., Roisin, E. B., Norbert, S., Wojciech, C., Nial, J. W., 2012. Cisplatin drug delivery using gold-coated iron oxide nanoparticles for enhanced tumour targeting with external magnetic fields., Inorganica Chimica Acta., 393., 328–333.

Anand, P., Kunnumakara, A. B., Sundaram, C., Harikumar, K. B., Tharakan, S. T., Lai, O. S., Aggarwal, B. B., 2008. Cancer is a Preventable Disease that Requires Major Lifestyle Changes. Pharmaceutical Research. 25-9., 2097-2116., doi: DOI 10.1007/s11095-008-9661-9.

Antonio, R., Massimiliano, B., Paolo, B., Barbara, B., Attilio, C. 2013. Chitosan nanoparticles: Preparation, size evolution and stability, International Journal of Pharmaceutics., 455., 219– 228.

B. Hu., C. Pan., Y. Sun., Z. Hou., H. Ye., B. Hu., X. Zeng., 2008. Optimization of Fabrication Parameters To Produce Chitosan-Tripolyphosphate Nanoparticles for Delivery of Tea Catechins., Journal of Agricultural and Food Chemistry., 56., 7451–7458.

Berger, J., Reist, M., Mayer, J.M., Felt, O., Peppas, N.A., Gurny, R., 2004. Structureand interactions in covalently and ionically crosslinked chitosan hydrogels forbiomedical applications. Eur. J. Pharm. Biopharm. 57, 19–34.

Birrenbach, G., Speiser, P.P., 1976. Polymerized micelles and their use as adjuvantsin immunology. J. Pharm. Sci. 65, 1763–1766.

Bodmeier, R., Chen, H., & Paeratakul, O. 1989. Pharmaceutical Research., 6., 413.

Bouallagui, Z., Han, J., Isoda, H., Sayadi, S., 2011. Hydroxytyrosol rich extract from olive leaves modulates cell cycle progression in MCF-7 human breast cancer cells, Food and Chemical Toxicology., 49., 179–184.

C-W. Chou., O. Batnyam., H-S Hung., H-J Harn., W-F. Lee., H-R. Lin., J-G. Chung., Y-C. Shih., S-Y. Yen., Y-H. Kuobj., M-H Tsaoa. 2013. Highly bioavailable anticancer herbal-loaded nanocarriers for use against breast and colon cancer in vitro and in vivo systems., Polymer Chemistry., 4., 2040.

Chris I.R. Gill., Boyd, A., McDermott, E., McCann, M., Servili, M., Selvaggini, R., Taticchi, A., Esposto, S., Montedoro, G., McGlynn, H., Rowland I., 2005.

Potential anti-cancer effects of virgin olive oil phenols on colorectal carcinogenesis models in vitro., International Journal of Cancer., 117., 1–7.

Corona, G., Deiana, M., Incani, A., Vauzour, D., Dessi, M-A., Spencer, J-P-E., 2009. Hydroxytyrosol inhibits the proliferation of human colon adenocarcinoma cells through inhibition of ERK1/2 and cyclin D1. Molecular Nutrition and Food Research., 53-7: 897-903.

Çınar A. et al., 2011. Phenolic Compounds of Olive by-products and Their Function in the Development of Cancer Cells. Biyoloji Bilimleri Araştırma Dergisi, 4-2: 55-58.

D. R. Nogueira., L. Tavano., M. Mitjans., L. Pérez., M. R. Infante., M. P. Vinardell. 2013. In vitro antitumor activity of methotrexate via pH-sensitive chitosan nanoparticles., Biomaterials., 34., 2758-2772.

D. R. Bhumkar et al., 2002. Studies on Effect of pH on Cross-linking of Chitosan With Sodium Tripolyphosphate: A Technical Note., AAPS PharmSciTech., 7., 2.

D. Baycın., E. Altıok., S. Ulku., O. Bayraktar., 2007. Adsorption of Olive Leaf (Olea europaea L.) Antioxidants on Silk Fibroin., Journal of Agricultural and Food Chemistry., 55., 1227-1236.

Dan, P., Jeffrey, M. K., Seungpyo, H., Omid, C. F., Rimona M., Robert L., 2007. Nanocarriers as an emerging platform for cancer therapy. Nat. Nano., 2., 751-760.

E, Tripoli., M. Giammanco., G. Tabacchi., D. D. Majo., S. Giammanco., M. La Guardia. 2005. The phenolic compounds of olive oil: structure, biological activity and beneficial effects on human health. Nutrition Research Reviews., 18., 98–112.

Fabiani, R.., De Bartolomeo, A., Rosignoli, P., Servili, M l., 2002. Cancer chemoprevention by hydroxytyrosol isolated from virgin olive oil through G1 cell cycle arrest and apoptosis. European Journal of Cancer Prevention., 11., 351–358.

Fortes, C., Forastiere, F., Farchi, S., Mallone, S., Trequattrinni, T., Anatra, F., Schmid, G., and Perucci, C. A., 2003. The Protective Effect of the Mediterranean Diet on Lung Cancer., Nutrition and Cancer., 46, 30–37.

H, Hosseinzadeh., F, Atyabi., R, Dinarvand., S. N. Ostad., 2012. Chitosan–Pluronic nanoparticles as oral delivery of anticancer gemcitabine: preparation and in vitro study, Hosseinzadeh et al, International Journal of Nanomedicine. 7 1851–1863.

Haag, R., Kratz, F., 2006. Polymer Therapeutics: Concepts and Applications. Angewandte Chemie International Edition., 45., 1198 – 1215.

Hamdi H.K., Castellon R., 2005. Oleuropein, a nontoxic olive iridoid, is an anti-tumor agent and cytoskeleton disruptor. Biochemical and Biophysical Research Communications., 334:769-778.

Han, J., Terence, P. N., Yamada, T.P., Isoda, H., 2009. Anti-proliferative and apoptotic effects of oleuropein and hydroxytyrosol on human breast cancer MCF-7 cells. Cytotechnology., 59., 45–53.

Hashim, Y. Z., Rowland, I. R., McGlynn, H., Servili, M. Et al., 2008. Inhibitory effects of olive oil phenolics on invasion in human colon adenocarcinoma cells in vitro. International Journal of Cancer., 122., 495–500.

Hengartner, M. O., 2000. The biochemistry of apoptosis. *Nature, 407*(6805), 770-776. doi: 10.1038/35037710.

Hıtesh, J., Josyula, V. R., Vasanth, R. P., Raghu C. H., Sagar, G. A. 2013. Nanoformulation Of SiRNA And Its Role In Cancer Therapy: *In Vitro* And *In Vivo* Evaluation, Cellular & Molecular Biology Letters., 18., 1., 120-136., DOI: 10.2478/s11658-012-0043-2.

Hong, Z., Megan O., Christine A., Eugenia K., 2004. Monodisperse Chitosan Nanoparticles for Mucosal Drug Delivery., Biomacromolecules., 5., 2461-2468.

http://www.lungcancer.org/find_information/publications/163-lung_cancer_101/265-what_is_lung_cancer

http://a549.com/ (accessed, 24 May 2014)

http://www.phe-culturecollections.org.uk/ (accessed, 24 May 2014)

http://www.lgcstandards-atcc.org/~/media/Attachments/B/8/0/F/33208.ashx (accessed, 24 May 2014)

http://www.cancer.org/cancer/breastcancer/ (accessed, 24 May 2014)

http://www.mcf7.com/ (accessed, 24 May 2014)

http://www.lgcstandards-atcc.org/~/media/Attachments/0/E/E/2/1980.ashx (accessed, 24 May 2014)

Ivan, C., Francesco, P., Adele, C., Rosa, S., Carmen, R., Paola, A., Vincenzo, P., 2013. Potential of olive oil phenols as chemopreventive and therapeutic agents against cancer: A review of in vitro studies. Molecular Nutrition & Food Research., 57., 71–83.

J. J, Wang., Z. W. Zeng., R. Z. Xiao., T. Xie., G. L. Zhou., X. R. Zhan., S. L. Wang., Recent advances of chitosan nanoparticles as drug carriers, International Journal of Nanomedicine., 6., 765–774.

J. Liu., L. Zhang., C. Wang., H, Xu., X. Zhao. 2009. Preparation and characterization of lectin-conjugated chitosan fluorescent nanoparticles., Molecular BioSystems, 6, 954–957, DOI: 10.1039/b927040j

Jacobson, M. D., Weil, M., & Raff, M. C., 1997. Programmed cell death in animal development. *Cell, 88*(3), 347-354.

Jennifer, H. G., Scott, E. M., 2012. Physics Today., Nanotechnology in Cancer Medicine., Citation: Physics Today 65(8), 38; doi: 10.1063/PT.3.1678 View online: http://dx.doi.org/10.1063/PT.3.1678

Jong-Ho Kim et. al., 2008. Antitumor efficacy of cisplatin-loaded glycol chitosan nanoparticles in tumor-bearing mice., Journal of Controlled Release., 127, 41–49.

Junkyu, H., Terence, P. N., Talorete P. Y., Hiroko I., 2009. Anti-proliferative and apoptotic effects of oleuropein and hydroxytyrosol on human breast cancer MCF-7 cells. Cytotechnology., 59:45–53

Knaul, J.Z., Hudson, S.M., Creber, K.A.M., 1999. Improved mechanical properties of chitosan fibres. J Appl Polym Sci., 72., 1721-1731.

Leist, M., & Jaattela, M., 2001. Four deaths and a funeral: from caspases to alternative mechanisms. *Nat Rev Mol Cell Biol, 2*(8), 589-598. doi: 10.1038/35085008.

M. Huang., E. Khor., L-Y. Lim., 2004. Uptake and Cytotoxicity of Chitosan Molecules and Nanoparticles: Effects of Molecular Weight and Degree of Deacetylation., Pharmaceutical Research., 21, 2.

M.P., Carrera-Gonzalez., M.J. Ramırez-Exposito., M.D. Mayas and J.M., Martınez-Martos. 2013. Protective role of oleuropein and its metabolite hydroxytyrosol on cancer. Trends in Food Science & Technology., 31., 92-99.

Meier, P., Finch, A., & Evan, G., 2000. Apoptosis in development. *Nature, 407*(6805), 796-801. doi: 10.1038/35037734.

Michael, M., 2002. Mechanisms Of Cancer Drug Resistance., Annual Review of Medicine., 53:615–27.

Mosmann, T., 1983. Rapid colorimetric assay for cellular growth and survival: application to proliferation and cytotoxicity assays. *J Immunol Methods, 65*(1-2), 55-63.

N. Pellegrini., M. Serafini., B. Colombi., D. D. Rio., S. Salvatore., M. Bianchi., F. Brighenti. 2003. Total Antioxidant Capacity of Plant Foods, Beverages and Oils Consumed in Italy Assessed by Three Different In Vitro Assays., The Journal of Nutrition., 133: 2812–2819.

Nasti, A., Zaki, N.M., De Leonardis, P., Ungphaiboon, S., Sansongsak, P., Rimoli, M.G.,Tirelli, N., 2009. Chitosan/TPP and chitosan/TPP-hyaluronic acid nanoparticles:systematic optimisation of the preparative process and preliminary biologicalevaluation. Pharm. Res. 26, 1918–1930.

Parveen, S., Misra, R., Sahoo, K. S., 2008. Nanoparticles: a boon to drug delivery, therapeutics, diagnostics and imaging., Nanomedicine: Nanotechnology, Biology, and Medicine., 8., 147–166.

Q. Gan., T. Wang., C. Cochrane., P. McCarron., 2005. Modulation of surface charge, particle size and morphological properties of chitosan–TPP nanoparticles intended for gene delivery., Colloids and Surfaces B: Biointerfaces., 44., 65–73.

S. Cicerale., L. Lucas., R. Keast. 2010. Biological Activities of Phenolic Compounds Present in Virgin Olive Oil, International Journal of Molecular Sciences., 11., 458-479.

Shi, X. Y., Fan, X. G., 2002. Advances in nanoparticle system for deliverying drugs across the biological barriers., J China Pharm Univ., 33(3): 169–172.

S. Isık et al., 2012., Proliferative and apoptotic effects of olive extracts on cell lines and healthy human cells. Food Chemistry. 134., 29–36.

S. Papadimitriou., D. Bikiaris., K. Avgoustakis., E. Karavas., M. Georgarakis., 2008. Chitosan nanoparticles loaded with dorzolamide and pramipexole, Carbohydrate Polymers., 73., 44–54.

T. López-León et al., 2005. Physicochemical characterization of chitosan nanoparticles: electrokinetic and stability behavior., Journal of Colloid and Interface Science., 283:344–351.

The Biology of Cancer, by Robert A. Weinberg.

The Cell: A Molecular Approach. 2nd edition, The Eukaryotic Cell Cycle, NCBI can be accessed, http://www.ncbi.nlm.nih.gov/books/NBK9876/, 28.05.2014.

Tuck, K.L., Freeman, M.P., Hayball, P.J., Stretch, G.L., Stupans, I. 2001. The in vivo fate of hydroxytyrosol and tyrosol, antioxidant phenolic constituents of olive oil, after intravenous and oral dosing of labeled compounds to rats. Journal of Nutrition., 131, 1993–1996.

Twan, L., 2010. Improving the efficacy of combined modality anticancer therapy using HPMA copolymer-based nanomedicine formulations. Adv. Drug Deliv. Rev. 62., 203–230.

Vaux, K., 1999. Law and lamb: AKEDAH and the search for a deep religious symbol for an ecumenical bioethics. *Christ Bioeth*, *5*(3), 213-219. doi: 10.1076/chbi.5.3.213.6893.

Waterman, E., Lockwood, B., 2007. Active components and clinical applications of olive oil. Alternative Medicine Review., 12-4: 331-342.

Wu, Y., Yang, W., Wang, C., Hu, J., & Fu, S. 2005. Chitosan nanoparticles as a novel delivery system for ammonium glycyrrhizinate. International Journal of Pharmaceutics, 295, 235–245.

www.altogen.com/a549php (accessed, 24 May 2014)

Xu, Y.M., Du, Y.M., 2003. Effect of molecular structure of chitosan on protein delivery properties of chitosan nanoparticles. Int. J. Pharm. 250, 215–226.

Yumi, Z., H-Y, Hashim., M Eng., Chris, I.R. G., Hugh McGlynn and Ian R. Rowland., 2005. Components of Olive Oil and Chemoprevention of Colorectal Cancer, Nutrition Reviews., 63., 11., 374–386.

Zhang, H., Oh, M., Allen, C., & Kumacheva, E. 2004. Monodisperse chitosan nanoparticles for mucosal drug delivery. Biomacromolecules, 5., 6., 2461., 8.

Zhang, L., Kosaraju, S. L. 2007. Biopolymeric delivery system for controlled release of polyphenolic antioxidants., Eur. Polym. J., 43., 2956–2966.

Zhang P., Gao W. Y., Turner S., Ducatman S. B., 2003. Gleevec (STI-571) inhibits lung cancer cell growth (A549) and potentiates the cisplatin effect in vitro, Molecular Cancer, 2:1.

.

APPENDIX A

MEDIAS

A.1. RPMI-1640 Growth Medium

Roswell Park Memorial Institute – 1640 (RPMI 1640) growth medium, fethal bovine serum (FBS) and gentamicine sulfate were obtained from Gibco, BRL.

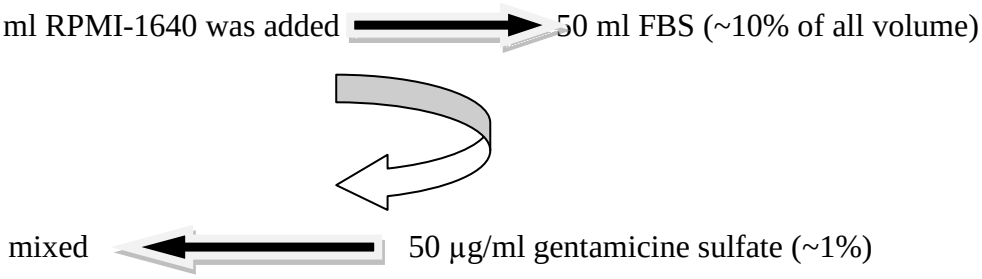

APPENDIX B

CHEMICALS, REAGENTS AND SOLUTIONS

Table.1. Chemicals and Reagents Used in Experiments

NO	CHEMICALS	COMPANY
1	Dimethyl Sulfoxide (DMSO)	Sigma
2	Trypan Blue Dye	Sigma
3	Phosphate Buffered Saline (PBS)	Invitrogen
4	Gentamicine Sulfate	Gibco
5	Fetal Bovine Serum (FBS)	Gibco
6	MTT Reagent (should not be exposed to light)	Sigma
7	Annexin-V Apoptosis Detection Kit I	BD Pharmingen
8	Absolute Ethanol	AppliChem
9	Phosphoric Acid	AppliChem
10	Trypsin	Sigma
11	Triton X-100	Sigma
12	RNase	Thermo
13	Chitosan	Sigma
14	Sodium tri polyphosphate (TPP)	Sigma
15	Sodium Hydroxyde (NaOH)	Sigma
16	Acetic Acid Glacial	Sigma
17	Folin Reagent	Merck
18	Sodium Carbonate ($Na_2CO_{3)}$	Sigma
19	ABTS reagent	Fluka
20	$K_2S_2O_8$	Merck
21	Aceto nitryl	Sigma

B.2. MTT Reaction Solution

In order to prepare a reaction solution sufficient for a 96-well plate 3-(4,5-Dimethylthiazol-2-yl)-2,5-diphenyltetrazolium bromide MTT solution was prepared in PBS to obtained a concentration of 5mg/ml. % 10 MTT solution was prepared with RPMI.

APPENDIX C

CALCULATIONS OF CHARACTERIZATION OF OLIVE LEAF EXTRACT

Calibration Curve For Total Phenolic Compound Content:

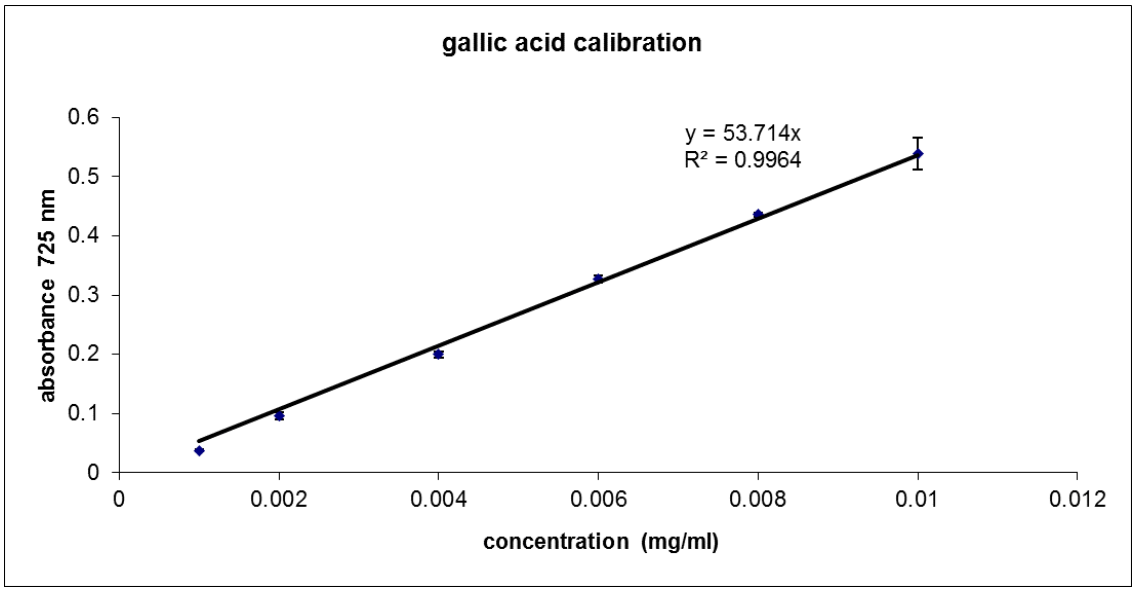

Figure C.1. Calibration curve for total phenol content as gallic acid equevalant

Sample Calculation For Percentage Inhibition:

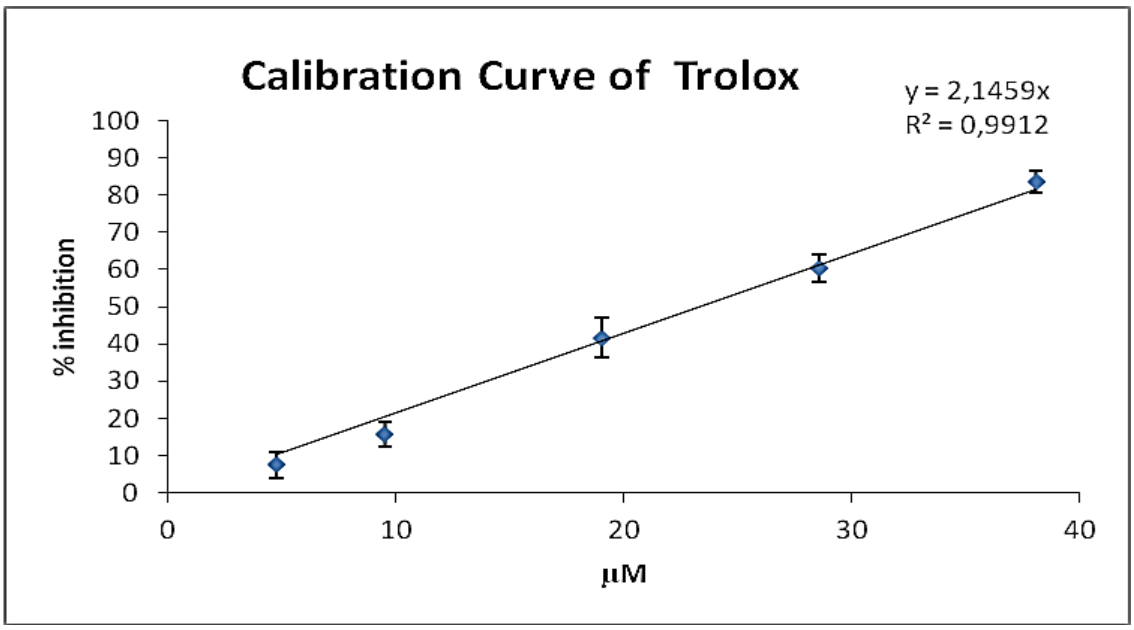

Figure C.2. Calibration curve for total antioxidant capacity as mmol TEAC/g OLE

Olive leaf extract solution was added to ABTS radical cation solution and the absorbance values were taken at each 1 minute during 60 minutes. Average of the first and last absorbance was taken for two diluted OLE solution and its decrease from the absorbance value of ABTS radical cation solution was calculated in order to find out percentage inhibition. The measured absorbance values after adding the olive leaf extract solution were, 0.4924 and 0.6016 for first absorbance and 0.298244 and 0.57723 for last absorbance. % inhibition was calculated as:

% 39.43 = [1-(0.4924/0.2982)]*100

and

% 4.05 = [1-(0.6016/0.57723)]*100

The concentrations of two solutions were calculated as 1.67 and 2.68 mM and the average was 2.18 mM per g of OLE. The result was concluded 2.18 mmol TEAC/ g of OLE.

Calculation For Analysis of Total Phenolic Compounds with HPLC:

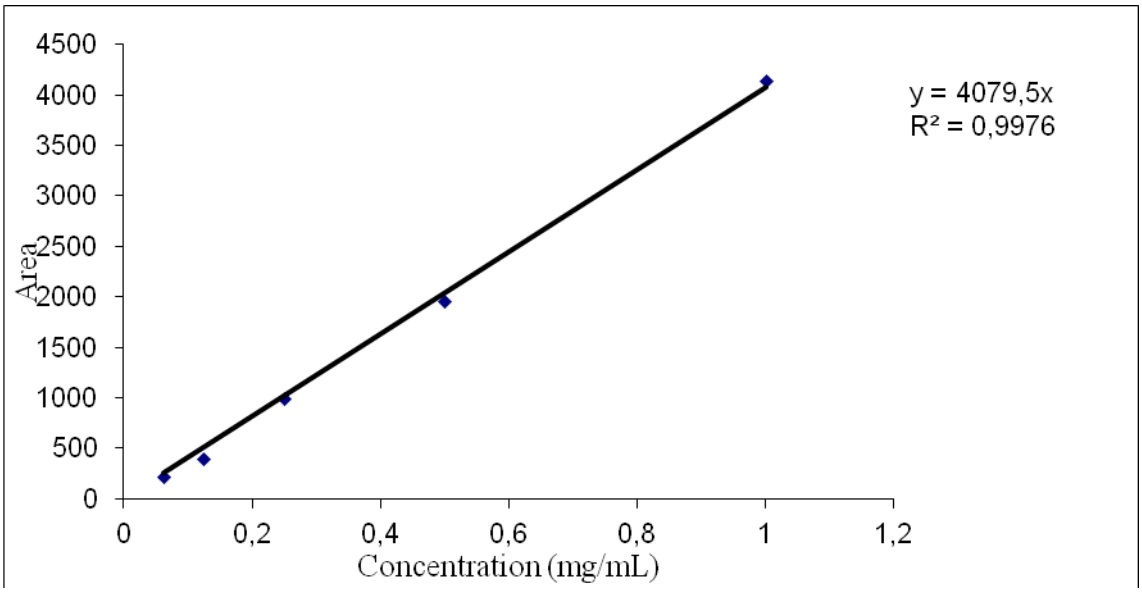

Figure C.3. Calibration curve of oleuropein

In order to find out the amount of oleuropein in olive leaf extract, the responses of HPLC in terms of areas were recorded. By using these areas and calibration curves, concentration of oleuropein was calculated. the HPLC response for oleuropein was 944.4. The equation of external calibration curve for oleuropein is:

y = 4079.5 x

where,

y = area

x = concentration

944.4 = 4079.5 x

x = 0.231 μg/mL = 0.00023 mg/mL.